1998

Ambiguities in the definition of spin-dependent parton distributions

Yuen-Wing Law
Iowa State University

INFORMATION TO USERS

This manuscript has been reproduced from the microfilm master. UMI films the text directly from the original or copy submitted. Thus, some thesis and dissertation copies are in typewriter face, while others may be from any type of computer printer.

The quality of this reproduction is dependent upon the quality of the copy submitted. Broken or indistinct print, colored or poor quality illustrations and photographs, print bleedthrough, substandard margins, and improper alignment can adversely affect reproduction.

In the unlikely event that the author did not send UMI a complete manuscript and there are missing pages, these will be noted. Also, if unauthorized copyright material had to be removed, a note will indicate the deletion.

Oversize materials (e.g., maps, drawings, charts) are reproduced by sectioning the original, beginning at the upper left-hand corner and continuing from left to right in equal sections with small overlaps. Each original is also photographed in one exposure and is included in reduced form at the back of the book.

Photographs included in the original manuscript have been reproduced xerographically in this copy. Higher quality 6" x 9" black and white photographic prints are available for any photographs or illustrations appearing in this copy for an additional charge. Contact UMI directly to order.

UMI

A Bell & Howell Information Company
300 North Zeeb Road, Ann Arbor MI 48106-1346 USA
313/761-4700 800/521-0600

Ambiguities in the definition of spin-dependent parton distributions

by

Yuen-Wing Law

A dissertation submitted to the graduate faculty

in partial fulfillment of the requirements for the degree of

DOCTOR OF PHILOSOPHY

Major: Nuclear Physics

Major Professor: Jianwei Qiu

Iowa State University

Ames, Iowa

1998

Graduate College
Iowa State University

This is to certify that the Doctoral dissertation of

Yuen-Wing Law

has met the dissertation requirements of Iowa State University

Signature was redacted for privacy.

Committee Member

Signature was redacted for privacy.

Committee Member

Signature was redacted for privacy.

Committee Member

Signature was redacted for privacy.

Committee Member

Signature was redacted for privacy.

Major Professor

Signature was redacted for privacy.

For the Major Program

Signature was redacted for privacy.

For the Graduate College

TABLE OF CONTENTS

LIST OF TABLES

LIST OF FIGURES

1 INTRODUCTION

Historical Background

Deep Inelastic Scattering (DIS) of leptons and nucleons has been used for decades to probe the parton structure inside nucleons. The results are tremendous. It has improved enormously our knowledge on the parton structure inside nucleon and understanding of the underlying interaction among theses partons. It has led to the discovery of quarks [1], and confirmation of scaling violation in structure functions [2], which itself is a direct evidence of the dynamics in Quantum Chromodynamics (QCD) theory. In the last decade, attention has been turning to the spin structure of nucleons.

The first polarized lepton-proton DIS experiment was conducted by the E80 and E130 Collaborations at SLAC [3]. Their results were in agreement with the predictions of Bjorken [4] and Ellis-Jaffe [5] sum rules. However, the big story came from the subsequent experiments carried out by the European Muon Collaboration (EMC) at CERN in 1987 [6]. With much higher luminosity and larger kinematic range, they found the data were inconsistent with the Ellis-Jaffe sum rule. The implication was that quarks inside proton carry only a very small fraction of the total proton spin. This surprising conclusion has caused great excitement in both experimental and theoretical communities. New experiments were designed to have even larger kinematic range and lower systematic and statistic errors, so that more accurate data could be obtained. Also, neutron and deuteron experiments were proposed to test the more fundamental Bjorken sum rule. On the theoretical side, it has simulated numerous studies on the

contribution from polarized sea quarks, polarized gluon, and even orbital momenta of quarks and gluons to the total spin of nucleons.

Such a big reaction of the community is the result of the obvious contradiction to the success of Quark Model [7], which has correctly explained the magnetic moments of proton and neutron. In simplistic Quark Model, proton consists of only u and d quarks; and since proton is the lowest energy state of the octet, the total orbital angular momentum of these constituent quarks is zero. That is, the wave function of the polarized proton is,

$$|p(\uparrow)\rangle = \frac{1}{\sqrt{6}}\Big[2\,|u(\uparrow)\rangle\,|u(\uparrow)\rangle\,|d(\downarrow)\rangle - |u(\uparrow)\rangle\,|u(\downarrow)\rangle\,|d(\uparrow)\rangle - |u(\downarrow)\rangle\,|u(\uparrow)\rangle\,|d(\uparrow)\rangle\Big]\,. \tag{1.1}$$

Clearly, quarks carry all the spin of the proton. Nevertheless, it is only a very simple model that, for instance, includes no contribution from sea quarks.

Experimentally, due to the confinement nature of the strong interaction, it is impossible to directly measure the angular momentum and polarization of individual constituent quarks. Instead, it is the asymmetry $A_{\parallel} = (d\sigma(\uparrow\downarrow) - d\sigma(\uparrow\uparrow))/(d\sigma(\uparrow\downarrow) + d\sigma(\uparrow\uparrow))$ being measured. From asymmetry $A_{\parallel}$, the structures function g_1 can be extracted. In Quark Model, proton structure function g_1^p is given by,

$$g_1^p(x,Q^2) = \frac{1}{2}\sum_q e_q^2\left[\Delta q(x,Q^2) + \Delta\bar{q}(x,Q^2)\right]\,, \tag{1.2}$$

where $\Delta q(x,Q^2) = \frac{1}{2}[q_\uparrow(x,Q^2) - q_\downarrow(x,Q^2)]$ is the polarized quark distribution inside proton. By decomposing the first moment of matrix element of g_1^p into different SU(3) singlet and octet pieces, the first moment of the proton structure function g_1^p is,

$$\begin{aligned}\Gamma_1^p(Q^2) &= \int_0^1 dx\, g_1^p(x,Q^2) \\ &= \frac{1}{18}(3F + D + 2\,\Sigma(Q^2))\,.\end{aligned} \tag{1.3}$$

It is the well-known Ellis-Jaffe sum rule [5]. In above, F and D are the axial charges in hyperon and neutron β-decay. The last term $\Sigma(Q^2) = \Delta u(Q^2) + \Delta d(Q^2) + \Delta s(Q^2)$ is

the total fraction of spin carried by the quarks in a proton. In the original work of Ellis and Jaffe, they assumed zero strange contribution that corresponds to $\Sigma = 3F - D$. Using $F = 0.459 \pm 0.008$ and $D = 0.798 \pm 0.008$ [8], it is found that $\Sigma = 0.597 \pm 0.032$. However, the EMC result was, $\Gamma_1^p = 0.116 \pm 0.012 \pm 0.026$. That implies,

$$\Sigma \approx 0\,. \tag{1.4}$$

Thus the so-called "Spin Crisis" was born and propelled the urgency to understand spin structure inside nucleons.

Since then, a flurry of studies have been published on the subject. Different theoretical explanations have been proposed, including the effect of a polarized sea and the contribution from polarized gluon. Among them, the most obvious choice is to add a negative contribution from the polarized sea quarks. However, due to the positivity limit of the polarized parton distributions, i.e. $|\Delta q/q| \leq 1$, negative polarized sea can only help a little. Recent calculation shows $\Delta s = -0.12 \pm 0.04$, i.e. $\Sigma = 0.2 \pm 0.1$ [9]. It indicates that the total spin carried by the light quarks, in fact, makes up only a small fraction of the total nucleon spin.

Even before the EMC data, it has been known that the intrinsic spin of quarks cannot account for all the nucleon spin [10]. In fact, the naive Quark Model predicts the weak axial charge $|g_A/g_V| = 5/3$ [11, 12], while the current experimental value is 1.2601 ± 0.0025 [13]. In order to fit the experimental result, it is necessary to include both the spin and orbital angular momentum in a relativistic model. Thus it has long been expected by some researchers that the true spin structure of nucleons is much more complicated than the naive low-energy Quark Model.

The general consensus now is that there is no magic bullet to "solve" the "Spin Crisis" because in QCD the total quark spin Σ is not longer a well-defined scale invariant quantity. It is often to consider the total spin of nucleon as,

$$\frac{1}{2} = \frac{1}{2}\Sigma + L_q + \Delta G + L_g, \tag{1.5}$$

where L_q and L_g are the orbital angular momenta of quarks and gluon respectively, and ΔG is the contribution from polarized gluon spin. It is important to note that such decomposition is artificial and scale-dependent. In term of Operator Product Expansion (OPE), the operators corresponding to the four terms are mixed. That is, contribution from one term may move to the other when energy scale changes. In a simpler evolution picture, as Q^2 increases, the observer can "see" more details inside a "quark" or "gluon", which has included radiation of both quarks and gluons; therefore the previously labeled total spin carried by quarks Σ may have included, say, some gluon spin ΔG into it. Furthermore, this artificial decomposition is neither gauge invariant nor renormalization/factorization scheme independent. In this sense, the so-called total intrinsic spin carried by quarks is ill-defined and meaningless.

Despite the mixing of operator in the decomposition, a recent study by Ji, Tang and Hoodbhoy [14] finds that the anomalous dimension of these operators has a zero eigenvalue. That is, in a very high Q^2 limit, the ratio of the quark and gluon spin contribution is a constant, namely,

$$\lim_{Q^2\to\infty} \frac{1}{2}\Sigma + L_q = \frac{1}{2}\frac{3N_f}{16+3N_f}, \tag{1.6}$$

$$\lim_{Q^2\to\infty} \Delta G + L_g = \frac{1}{2}\frac{16}{16+3N_f}, \tag{1.7}$$

where N_f is the number of flavors of quarks involved. This result is similar to the well-known momentum sum rule in unpolarized case. However, it is still uncertain how to use this asymptotic result in lower energy situation.

On the other hand, Bjorken sum rule is more fundamental as it is a rigorous prediction of QCD based on current algebra. It states that,

$$\Gamma_1^p - \Gamma_1^n = \frac{1}{6}\left|\frac{g_A}{g_V}\right| \Delta\bar{C}_q, \tag{1.8}$$

where $\Delta\bar{C}_q$ is the first moment of the non-singlet quark coefficient function. In leading

order, $\Delta\bar{C}_q^{(0)} = 1$. The experimental value measured from polarized DIS by SMC [15] is,

$$\Gamma_1^p - \Gamma_1^n = 0.199 \pm 0.025 \qquad (Q_0^2 = 5\,\mathrm{GeV}^2)\,, \tag{1.9}$$

while the corresponding theoretical value, including up to $O(\alpha_s^3)$ perturbative QCD radiative correction, is given by,

$$\Gamma_1^p - \Gamma_1^n = 0.181 \pm 0.003 \qquad (Q_0^2 = 5\,\mathrm{GeV}^2)\,. \tag{1.10}$$

Clearly, the two values are in agreement with each other. Figure 1.1 summarizes the current experimental results and theoretical predictions for Bjorken and Ellis-Jaffe sum rules.

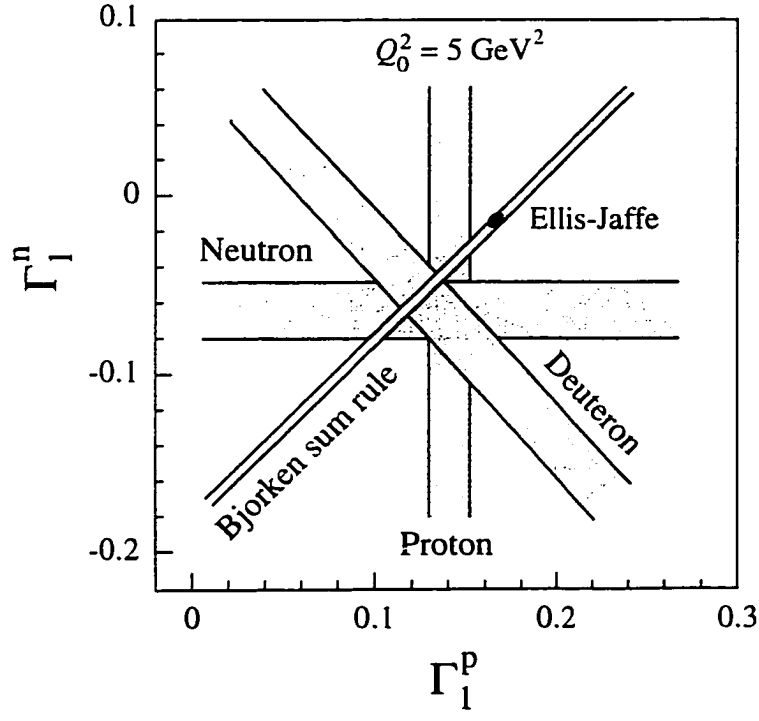

Figure 1.1 Comparison of combined experimental data of Γ_1^p, Γ_1^n, and Γ_1^d with theoretical predictions for the Bjorken and Ellis-Jaffe sum rules. The prediction of Ellis-Jaffe sum rule is represented by the black dot. This figure is obtained from Ref. [15].

Although, the "Spin Crisis" no longer exists, there are still numerous unanswered questions about spin structure of nucleons. In particular, despite the high quality data [9, 16, 17] collected in the past few years, the exact contributions of sea and gluon polarization are still unknown. Even the sign of the gluon polarization is subjected to debate. To resolves these remaining issues, many experiments have been proposed. To name a few: HERMES experiments is currently running at DESY [16]; COMPASS at CERN, HERA at DESY and RHIC at Brookhaven are being planned and will soon be on-line.

To understand nucleon spin, experimental data alone are not enough, we also need theories. In fact, theorists are working very hard to obtain better theoretical models and predictions [18, 19, 20, 21]. In order to construct more accurate models, it is necessary to have a good working set of polarized parton distributions. However, due to its *non-local* nature, the definition of polarized parton distribution is ambiguous. In addition to the renormalization/factorization scheme dependence, which is well-studied in the case of unpolarized distributions, polarized parton distributions have extra ambiguities that come from the definition of γ_5 in d-dimension and the question of where to include the anomalous contribution.

In this work, various theoretical ambiguities in extracting polarized parton distributions are being explored. Using the language of QCD factorization theorem [22, 23, 24], we pin point the sources of these ambiguities, and present a systematic method to handle them.

QCD Factorization and Parton Distributions

Extraction of structure functions from polarized DIS cross-sections has very little to do with QCD. In fact, structure functions can be thought of as physically measurable quantities like cross-sections. On the other hand, parton distributions are some theoret-

ical objects defined as matrix elements of non-local operators of parton fields in QCD, and are not direct measurables in experiments. It is the QCD factorization theorem that links these parton distributions to the measurable structure functions (or cross-sections). For example, nucleon's structure function g_1, measured in a polarized DIS experiment, can be expressed in terms of non-perturbative parton distributions,

$$g_1^h(x,Q^2) = \sum_a \Delta C_a(x,Q^2/\mu_f^2) \otimes \Delta\phi_{a/h}(x,\mu_f^2) + O\left(\frac{1}{RQ}\right) , \tag{1.11}$$

where $\sum_a$ runs over all parton flavor, and $\Delta\phi_{a/h}(x,\mu^2)$ represents polarized parton distribution of flavor a within a hadron h, and μ_f is the factorization scale. This factorization of structure function g_1^h into two different parts is shown in Figure 1.2. The last term $O(1/RQ)$, where R is the hadron radius, corresponds to all power-suppressed terms. The convolution, $\otimes$, for two functions, $A(x)$ and $B(x)$, is defined as,

$$A(x) \otimes B(x) \equiv \int_x^1 \frac{dx'}{x'} A(x')\, B(\frac{x}{x'}) . \tag{1.12}$$

In terms of quark fields, polarized quark distribution of flavor q is defined as a matrix element of a non-local twist-2 operator (see also Eq. (3.6)),

$$\Delta\phi_{q/h}(x,\mu_f^2) = \int \frac{dy^-}{4\pi} e^{ixp^+y^-} \langle h(p,s)|\bar{\psi}_q(y^-)\,\gamma^+\gamma_5\,\psi_q(0)|h(p,s)\rangle , \tag{1.13}$$

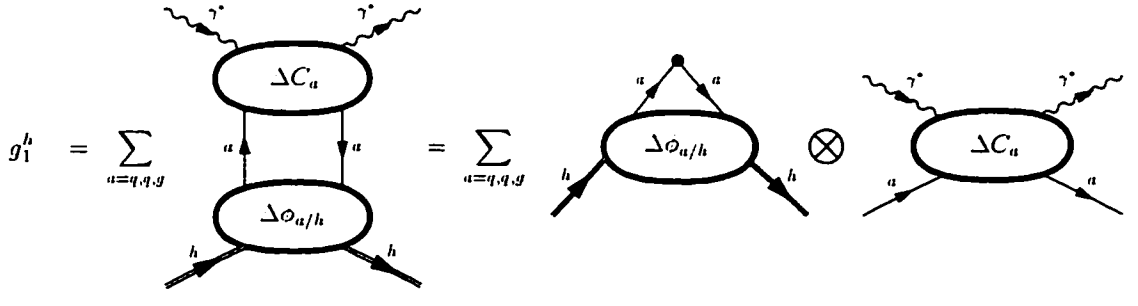

Figure 1.2 Factorization of structure function g_1^h.

where p and s are hadron's momentum and spin, respectively, and s is parallel to p. The definition of polarized quark distribution given in Eq. (1.13) is in light-cone gauge so that the path-ordered phase between $\bar{\psi}_q$ and ψ_q is reduced to 1. Similar definitions for antiquark and gluon have been introduced in Ref. [25]. These polarized parton distributions in a hadron, $\Delta\phi_{a/h}$, are non-perturbative in nature, and thus cannot be calculated in QCD perturbation theory. In Eq. (1.11), all power-suppressed terms are grouped into $O(1/RQ)$. These power-suppressed terms are normally proportional to matrix elements of higher twist operators, which are once again non-perturbative in general.

In principle, there are infinite number of terms on the right hand side of Eq. (1.11), and such decomposition does not have much predicting power. However, at high energy, i.e. energy exchange $Q \gg 1/R$, all power-suppressed terms can be ignored. Then the physical quantity, $g_1^h(x, Q^2)$, can be expressed in terms of a few unknown polarized parton distributions. Effectively, these parton distributions become measurable once we know the coefficients $\Delta C_a(x)$. Because of this, the extraction of parton distributions from measured structure function, g_1^h, depends on how we calculate these coefficients, $\Delta C_a(x)$.

According to QCD factorization theorem, coefficients $\Delta C_a(x)$ in Eq. (1.11) include only short-distance physics, and free of any mass singularities. In other words, coefficients $\Delta C_a(x)$ are independent of the long-distance details of the hadron state h. It is therefore assumed that $\Delta C_a(x)$ are the same for any long-distance state h, even when the state is a parton of flavor f.

After applying factorization decomposition onto a parton state f, both $g_{1_f}(x)$ and $\Delta\phi_{a/f}(x)$ can be written in terms of Feynman diagrams in perturbative QCD as shown in Figure 1.3. Although Feynman diagrams for $g_{1_f}(x)$ and $\Delta\phi_{a/f}(x)$ may include some long-distance physics, it is the short-distance nature of the coefficient functions $\Delta C_a(x)$ that ensures cancellation of the long-distance behavior between $g_{1_f}(x)$ and $\Delta\phi_{a/f}(x)$.

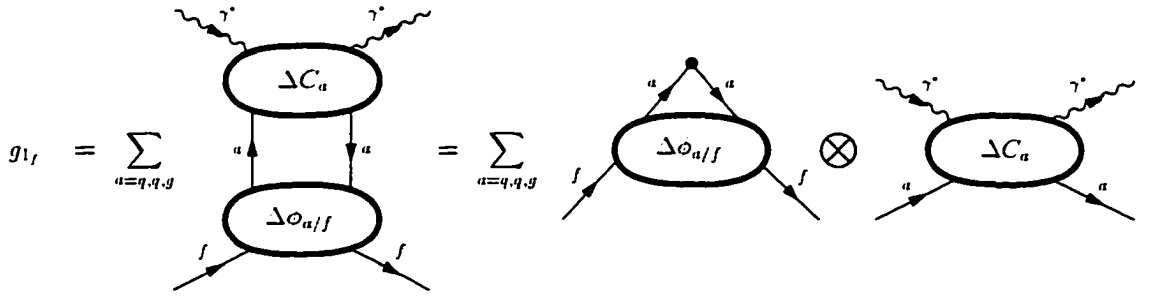

Figure 1.3 Factorization of partonic structure function g_{1_f}.

Such cancellation in turns allows us to extract these coefficient functions $\Delta C_a(x)$ from Eq. (1.11) by calculating $g_{1_f}(x)$ and $\Delta\phi_{a/f}(x)$ order by order in α_s.

In particular, quark coefficient function $\Delta C_q(x)$ can be extracted by replacing h with a quark state in Eq. (1.11). At zeroth order in α_s, $\Delta C_q^{(0)}(x)$ are given by,

$$g_{1_q}^{(0)}(x) = \Delta C_q^{(0)}(x) \otimes \Delta\phi_{q/q}^{(0)}(x) \quad \Rightarrow \quad \Delta C_q^{(0)}(x) = g_{1_q}^{(0)}(x) \ . \tag{1.14}$$

In the last statement, we use Eq. (1.12), Eq. (3.18), and $\Delta\phi_{q/q}^{(0)}(x) = \delta(1-x)$. As shown in Chapter 4, $g_{1_q}^{(0)}(x)$ can be extracted by calculating the tree-level photon-quark DIS Feynman diagram. Similarly, at the order of α_s, we have,

$$g_{1q}^{(1)}(x) = \Delta C_q^{(1)}(x) \otimes \Delta\phi_{q/q}^{(0)}(x) + \Delta C_q^{(0)}(x) \otimes \Delta\phi_{q/q}^{(1)}(x) \ , \tag{1.15}$$

or

$$\Delta C_q^{(1)}(x) = g_{1q}^{(1)}(x) - \Delta C_q^{(0)}(x) \otimes \Delta\phi_{q/q}^{(1)}(x) \ . \tag{1.16}$$

In Eq. (1.16), $\Delta C_q^{(0)}(x)$ is given by Eq. (1.14), and both $g_{1q}^{(1)}(x)$ and $\Delta\phi_{q/q}^{(1)}(x)$ are obtained by calculating the order of α_s Feynman diagrams, as discussed in Chapter 4. Iteratively, Eq. (1.16) can be generalized to all orders of $\Delta C_f^{(n)}(x)$,

$$\Delta C_f^{(n)}(x) = g_{1_f}^{(n)}(x) - \sum_{m=0}^{n-1} \sum_{a=q,\bar{q},g} \Delta C_a^{(m)}(x) \otimes \Delta\phi_{a/f}^{(n-m)}(x) \ , \tag{1.17}$$

for any flavor $f = q, \bar{q}, g$. From the above equation, we conclude that under QCD factorization theorem, once we specify the rules for calculating parton-level structure function $g_{1_f}(x)$ and parton-level parton distribution $\Delta\phi_{a/f}(x)$, all short-distance coefficients $\Delta C_a(x)$ in Eq. (1.11) can be uniquely determined.

However, rules for calculating the parton-level $g_{1_f}(x)$ and $\Delta\phi_{a/f}(x)$ are not unique under factorization theorem — because of the freedom in regularization and renormalization. In terms of Feynman diagrams, both parton-level $g_{1_f}(x)$ and $\Delta\phi_{a/f}(x)$ have following general form,

$$g_{1_f}(x) \ \Big(\text{or } \Delta\phi_{a/f}(x)\Big) = \text{Regularized Feynman diagrams + UV-counterterms .} \tag{1.18}$$

When calculating Feynman diagrams of $g_{1_f}(x)$ and $\Delta\phi_{a/f}(x)$ for massless partons, we have to deal with three types of divergences: Infrared (IR), Collinear (CO) and Ultraviolet (UV). All IR divergences are canceled among the regularized Feynman diagrams, while the UV divergences are removed by UV counterterms. But, because of the massless partons, both $g_{1_f}(x)$ and $\Delta\phi_{a/f}(x)$ have CO divergences. As a result, expressions for $g_{1_f}(x)$ and $\Delta\phi_{a/f}(x)$ depend on collinear regularization (i.e., the choice of collinear regulator). According to QCD factorization theorem, coefficient functions $\Delta C_a(x)$ should include only short-distance physics, and are collinear insensitive. In other words, it should not depend on the choice of CO regulators, even though both $g_{1_f}(x)$ and $\Delta\phi_{a/f}(x)$ do. Such cancellation of collinear regulator dependence can be a powerful tool for checking consistency of any set of rules for calculating the parton-level $g_{1_f}(x)$ and $\Delta\phi_{a/f}(x)$.

Although the divergent parts of UV counterterms are well-determined, ambiguities of their finite pieces remain. Consequently, analytical expressions for $g_{1_f}(x)$ and $\Delta\phi_{a/f}(x)$ also depend on UV renormalization (i.e., the choice of the finite part of the UV counterterms). The UV counterterms for $g_{1_f}(x)$ in Eq. (1.18) is in principle fixed by the renormalized QCD Lagrangian. However, UV counterterms for the $\Delta\phi_{a/f}(x)$ are not

fixed by the same renormalized QCD Lagrangian. Again, it is because $\Delta\phi_{a/f}(x)$ are defined as matrix elements of composite non-local operators, which are not the fundamental terms in the original QCD Lagrangian. In addition, parton distribution within a parton, $\Delta\phi_{a/f}(x)$, is not a direct physical observable. Therefore, UV counterterms cannot be fixed by any physical observable. From Eq. (1.17), different choice of the UV counterterms for $\Delta\phi_{a/f}(x)$ leads to different expressions for the coefficient functions $\Delta C_a(x)$. Since UV counterterms represent short-distance physics, such freedom or ambiguity in renormalization does not contradict QCD factorization theorem. That is, coefficient functions $\Delta C_a(x)$ are still short-distance, even though not unique.

In summary, polarized parton distributions are defined as matrix elements of non-local operators on a polarized hadron state; extraction of these distributions from experimentally measured structure functions or cross-sections depends on theoretically calculated short-distance coefficient functions $\Delta C_a(x)$; ambiguities in polarized parton distributions are results of ambiguities in calculating $\Delta C_a(x)$, which arise from the freedom to renormalize the parton distributions within a parton, $\Delta\phi_{a/f}(x)$.

From Eq. (1.17), it is clear that for every short-distance coefficient function, $\Delta C_a^{(n)}(x)$, the role of the second term on the right hand side is to remove all possible long-distance physics from the partonic process, $g_{1_f}^{(n)}(x)$. This program to remove all collinear sensitive information is a factorization procedure that factorizes the short-distance $\Delta C_a^{(n)}(x)$ out of partonic process $g_{1_f}^{(n)}(x)$. The freedom to renormalize $\Delta\phi_{a/f}^{(n)}(x)$ makes the products of the factorization not unique.

A factorization scheme can be referred to as a systematic choice of UV counterterms that fix the renormalization of parton-level parton distributions, $\Delta\phi_{a/f}^{(n)}(x)$. Well-known factorization schemes include DIS, MS or $\overline{\text{MS}}$ schemes. Since the same renormalized QCD Lagrangian is used for both polarized and unpolarized calculations, naively, one might expect that fixing ambiguities in unpolarized calculation is sufficient to eliminate all ambiguities in polarized calculation. But, since polarized and unpolarized parton dis-

tributions are defined by different non-local operators, there are new types of ambiguities for polarized calculations.

If Dimensional Regularization is being used to regulate both the UV and CO divergences, all parton-level parton distributions, $\Delta\phi_{a/f}(x)$ (or $\phi_{a/f}(x)$ for unpolarized case), in $d = 4 - 2\epsilon$ dimension have following generic form,

$$\begin{aligned}\Delta\phi_{a/f}(x) &= \left[\left(\frac{1}{\epsilon}\right)_{\rm UV} + \left(-\frac{1}{\epsilon}\right)_{\rm CO}\right]\left[1 + \epsilon\,\ln\left(4\pi e^{-\gamma_E}\right)\right]\left[A(x) + \epsilon\,B(x)\right] \\ &+ \text{UV-counterterms}\,, \end{aligned} \tag{1.19}$$

where functions $A(x)$ and $B(x)$ are finite as $\epsilon \to 0$, and γ_E is the Euler constant. In a traditional $\overline{\rm MS}$ scheme, the UV counterterms are defined as,

$$\text{UV-counterterms}\Big|_{\overline{\rm MS}} = -\left(\frac{1}{\epsilon}\right)_{\rm UV}\left[1 + \epsilon\,\ln\left(4\pi e^{-\gamma_E}\right)\right]A(x). \tag{1.20}$$

Obviously, the $\overline{\rm MS}$ UV counterterms remove the UV divergence as well as a phase space constant $\ln(4\pi e^{-\gamma_E})$ in Eq. (1.19). Substituting Eq. (1.20) into Eq. (1.19), we obtain a generic form for the parton-level parton distribution, $\Delta\phi_{a/f}(x)$,

$$\begin{aligned}\Delta\phi_{a/f}(x)\Big|_{\overline{\rm MS}} &= -\left(\frac{1}{\epsilon}\right)_{\rm CO}\left[1 + \epsilon\,\ln\left(4\pi e^{-\gamma_E}\right)\right]\left[A(x) + \epsilon\,B(x)\right] \\ &+ \left[B(x)\right]_{\rm UV}\,. \end{aligned} \tag{1.21}$$

The first line in Eq. (1.21) depends on the collinear regulator, and we refer it as a collinear sensitive term. It should be noted that all collinear sensitive terms must be canceled during the calculation of any short-distance partonic quantities. However, the second line in Eq. (1.21) is actually short-distance in nature as the subscript "UV" indicates. Therefore, Eq. (1.21) shows explicitly that by adopting a traditional $\overline{\rm MS}$ renormalization scheme, the parton-level parton distribution $\Delta\phi_{a/f}(x)$ may carry some short-distance information.

In the case of polarized quark distribution, defined in Eq. (3.6), finite function $B(x)$ in Eq. (1.19) is not fixed in $\overline{\rm MS}$ scheme, due to the presence of γ_5 in its operator definition.

Different choice of γ_5 prescription in d-dimension gives different expression of $B(x)$, which leads to different $\Delta\phi_{q/f}(x)|_{\overline{\rm MS}}$, and eventually different DIS coefficient functions $\Delta C_a(x)$ in Eq. (1.17) [26, 27]. Therefore, in the usual $\overline{\rm MS}$ renormalization/factorization scheme, polarized parton distributions extracted from Eq. (1.11) have an extra ambiguity due to γ_5 in d-dimension, while the physical observable $g_1^h(x,Q^2)$ does not.

Such γ_5 ambiguity first shows up in one-loop polarized quark distribution, $\Delta\phi_{q/f}^{(1)}(x)$ with $f = q, \bar{q}, g$, as demonstrated in the next chapter. According to QCD factorization theorem, this γ_5 ambiguity in $\Delta\phi_{q/f}^{(1)}(x)$ leads to ambiguity in all one-loop perturbatively calculated short-distance partonic quantities, such as coefficient functions for DIS, partonic cross-sections for Drell-Yan, direct photon and all other polarized hadronic processes. To complicate the issue even further, it also affects the two-loop evolution kernel for polarized parton distributions, as well as higher order short-distance partonic parts following Eq. (1.17). Since physically measured structure functions or cross-sections do not depend on the definition of γ_5 in d-dimension, the ambiguities in the calculated short-distance partonic parts must have their counterparts in the extracted polarized parton distributions.

Within the scope of QCD factorization theorem, any choice of UV counterterms that remove all UV divergences is equally acceptable. Different choice of UV counterterms corresponds to different renormalization/factorization scheme. After the removal of UV divergences, all schemes can only differ by a finite term which is short-distance in nature and perturbatively calculable. In the traditional $\overline{\rm MS}$ scheme, the finite function $B(x)$ in Eq. (1.19) in general does not equal to zero. In other words, an extra finite short-distance piece, $B(x)$, is introduced to parton-level parton distributions due to our choice of $\overline{\rm MS}$ scheme. Consequently, partonic quantities such as short-distance coefficient functions, from $\overline{\rm MS}$ parton-level distributions, do not contain all the short-distance dynamics of the corresponding partonic subprocesses. For instance, using the $\overline{\rm MS}$ parton-level parton distributions in DIS, $\Delta C_q^{(1)}(x)$ in Eq. (1.16) will have an extra short-distance subtraction

term, $-C_q^{(0)}(x) \otimes B(x)$, which removes certain short-distance physics from the original partonic process, $g_{1_q}^{(1)}(x)$. Furthermore, owing to its short-distance nature, this finite term $B(x)$ can have γ_5 dependence. So by including this finite piece in parton-level parton distributions $\Delta\phi_{a/f}(x)$, we not only subtract certain short-distance physics but also introduce extra γ_5 prescription ambiguity.

In the next chapter, we propose a new factorization scheme called UV Subtraction (UVS) scheme, which is defined by requiring all parton distributions within a parton include *only* collinear sensitive information. That is, any subtraction term, such as the second term on right hand side of Eq. (1.17), removes only collinear sensitive information from the original partonic subprocesses. Effectively, UVS scheme is defined by choosing the UV counterterms as,

$$\text{UV-counterterms}\Big|_{\text{UVS}} = -\left(\frac{1}{\epsilon}\right)_{\text{UV}} \left[1 + \epsilon \ln\left(4\pi e^{-\gamma_E}\right)\right] \left[\, A(x) + \epsilon\, B(x) \,\right] \ . \tag{1.22}$$

In UVS scheme, by definition, parton-level parton distributions have only collinear sensitive information. As a result, all perturbatively calculable quantities in UVS scheme include all possible short-distance dynamics from the corresponding partonic processes. Moreover, perturbative quantities will not have any dependence on γ_5 prescription because QCD Lagrangian has only vector interactions. Although there could be γ_5 dependence left in parton-level parton distributions if Dimensional Regularization is being used for regulating CO divergence, such γ_5 dependence is collinear sensitive, and therefore, must be canceled in any short-distance perturbative quantities.

In addition to the γ_5 problem, there is the issue of proper handling of the axial anomalous contribution [28, 29, 30], whose first moment is the usual axial anomaly. From Eq. (1.17), it is obvious that ΔC_g depends on how quark distribution within a gluon $\Delta\phi_{q/g}$ is renormalized and its finite part after the renormalization. The first moment of $\Delta\phi_{q/f}$ corresponds to a matrix element of a local operator which is proportional

to the axial vector current. Because of the local nature of axial anomaly, where to include the anomalous contribution becomes an issue when we renormalize $\Delta\phi^{(1)}_{q/g}$ in Eq. (1.17). One can either treat the anomalous contribution as an explicit gluonic contribution, which leads to a non-vanishing $\Delta C^{(1)}_g(x)$ at first moment, or leave it as a part of polarized quark distribution $\Delta\phi_{q/g}$ [30]. No matter where to include the anomalous contribution at first moment, one has to have a consistent treatment for the x-dependent distributions $\Delta\phi^{(1)}_{q/f}(x)$ in calculating coefficient functions in DIS, as well as partonic parts in hadron-hadron collisions. In this work, we extract the explicit x-dependent expression of the anomalous contribution inside parton distribution $\Delta\phi^{(1)}_{q/g}(x)$ by two very different methods. First, we make use of the inconsistent results of CFH γ_5 prescription in the presence of anomaly. Secondly, we formally calculate the chirality violating part of HVBM γ_5 prescription and the corresponding diagrams in Fig. 4.6 for $\Delta\phi^{(1)}_{q/g}(x)$. We find both methods give the same result. Using this result, we obtain the explicit x-dependent expressions for both $\Delta\phi^{(1)}_{q/g}(x)$ and $\Delta\phi^{(1)}_{q/g}(x)\Big|_{\text{no-anomaly}}$ so that one may make use of them consistently for other polarized processes. Moreover, we show that in the new UVS scheme, the anomalous ambiguity, due to its short-distance nature, can be eliminated.

According to QCD factorization theorem, all calculable short-distance quantities can be uniquely derived once we fix (a) renormalization of QCD Lagrangian, such as wave functions, coupling, masses, and etc; and (b) all possible parton-level parton distributions $\Delta\phi^{(n)}_{a/f}(x)$, order by order in α_s. Here, the traditional $\overline{\text{MS}}$ scheme is chosen for the renormalized QCD Lagrangian. For completeness, in the next chapter we first derive the operator definition for all polarized parton distributions; and then calculate the parton-level parton distributions at the leading and next-to-leading orders in both $\overline{\text{MS}}$ scheme and UVS scheme. In addition, we calculate these distributions with different CO regulators to demonstrate the fact that perturbatively calculable quantities are collinear insensitive. We also provide explicit conversion between the results in $\overline{\text{MS}}$ distributions

and those in UVS scheme. Having all parton-level parton distributions at one-loop level, in principle, one can derive next-to-leading order short-distance quantities for all perturbatively calculable processes, such as DIS, Drell-Yan, direct photon, and etc. In Chapter 4, we use polarized DIS as an example to explore possible ambiguities in calculating perturbative coefficient functions, and to study the dependence of different choice of collinear regulators and γ_5 prescriptions. We provide explicit comparison of different perturbative results in both traditional $\overline{\rm MS}$ scheme and the new UVS scheme. In Chapter 5, we discuss the impact of these ambiguities on polarized Drell-Yan. We also explore the difference between the $\overline{\rm MS}$ and UVS schemes for Drell-Yan process. Finally, in Chapter 6, we provide our summaries and conclusions.

2 REGULARIZATION, RENORMALIZATION AND γ_5

In this chapter, we present several key ideas that are crucial for the discussion on ambiguities in polarized parton distributions. In fact, all ambiguities in polarized parton distributions can be traced back to different treatments of regularization, renormalization or γ_5 prescriptions.

Regularization

It is known that when going beyond zeroth order, diagrams in both $g_{1f}^{(1)}$ and $\Delta\phi_{f'/f}^{(1)}$ are divergent, and thus require regularization. Since regularization is only a mathematical procedure to render infinities manageable, all results should have no dependence on the choice of regularization method. Otherwise, the regularization procedure is deemed as inconsistent. In our calculation, there are three types of divergences: Ultraviolet (UV), Infrared (IR) and Collinear (CO). The first two are well-studied and present in almost all Feynman diagrams. For UV divergences, they are removed by renormalization, while IR divergences cancel each other.

In this work, we use Dimensional Regularization (DR) to handle all UV divergences. The basic idea of Dimensional Regularization is to analytically continue the 4-dimensional physical world to an unphysical world of $d = 4 - 2\epsilon$ dimensions. Then all divergences are regulated as poles of $1/\epsilon$. Only after all divergences are being systematically removed, we take $\epsilon \to 0$ and return to the 4-dimensional physical world. It is shown in Figure 2.1 that after dimensional continuation to d-dimension, which is

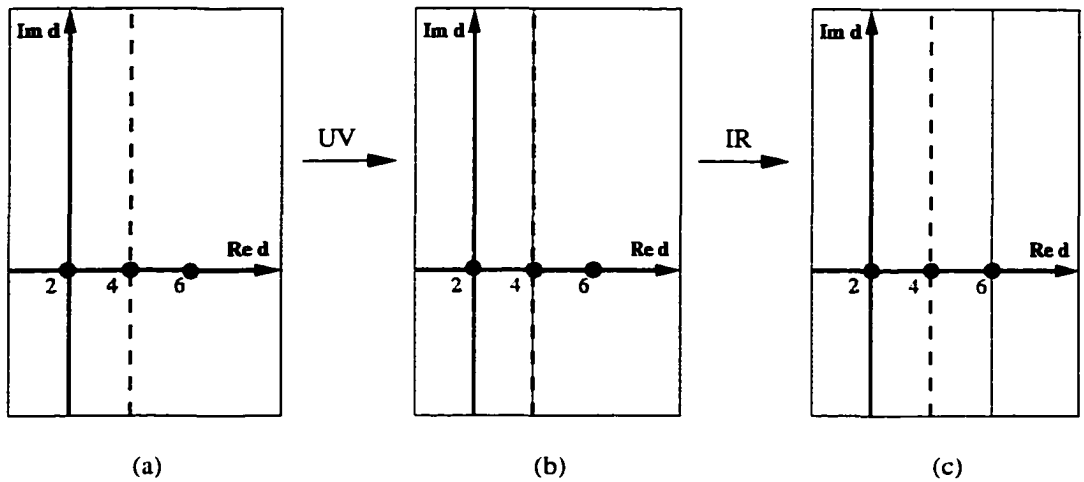

Figure 2.1 Illustration of the removal of both UV and IR divergences in the complex d-dimensional plane.

complex, we should first perform renormalization to get rid of all UV poles and only then add all subgraphs together and allow their IR poles to cancel. In Figure 2.1, shaded area represents divergent region and blank area represents convergent region.

Dimensional Regularization was first applied in statistical physics [31, 32], but later exported to regulate non-abelian gauge theories [33]. Beside its simplicity and ease to use, Dimensional Regularization's main appeal lies in its ability to preserve gauge and Lorentz invariances [33]. And because of this crucial property, it is used to prove renormalizabilty of non-abelian gauge theories [34, 35], such as QCD.

The main concern in QCD factorization is how to treat collinear divergences consistently and ensure their cancellation in all perturbatively calculable short-distance quantities. The nature of collinear divergence can be understood by examining the diagram of $q(p) \to q(p-k) + g(k)$ in Figure 2.2. For a massless quark with momentum p, $p^2 = 0$, the quark propagator of momentum $p-k$, i.e. $i\gamma \cdot (p-k)/(p-k)^2$, has poles at $k = 0$ and $k \parallel p$. The first one is our usual IR pole which will eventually be canceled when we combine all other diagrams. But the last one is different — it remains even after adding all the other subgraphs — and is the result of a collinear gluon that is real

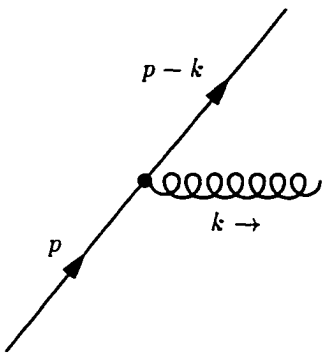

Figure 2.2 Quark splitting to a gluon and another quark, $q \to g + q$.

($k^2 = 0$). Of course, such collinear pole is long-distance in nature and eventually must be removed from all short-distance quantities.

For collinear divergence, we however adopt two different collinear regulators, namely, Dimensional Regularization and off-shell momentum regulator ($p^2 \neq 0$) for checking the consistency of various γ_5 prescriptions. In Dimensional Regularization, as shown earlier, all collinear poles are regulated as $(-1/\epsilon)_{CO}$. While in the case of off-shell momentum regulator, the momentum p of the incoming parton is taken off-shell, in fact, $p^2 < 0$. The resulting collinear divergence will appear as $\ln(-Q^2/p^2)$.

Renormalization

As mentioned, the purpose of renormalization is to consistently remove all UV divergences associated with short-distance quantum fluctuations that cannot be probed or measured in experiments. In theoretical sense, it is a reparameterization of the basic Lagrangian in terms of finite renormalized fields, coupling, and mass etc. In practical sense, it is a procedure allows us to systematically discard all those ubiquitous UV divergences in Feynman diagram calculations by adding necessary UV counterterms.

Any renormalization procedure is therefore by definition ambiguous, as it is always

legitimate to remove some finite pieces in addition to the unwanted UV divergence. This kind of ambiguity is generally referred as the freedom of choosing a renormalization scheme. For instance, in Minimal Subtraction (MS) [36] scheme, the UV counterterms are simply the UV poles of the Feynman diagrams. For physical quantities composed only of fundamental objects, e.g. local operators, of the basic Lagrangian, they have the same renormalization scheme as the basic Lagrangian. One example is the structure function g_1. Once we choose the renormalization scheme for the QCD Lagrangian, that of the structure function g_1 is also fixed. But, this is not true in the case of parton distributions. Because parton distributions are matrix element of non-local operators that are not fundamental in QCD Lagrangian. Consequently, there is an extra ambiguity or freedom to choose renormalization scheme for parton distributions. In our later discussion, this freedom is being exploited to cancel the ambiguity associated with γ_5 prescription in UVS renormalization scheme.

γ_5 in d-Dimension

Since Dimensional Regularization is being used as the UV regulator, it is necessary to have some prescription to manipulate γ_5 in d-dimension. In our calculations, two prescriptions, namely, HVBM (denoted as γ_5) and Modified CFH (denoted as γ_5') are being used. More details of their definitions are presented in the Appendix A. The choice of HVBM prescription is an obvious one because it has been widely used and perhaps is the most popular. For the Modified CFH prescription, it is chosen for its chiral symmetric definition. In fact, CFH prescription is commonly used in symbolic calculations because of this anticommuting feature in d-dimension. As in Dimensional Regularization, all calculations are being analytically continued to d-dimension, γ_5 in d-dimension can only be defined formally by its algebraic properties.

It is known that both d-dimensional prescriptions have the same 4-dimensional be-

haviors, and the differences are of $(d-4)$-dimension only. Since pole behavior is of 4-dimension, the two prescriptions give the same singularities in Dimensional Regularization. In other words, the choice of γ_5 prescription in d-dimension does not affect the renormalizabilty of the theory. Nevertheless, the finite pieces may be different and that can affect the result of factorization.

Nevertheless, due to different treatments of chiral symmetry, the two prescriptions behave very differently when chirality is concerned. Just by looking at the definition of HVBM γ_5, it is certain that HVBM prescription does not respect chiral symmetry; consequently the results obtained by this method may violate chirality as well. Thus, if conservation of chiral symmetry is essential, one should be cautious about applying this prescription. Whereas, the Modified CFH γ_5 is constructed with chiral symmetry in mind, and therefore manifestly conserved chirality. Such benefit is of course not without penalty. To insist a chiral symmetric definition, the cyclicity in spinor trace calculation is being sacrificed. Owing to this special feature, all traces of the diagrams have to start at the same vertex, which is called the *reading point.* Furthermore, it is shown that under certain circumstances CFH γ_5 leads to inconsistent result in calculation that involves QCD factorization [37].

3 POLARIZED PARTON DISTRIBUTION WITHIN A PARTON

Within the framework of QCD factorization, the chief ambiguity in calculating short-distance partonic quantities for hadronic processes comes from the freedom to renormalize the parton-level parton distributions (or parton distributions within a parton). In this chapter, we define the parton-level parton distributions $\Delta\phi_{a/f}(x)$, and discuss how ambiguities arises from renormalization. Furthermore, we present a complete set of leading and next-to-leading order polarized parton-level parton distributions, from which one can readily derive the associated next-to-leading order short-distance quantities for all interesting polarized hadronic processes.

Definition and Normalization

For simplicity, we employ the $n \cdot A(x) = 0$ physical gauge in the following discussion. The $A^\mu(x)$ field here is the usual gluon field, and the vector n^μ will be specified later. First, we rederive the operator definition for all twist-2 polarized parton distributions for completeness.

Consider a general forward scattering process as shown in Figure 3.1(a). In the scattering process, the parton f has momentum p and spin s, which is polarized along the direction of p, and the momentum of the quark q is k. The blob labeled by H_q represents the hard physics at a large energy scale Q. The dashed lines represents interaction between H_q and the other colliding particle. Assuming the momentum p is

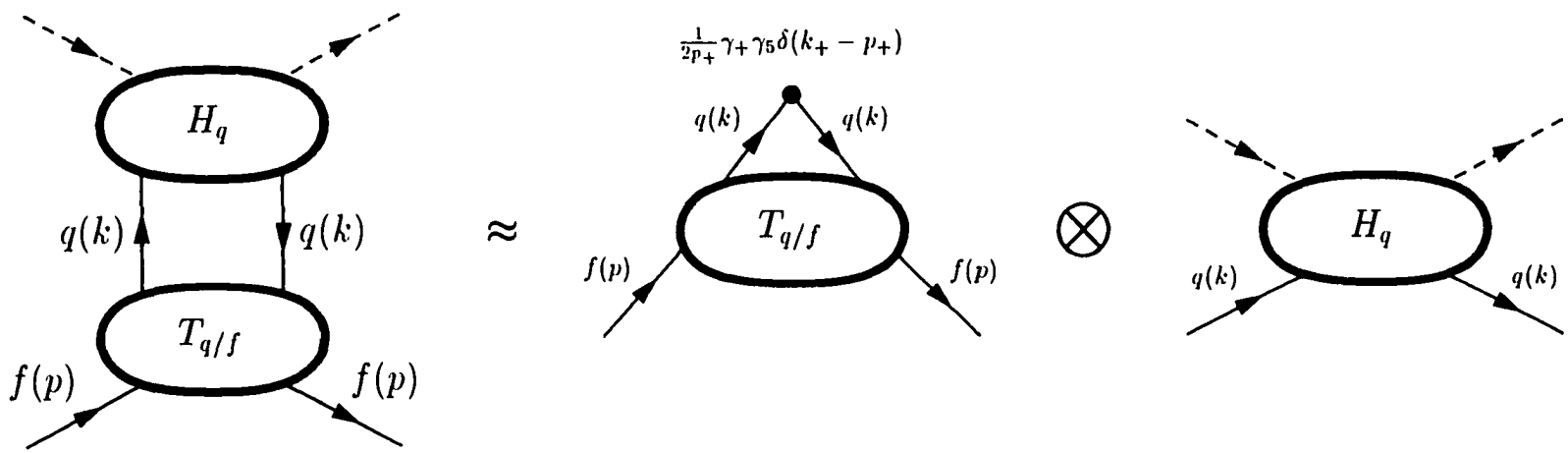

Figure 3.1 (a) Forward scattering of a quark inside parton f. (b) Factorized result in terms of long-distance $T_{q/f}$ and short-distance H_q parts.

in the "+" direction, and the transverse and "−" components of k, i.e. k_T and k_-, are much smaller than the large energy scale Q, we can factorize the general diagram in Figure 3.1(a) into a hard part at energy scale Q convoluted with a quark distribution within parton f as follows,

$$I_{q/f} \equiv \int \frac{d^4k}{(2\pi)^4} \,\mathrm{Tr}\left[\hat{T}_{q/f}(p,s;k)\,\hat{H}_q(k,Q)\right] , \tag{3.1}$$

$$\approx \int dx \,\mathrm{Tr}\left[\hat{T}_{q/f}(p,s;x)\,\hat{H}_q(k=xp,Q)\right] , \tag{3.2}$$

$$\approx \int \frac{dx}{x}\,\Delta\phi_{q/f}(x)\,\Delta H_q(k=xp,Q) . \tag{3.3}$$

In obtaining Eq. (3.2), we use the collinear expansion of $k = xp$ in H_q and drop all terms suppressed by power of $1/Q$. The $\hat{T}_{q/f}(p,s;x)$ in Eq. (3.2) is given by,

$$\hat{T}_{q/f}(p,s;x) = \int \frac{d^4k}{(2\pi)^4}\,\delta\left(x - \frac{k^+}{p^+}\right)\,\hat{T}_{q/f}(p,s;k) . \tag{3.4}$$

To derive Eq. (3.3), we first decouple the quark's spinor trace between $\hat{H}_q$ and $\hat{T}_{q/f}$; then drop all quark mass terms and power corrections (i.e. $1/Q$ or higher); and finally keep only those terms contribute to the polarized cross-sections. By doing so, we arrive at the operator definition for the polarized quark distribution in $n\cdot A = 0$ gauge,

$$\Delta\phi_{q/f}(x) \equiv \int \frac{d^4k}{(2\pi)^4}\,\mathrm{Tr}\left[\frac{1}{2p^+}\,\gamma^+\gamma_5\,\hat{T}_{q/f}(p,s;k)\right]\,\delta\left(x-\frac{k^+}{p^+}\right) , \tag{3.5}$$

$$= \int \frac{dy^-}{4\pi}\,\mathrm{e}^{-ixp^+y^-}\,\langle f(p,s)|\bar{\psi}_q(y^-)\,\gamma^+\gamma_5\,\psi_q(0)|f(p,s)\rangle , \tag{3.6}$$

and the corresponding hard part at scale Q is ,

$$\Delta H_q(k=xp,Q) \equiv \mathrm{Tr}\left[\frac{1}{2}\,\gamma_5\,\gamma\cdot(xp)\,\hat{H}_q(k=xp,Q)\right] . \tag{3.7}$$

Eq. (3.6) is the familiar polarized quark distribution in $n\cdot A = 0$ gauge. In general, a path-ordered integral,

$$P\,\exp\left[-ig\int_0^{y^-} dy'^-\,\mathrm{A}_a^+(0,y'^-,0_\perp)\,t_a\right] , \tag{3.8}$$

where t_a is the generator of the color SU(3), should be added between the two quark field operators in Eq. (3.6) [25]. But by choosing $n \cdot A = 0$, the above path-ordered integral is reduced to 1. Eq. (3.3) can be graphically represented by the convolution shown in Figure 3.1(b), and the convolution $\otimes$ is defined in Eq. (1.12). In terms of the cut-vertex concept introduced in Ref. [38], the operator $(1/2p^+)\gamma^+\gamma_5\delta(x - k^+/p^+)$ in Eq. (3.5) can be identified as the cut-vertex that defines polarized quark distribution. Note that a cut-vertex is very different from a normal vertex in usual Feynman diagram because it is non-local — it links two fields at different positions, see Eq. (3.6).

Similarly, we derive the operator definition of polarized gluon distribution within a parton of flavor f by considering the general forward scattering diagram shown Figure 3.2(a). With the same approximation used to obtain Eq. (3.3), we have,

$$I_{g/f} \equiv \int \frac{d^4k}{(2\pi)^4} \left[T^{\mu\nu}_{g/f}(p,s;k)\, H_{g_{\mu\nu}}(k,Q)\right] \tag{3.9}$$

$$\approx \int dx \left[T^{\mu\nu}_{g/f}(p,s;x)\, H_{g_{\mu\nu}}(k=xp,Q)\right] \tag{3.10}$$

$$\approx \int \frac{dx}{x}\, \Delta\phi_{g/f}(x)\, \Delta H_g(k=xp,Q)\,. \tag{3.11}$$

As before, in deriving Eq. (3.10) from Eq. (3.9), we use the collinear expansion of $k = xp$ in $H_{g_{\mu\nu}}$, and drop all terms suppressed by power of $1/Q$. The $T^{\mu\nu}_{g/f}(p,s;x)$ in Eq. (3.10) is given by,

$$T^{\mu\nu}_{g/f}(p,s;x) = \int \frac{d^4k}{(2\pi)^4}\, \delta\left(x - \frac{k^+}{p^+}\right)\, T^{\mu\nu}_{g/f}(p,s;k)\,. \tag{3.12}$$

From Eq. (3.10) to Eq. (3.11), we decouple the gluon's Lorentz indices μ and ν between H_g and $T_{g/f}$. In light-cone gauge, after dropping all power corrections, the only surviving terms are those with transversely polarized μ and ν. Since we are interested only in polarized cross-sections, only those terms antisymmetric in μ and ν contribute. After decoupling the Lorentz indices, the operator definition of polarized gluon distribution in

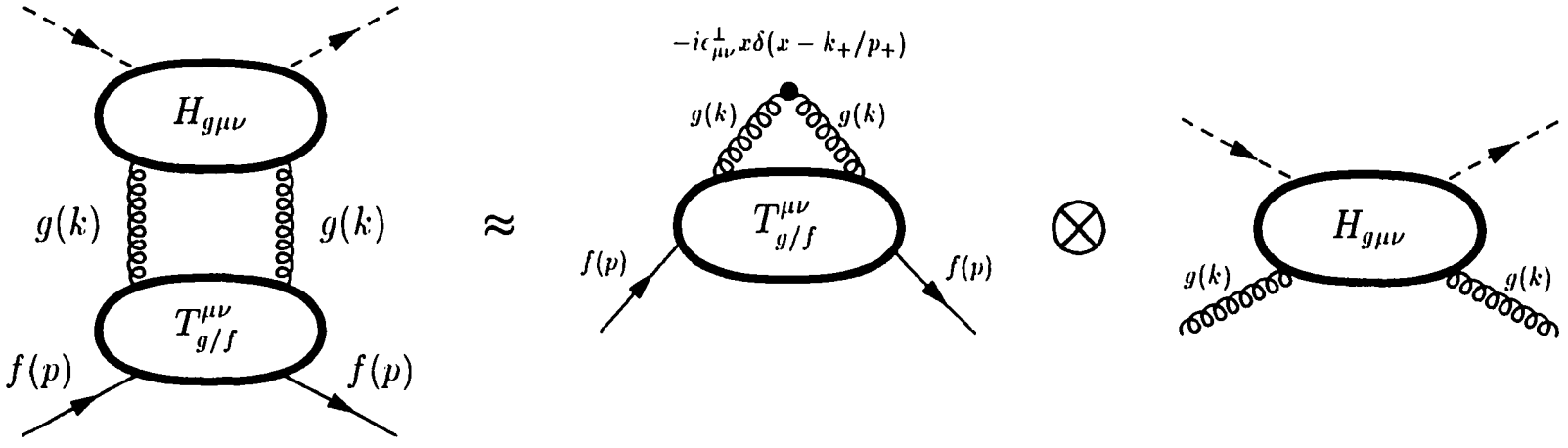

Figure 3.2 (a) Forward scattering of a quark inside parton f. (b) Factorized result in terms of long-distance $T_{q/f}$ and short-distance H_q parts.

$n \cdot A = 0$ gauge is,

$$\Delta\phi_{g/f}(x) \equiv \int \frac{d^4k}{(2\pi)^4} \left[\left(-i\epsilon_{\mu\nu}^{\perp}\right) T_{g/f}^{\mu\nu}(p,s;k)\right] x\,\delta\left(x - \frac{k^+}{p^+}\right) \tag{3.13}$$

$$= \frac{1}{xp^+} \int \frac{dy^-}{4\pi} e^{-ixp^+y^-} \left(-i\epsilon_{\mu\nu}^{\perp}\right) \langle f(p,s)|F^{+\mu}(y^-)\,F^{+\nu}(0)|f(p,s)\rangle, \tag{3.14}$$

and the corresponding hard part at scale Q is,

$$\Delta H_g(k = xp, Q) \equiv \frac{i}{2}\,\epsilon_{\perp}^{\mu\nu}\,H_{g_{\mu\nu}}(k = xp, Q)\ . \tag{3.15}$$

Like Figure 3.1(b), Eq. (3.11) can be graphically represented by the convolution shown in Figure 3.2(b).

In Eq. (3) and Eq. (3.15), the antisymmetric tensor is defined as,

$$\epsilon_{\mu\nu}^{\perp} = \epsilon_{\alpha\beta\mu\nu}\,n^{\alpha}\,\bar{n}^{\beta} = \epsilon_{03\mu\nu}\ , \tag{3.16}$$

with $n^{\alpha} = \delta^{\alpha-}$, $\bar{n}^{\beta} = \delta^{\beta+}$. The totally antisymmetric tensor $\epsilon_{\alpha\beta\mu\nu}$ is normalized as $\epsilon_{0123} = 1$. Note that the totally antisymmetric tensor $\epsilon_{\alpha\beta\mu\nu}$ is defined only in 4-dimension.

Eq. (3.14) is our definition of polarized gluon distribution in $n \cdot A = 0$ gauge. As mentioned earlier, in general a path-ordered integral should be added to above definition. Our definitions for polarized quark and gluon distributions, given in Eq. (3.6) and Eq. (3.14), are very similar to those of the unpolarized quark and gluon distributions introduced in Ref. [25]. The only difference is that polarized quark distribution has an extra γ_5, while in the case of gluon distribution the unpolarized "$-g_{\mu\nu}$" operator in Ref. [25] is replaced by the polarized "$-i\epsilon_{\mu\nu}^{\perp}$" operator. Again, using the concept of cut-vertex, operator "$(-i\epsilon_{\mu\nu}^{\perp})\,x\delta(x - k^+/p^+)$" is identified as the cut-vertex that defines polarized gluon distribution. The definitions given here is only for $n \cdot A$ gauge. A more general gauge invariant formulation is given in Appendix B.

At parton-level, polarized quark and gluon distributions within a parton of flavor f, defined in Eq. (3.6) and Eq. (3.14), can be expressed in terms of Feynman diagrams

order by order in the power of α_s. For a parton distribution of flavor $a = q, \bar{q}, g$, we define,

$$\Delta\phi_{a/f}(x) \equiv \sum_{n=0} \left(\frac{\alpha_s}{2\pi}\right)^n \Delta\phi^{(n)}_{a/f}(x)\,. \tag{3.17}$$

At the zeroth order in α_s, the parton-level distributions are given by,

$$\begin{aligned}
\Delta\phi^{(0)}_{q/q'}(x) &= \delta_{qq'}\,\mathrm{Tr}\left[\left(\frac{1}{2p^+}\gamma^+\gamma_5\right)\left(\frac{1}{2}\gamma_5\gamma\cdot p\right)\right]\delta(x-1) \\
&= \delta_{qq'}\,\delta(x-1)\,, && (3.18)\\
\Delta\phi^{(0)}_{q/g}(x) &= 0\,, && (3.19)\\
\Delta\phi^{(0)}_{g/q}(x) &= 0\,, && (3.20)\\
\Delta\phi^{(0)}_{g/g}(x) &= \left(-i\epsilon^{\perp}_{\mu\nu}\right)\left(\frac{i}{2}\epsilon^{\mu\nu}_{\perp}\right)x\delta(x-1) \\
&= \delta(x-1)\,. && (3.21)
\end{aligned}$$

Eq. (3.18) and Eq. (3.21) are derived by calculating the lowest order diagrams shown in Figure 3.3.

Beyond zeroth order, Feynman diagrams for parton-level parton distributions have IR, CO and UV divergences. In following sections, we calculate one-loop polarized

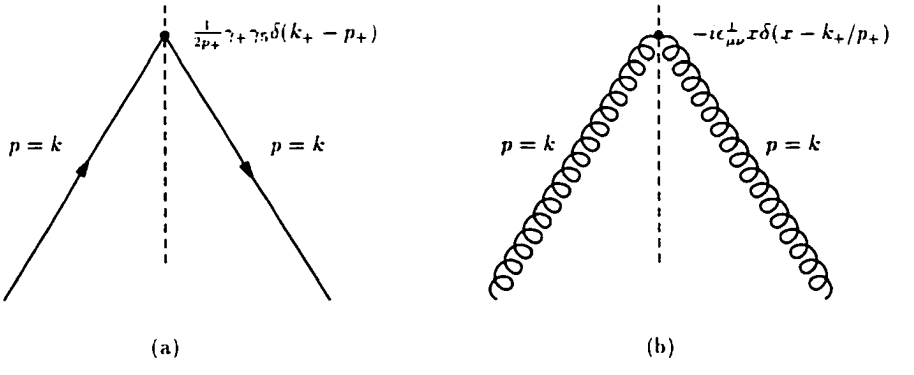

Figure 3.3 (a) Cut-vertex diagram for the leading order quark distribution inside a quark. (b) Cut-vertex diagram for the leading order gluon distribution inside a gluon.

parton-level distributions, discuss the role of the regularization, and explore the ambiguities arising from renormalization.

Dimensional Regularization, HVBM γ_5 Prescription, and $\overline{\rm MS}$ Scheme

In this section, we present the order of α_s polarized parton-level parton distributions. Dimensional regularization (DR) is used for both UV and CO divergences. For γ_5 in d-dimension, we use the HVBM prescription, which was first proposed by 't Hooft and Veltman [33], and later systematized by Breitenlohner and Maison [39]. In order to distinguish the HVBM γ_5 prescription from that of CFH, we adopt the notation that $\gamma_5 \equiv \gamma_5(\text{HVBM})$ and $\gamma_5' \equiv \gamma_5(\text{CFH})$. For more details, please refer to the Appendix A. Also the traditional $\overline{\rm MS}$ renormalization/factorization scheme is used to remove the UV divergences of the one-loop distributions.

Quark distribution within a quark

Applying our operator definition of quark distribution in Eq. (3.6) onto a quark state of flavor q', the first order quark distribution, $\Delta\phi^{(1)}_{q/q'}(x)$, can be obtained by calculating the Feynman diagrams shown in Figure 3.4 in axial gauge or Feynman diagrams shown in Figure 3.5 in a covariant gauge. The double dashed lines in Figure 3.5 are eikonal lines defined in Ref. [25] or Appendix B. Using Dimensional Regularization in $d = 4-2\epsilon$ dimensions to treat all UV and CO divergences and HVBM γ_5 prescription, we obtain (see Appendix B for details),

$$\begin{aligned}\Delta\phi^{(1)}_{q/q'}\Big|_{\gamma_5,\text{DR}} &= \delta_{qq'}\left(\frac{\mu^2}{\mu_f^2}\right)^{\epsilon}\left[\left(\frac{1}{\epsilon}\right)_{\text{UV}}+\left(-\frac{1}{\epsilon}\right)_{\text{CO}}\right]\left[1+\epsilon\,\ln\left(4\pi e^{-\gamma_E}\right)\right]\\ &\quad\times\left[\Delta P^{(1)}_{qq}(x)\,+\,\epsilon\,3\,C_F\,(1-x)\right]\\ &\quad+\text{UV-counterterms}\Big|_{q/q'}\,,\end{aligned}\tag{3.22}$$

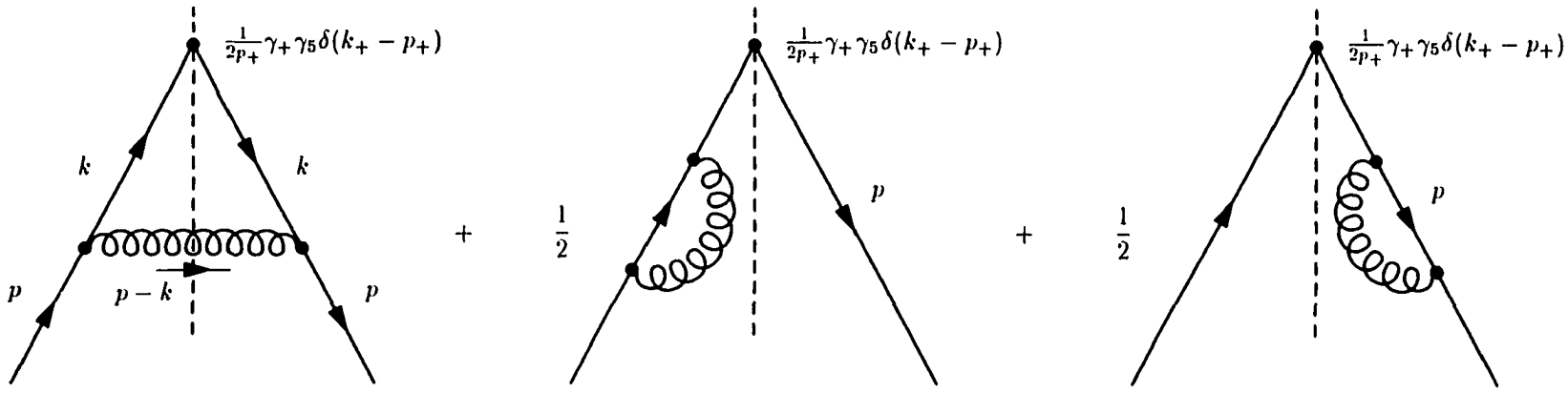

Figure 3.4 Next-to-leading order cut-vertex diagrams for quark distribution inside a quark.

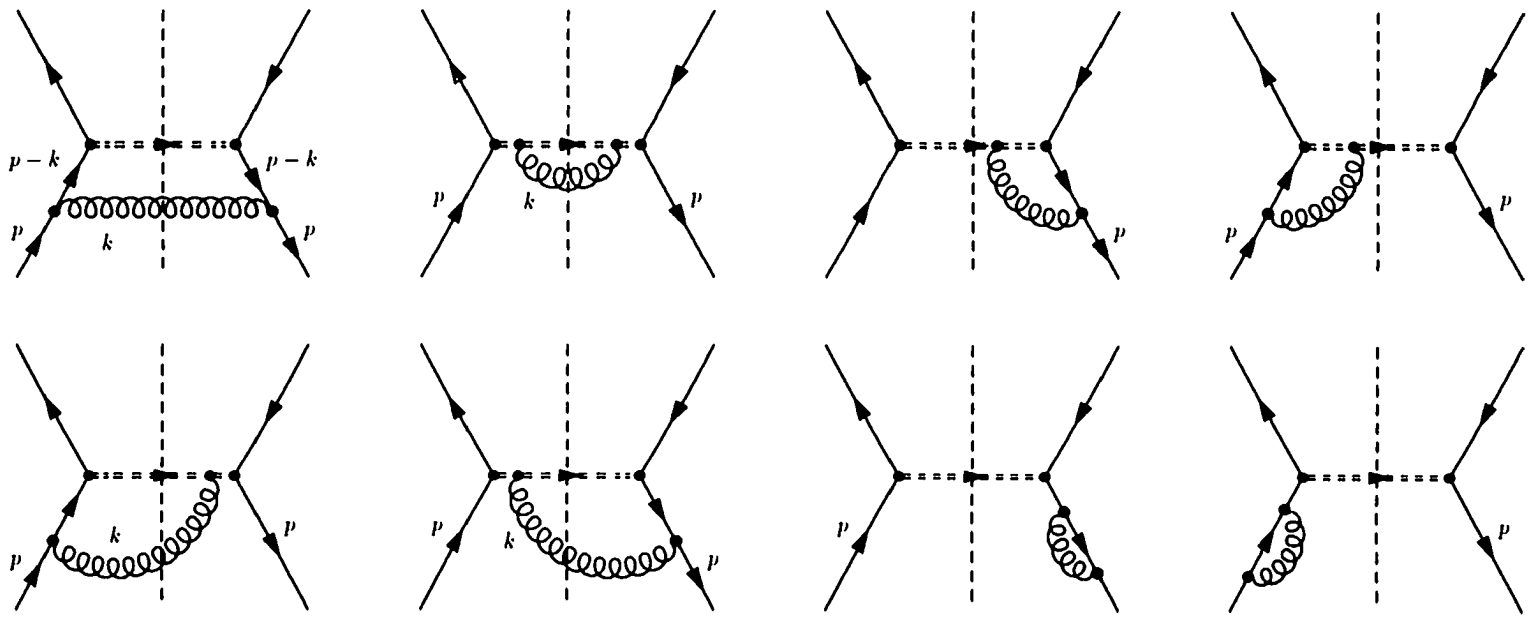

Figure 3.5 Gauge invariant Feynman diagrams of the $O(\alpha_s)$ quark distribution inside a quark.

where μ is the renormalization scale that comes from dimensional continuation $g \to g\mu^{\epsilon}$. μ_f is the factorization scale (see Appendix B), and $C_F = 4/3$ is a color factor for SU(3) color. In Eq. (3.22), $\Delta P_{qq}^{(1)}(x)$ is the well-known quark-to-quark splitting function,

$$\Delta P_{qq}^{(1)}(x) = C_F \left[\frac{1+x^2}{(1-x)_+} + \frac{3}{2}\delta(1-x) \right] . \tag{3.23}$$

The subscript "+" denotes the "+" distribution treatment of the divergence in $1/(1-x)$ as $x \to 1$. It is defined in such a way that for any function $f(x)$ smooth at $x = 1$, we have,

$$\int_0^1 dx \, \frac{f(x)}{(1-x)_+} \equiv \int_0^1 dx \, \frac{f(x) - f(1)}{(1-x)} . \tag{3.24}$$

In traditional $\overline{\rm MS}$ scheme, the UV counterterms are chosen to be the UV pole with a phase factor,

$$\text{UV-counterterms}\Big|_{q/q',\overline{\rm MS},\gamma_5} = -\delta_{qq'} \left(\frac{\mu^2}{\mu_f^2}\right)^{\epsilon} \left(\frac{1}{\epsilon}\right)_{\rm UV} \left[1 + \epsilon \, \ln\left(4\pi e^{-\gamma_E}\right)\right] \left[\Delta P_{qq}^{(1)}(x)\right] . \tag{3.25}$$

Using the given UV counterterms, the corresponding first order polarized quark distribution within a quark is,

$$\begin{aligned} \Delta\phi_{q/q'}^{(1)}\Big|_{\overline{\rm MS},\gamma_5,{\rm DR}} = \delta_{qq'} \left(\frac{\mu^2}{\mu_f^2}\right)^{\epsilon} \Bigg\{ & \left(-\frac{1}{\epsilon}\right)_{\rm CO} \Delta P_{qq}^{(1)}(x) \\ & - \left[\Delta P_{qq}^{(1)}(x) \, \ln\left(4\pi e^{-\gamma_E}\right) + 3\, C_F\, (1-x)\right]_{\rm CO} \\ & + 3\, C_F\, (1-x)_{\rm UV} \Bigg\} . \end{aligned} \tag{3.26}$$

In the above equation, the finite piece, $-[\Delta P_{qq}^{(1)}(x) \ln(4\pi e^{-\gamma_E}) + 3C_F(1-x)]_{\rm CO}$ arises from our choice of collinear regulator; whereas the remaining piece $3C_F(1-x)_{\rm UV}$ is a left-over from $\overline{\rm MS}$ renormalization. Although $-3C_F(1-x)_{\rm CO}$ and $3C_F(1-x)_{\rm UV}$ cancel each other numerically, the subscripts CO and UV indicate the different origins of these two finite terms. Such explicit separation of finite pieces based on CO and UV origins is very important for our later discussions.

Quark distribution within a gluon

In the case of quark distribution within a gluon $\Delta\phi^{(1)}_{q/g}(x)$, it can also be expressed by either cut-vertex type of Feynman diagrams shown in Figure 3.6(a) or those of covariant type in Figure 3.6(b). However, $\Delta\phi^{(1)}_{q/g}(x)$ is special in the sense that the two sets of diagrams are identical. That is, they effectively have the same Feynman rules. The reason is that all diagrams in Figure 3.6(a) with gluon attached to the eikonal line are zero. This is, of course, must be true because there is no internal gluon in $\Delta\phi^{(1)}_{q/g}(x)$, i.e. $\Delta\phi^{(1)}_{q/g}(x)$ is manifestly gauge invariant. The result obtained is ,

$$\begin{aligned}\Delta\phi^{(1)}_{q/g}\Big|_{\gamma_5,\mathrm{DR}} &= \left(\frac{\mu^2}{\mu_f^2}\right)^{\epsilon}\left[\left(\frac{1}{\epsilon}\right)_{\mathrm{UV}}+\left(-\frac{1}{\epsilon}\right)_{\mathrm{CO}}\right]\left[1+\epsilon\,\ln\left(4\pi\mathrm{e}^{-\gamma_E}\right)\right]\\ &\times\ \left[\Delta P^{(1)}_{qg}(x)\ -\ \epsilon\,2\,T_F\,(1-x)\right]\\ &+\ \text{UV-counterterms}\Big|_{q/g}\ ,\end{aligned}\tag{3.27}$$

where color factor $T_F = 1/2$ and the gluon-to-quark splitting function $\Delta P^{(1)}_{qg}(x)$ is,

$$\Delta P^{(1)}_{qg}(x) = T_F\,\left[x^2-(1-x)^2\right]\ .\tag{3.28}$$

Choosing the $\overline{\mathrm{MS}}$ UV counterterms that remove only the UV pole and the associated phase factor,

$$\text{UV-counterterms}\Big|_{q/g,\overline{\mathrm{MS}},\gamma_5} = -\left(\frac{\mu^2}{\mu_f^2}\right)^{\epsilon}\left(\frac{1}{\epsilon}\right)_{\mathrm{UV}}\left[1+\epsilon\,\ln\left(4\pi\mathrm{e}^{-\gamma_E}\right)\right]\left[\Delta P^{(1)}_{qg}(x)\right]\ ,\tag{3.29}$$

we find the first order polarized quark distribution within a gluon is,

$$\begin{aligned}\Delta\phi^{(1)}_{q/g}(x)\Big|_{\overline{\mathrm{MS}},\gamma_5,\mathrm{DR}} &= \left(\frac{\mu^2}{\mu_f^2}\right)^{\epsilon}\Bigg\{\left(-\frac{1}{\epsilon}\right)_{\mathrm{CO}}\Delta P^{(1)}_{qg}(x)\\ &\qquad-\left[\Delta P^{(1)}_{qg}(x)\,\ln\left(4\pi\mathrm{e}^{-\gamma_E}\right)-2\,T_F\,(1-x)\right]_{\mathrm{CO}}\\ &\qquad-2\,T_F\,(1-x)_{\mathrm{UV}}\Bigg\}\ .\end{aligned}\tag{3.30}$$

Just as the case of $\Delta\phi^{(1)}_{q/q'}(x)$ in Eq. (3.26), the first two lines in Eq. (3.30) depend on our choice of collinear regulator, while the last term, $-2T_F\,(1-x)_{\mathrm{UV}}$, is a short-distance piece, which comes from our UV regulator and $\overline{\mathrm{MS}}$ renormalization.

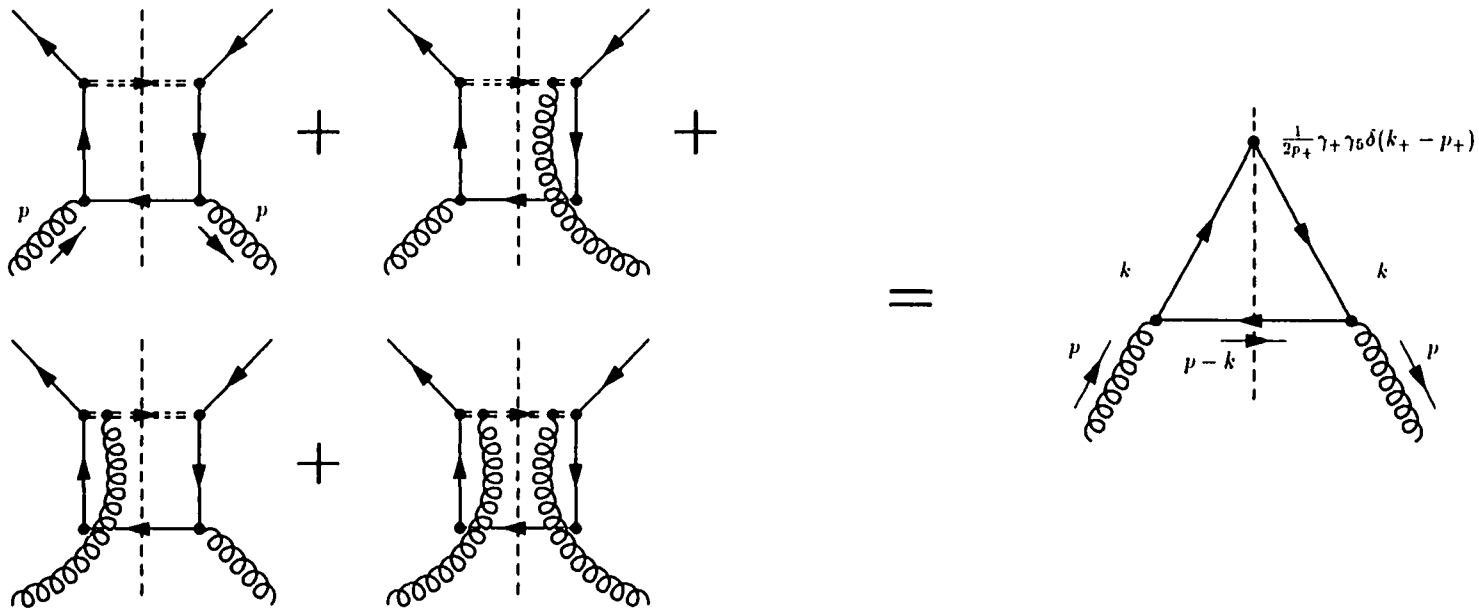

(a) (b)

Figure 3.6 The $O(\alpha_s)$ quark distribution inside a gluon. (a) In gauge invariant Feynman diagrams. (b) In light-cone gauge cut-vertex diagram.

Gluon distribution within a quark

Feynman diagram in figure 3.7 gives full contribution to $\Delta\phi^{(1)}_{g/q}(x)$ in the light-cone gauge. After evaluating the diagram, we obtain,

$$\begin{aligned}\Delta\phi^{(1)}_{g/q}(x)\Big|_{\gamma_5,\mathrm{DR}} &= \left(\frac{\mu^2}{\mu_f^2}\right)^{\epsilon}\left[\left(\frac{1}{\epsilon}\right)_{\mathrm{UV}}+\left(-\frac{1}{\epsilon}\right)_{\mathrm{CO}}\right]\left[1+\epsilon\,\ln\left(4\pi\mathrm{e}^{-\gamma_E}\right)\right]\\ &\quad\times\left[\Delta P^{(1)}_{gq}(x)+\epsilon\,2C_F\,(1-x)\right]\\ &\quad+\text{UV-counterterms}\Big|_{g/q}\,,\end{aligned}\tag{3.31}$$

where the quark-to-gluon splitting function $\Delta P^{(1)}_{gq}(x)$ is,

$$\Delta P^{(1)}_{gq}(x)=C_F\left[\frac{1-(1-x)^2}{x}\right]\,.\tag{3.32}$$

Substituting the traditional $\overline{\mathrm{MS}}$ UV counterterms,

$$\text{UV-counterterms}\Big|_{g/q,\overline{\mathrm{MS}},\gamma_5}=-\left(\frac{\mu^2}{\mu_f^2}\right)^{\epsilon}\left(\frac{1}{\epsilon}\right)_{\mathrm{UV}}\left[1+\epsilon\,\ln\left(4\pi\mathrm{e}^{-\gamma_E}\right)\right]\left[\Delta P^{(1)}_{gq}(x)\right]\,,\tag{3.33}$$

into Eq. (3.31), we derive the first order polarized gluon distribution within a quark,

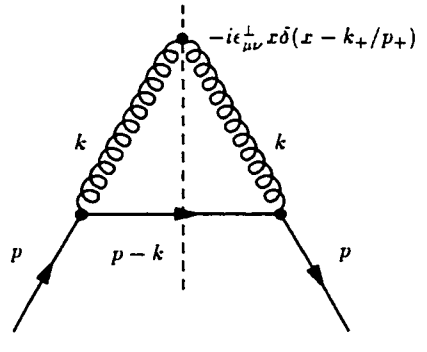

Figure 3.7 Next-to-leading order cut-vertex Feynman diagram for gluon distribution inside a quark.

$$\Delta\phi^{(1)}_{g/q}(x)\Big|_{\overline{\rm MS},\gamma_5,{\rm DR}} = \left(\frac{\mu^2}{\mu_f^2}\right)^{\epsilon}\Bigg\{\left(-\frac{1}{\epsilon}\right)_{\rm CO}\Delta P^{(1)}_{qg}(x) - \left[\Delta P^{(1)}_{qg}(x)\ln\left(4\pi e^{-\gamma_E}\right) + 2C_F(1-x)\right]_{\rm CO} + 2C_F(1-x)_{\rm UV}\Bigg\}. \tag{3.34}$$

In the last equation, the first two lines depend on our choice of collinear regulator, but the last term is a short-distance piece.

Gluon distribution within a gluon

In light-cone gauge, the one-loop gluon distribution within a gluon is given by Feynman diagrams shown in Figure 3.8. Since our normalization for polarized parton distributions, defined in Eq. (3.18), is the same as the unpolarized parton distributions, the contributions from the diagrams with a virtual loop are the same as those of unpolarized gluon distributions. Calculating the symmetric real diagram in Figure 3.8 in light-cone gauge, we obtain,

$$\Delta\phi_{g/g}\Big|_{\rm DR} = \left(\frac{\mu^2}{\mu_f^2}\right)^{\epsilon}\left[\left(\frac{1}{\epsilon}\right)_{\rm UV} + \left(-\frac{1}{\epsilon}\right)_{\rm CO}\right]\left[1+\epsilon\ln\left(4\pi e^{-\gamma_E}\right)\right] \times\left[\Delta P^{(1)}_{gg}(x) + \epsilon\, 4C_A(1-x)\right] + \text{UV-counterterms}\Big|_{g/g}, \tag{3.35}$$

where $C_A = 3$ is a color factor. There is no γ_5 subscript because there is no γ_5 in $\Delta\phi^{(1)}_{g/g}(x)$. In Eq. (3.35), the gluon-to-gluon splitting function $\Delta P^{(1)}_{gg}(x)$ is,

$$\Delta P^{(1)}_{gg}(x) = 2C_A\left[\frac{1}{(1-x)_+} + (1-2x) + \left(\frac{11}{12} - \frac{N_f}{6C_A}\right)\delta(1-x)\right], \tag{3.36}$$

where the "+" prescription is defined in Eq. (3.24). Substituting the corresponding $\overline{\rm MS}$ UV counterterms,

$$\text{UV-counterterms}\Big|_{g/g,\overline{\rm MS},\,{\rm DR}} = -\left(\frac{\mu^2}{\mu_f^2}\right)^{\epsilon}\left(\frac{1}{\epsilon}\right)_{\rm UV}\left[1+\epsilon\ln\left(4\pi e^{-\gamma_E}\right)\right]\left[\Delta P^{(1)}_{gg}(x)\right], \tag{3.37}$$

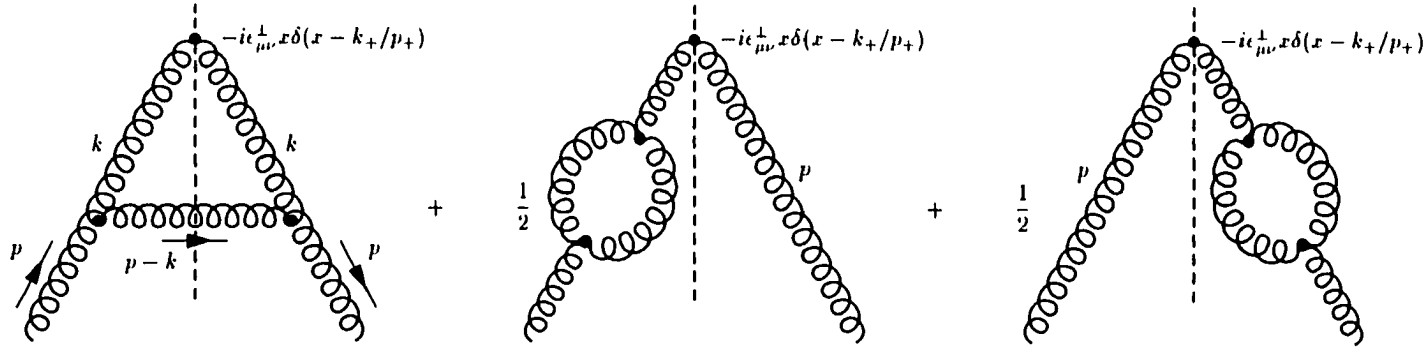

Figure 3.8 Cut-vertex Feynman diagrams of the $O(\alpha_s)$ gluon distribution inside a gluon.

into Eq. (3.35), we arrive at the first order polarized gluon distribution within a gluon,

$$\Delta\phi_{g/g}^{(1)}(x)\Big|_{\overline{\rm MS},\,{\rm DR}} = \left(\frac{\mu^2}{\mu_f^2}\right)^{\epsilon}\left\{\left(-\frac{1}{\epsilon}\right)_{\rm CO}\Delta P_{gg}^{(1)}(x) - \left[\Delta P_{gg}^{(1)}(x)\ln\left(4\pi {\rm e}^{-\gamma_E}\right) + 4\,C_A\,(1-x)\right]_{\rm CO} + 4\,C_A\,(1-x)_{\rm UV}\right\}. \tag{3.38}$$

Again, like Eqs. (3.26), (3.30) and (3.34), the first two lines in Eq. (3.38) are related to the choice of our collinear regulator, but the last term is a remainder of UV origin, i.e. short-distance.

Using Dimensional Regularization, $d = 4 - 2\epsilon$, and HVBM γ_5 prescription, the $\overline{\rm MS}$ parton-level parton distributions are summarized in Eqs. (3.26), (3.30), (3.34) and (3.38). From these four equations, a common feature emerges: In traditional $\overline{\rm MS}$ renormalization/factorization scheme, parton-level parton distributions include some short-distance information. More discussion on this point will be given later.

Dimensional Regularization, CFH γ_5 Prescription, and $\overline{\rm MS}$ Scheme

In order to demonstrate the ambiguities of polarized parton distributions on choice of γ_5 definition in d-dimension, we derive the parton-level parton distributions in another γ_5 prescription — CFH γ_5 or γ_5' in our notation.

In CFH γ_5 prescription, one has to assign a vertex as the reading point for all spinor traces. In QCD factorization, short-distance partonic quantities are extracted by calculating parton-level cross-section with subtraction terms to remove all possible collinear singularities. For example, in the calculation of the first order DIS coefficient function in Eq. (1.16), $g_{1q}^{(1)}(x)$ represents the partonic cross-section, and $\Delta C_q^{(0)}(x) \otimes \Delta\phi_{q/q}^{(1)}(x)$ is the subtraction term. To ensure consistency under factorization procedure, only corresponding vertices in both partonic cross-section and the subtraction terms should be chosen as reading points. Since a cut-vertex is not a normal vertex, and only

appears in the subtraction term, it should not be used as a reading point.

To derive the quark distribution within a quark, we can again use the Feynman diagrams shown in Figure 3.4 or Fig. 3.5 depending on the gauge choice. To use CFH γ_5 prescription, either one of the two quark-gluon vertices in Feynman diagrams shown in Figure 3.4 or Fig. 3.5 can be chosen as the reading point. Using Dimensional Regularization for both UV and CO divergences, we obtain,

$$\begin{aligned}\Delta\phi^{(1)}_{q/q'}\Big|_{\gamma_5',\mathrm{DR}} &= \delta_{qq'}\left(\frac{\mu^2}{\mu_f^2}\right)^{\epsilon}\left[\left(\frac{1}{\epsilon}\right)_{\mathrm{UV}}+\left(-\frac{1}{\epsilon}\right)_{\mathrm{CO}}\right]\left[1+\epsilon\,\ln\left(4\pi\mathrm{e}^{-\gamma_E}\right)\right]\\ &\quad\times\left[\Delta P^{(1)}_{qq}(x)\,-\,\epsilon C_F\,(1-x)\right]\\ &\quad+\text{UV-counterterms}\Big|_{q/q'}\,,\end{aligned}\tag{3.39}$$

Since by definition, UV counterterms in $\overline{\mathrm{MS}}$ scheme are independent of any γ_5 prescription, the UV counterterms for the above distribution are simply the one given by Eq. (3.25). The $\overline{\mathrm{MS}}$ renormalized distribution is,

$$\begin{aligned}\Delta\phi^{(1)}_{q/q'}\Big|_{\overline{\mathrm{MS}},\gamma_5',\mathrm{DR}} &= \delta_{qq'}\left(\frac{\mu^2}{\mu_f^2}\right)^{\epsilon}\Bigg\{\left(-\frac{1}{\epsilon}\right)_{\mathrm{CO}}\Delta P^{(1)}_{qq}(x)\\ &\qquad-\left[\Delta P^{(1)}_{qq}(x)\,\ln\left(4\pi\mathrm{e}^{-\gamma_E}\right)-C_F\,(1-x)\right]_{\mathrm{CO}}\\ &\qquad-C_F\,(1-x)_{\mathrm{UV}}\Bigg\}\,.\end{aligned}\tag{3.40}$$

Similar to the HVBM result in Eq. (3.26), only the last term $-C_F(1-x)_{\mathrm{UV}}$ in the above equation is short-distance. The rest in Eq. (3.40) depends on the choice of the collinear regulator, and hence, should not appear in any calculable short-distance quantities.

Comparing the short-distance piece $3C_F(1-x)_{\mathrm{UV}}$ from HVBM in Eq. (3.26) with $-C_F(1-x)_{\mathrm{UV}}$ from CFH in Eq. (3.40), it is obvious that even with the same $\overline{\mathrm{MS}}$ UV renormalization scheme, the first order polarized quark distribution within a quark gets different short-distance contribution from different choice of γ_5 prescription. In other words, one derives different short-distance quantities depending on whether HVBM result, Eq. (3.26), or CFH result, Eq. (3.40), is used for the $\Delta\phi^{(1)}_{q/q'}(x)$.

Clearly, from Eq. (3.26) and Eq. (3.40), those collinear sensitive terms depend on γ_5 prescription in d-dimension. It is therefore very important to ensure that this collinear γ_5 dependence does not appear in any calculable short-distance quantities. (However, those UV γ_5-dependent terms may show up in short-distance hard parts and lead to explicit γ_5 dependence.) We will provide such consistency check in the next chapter.

To derive the quark distribution within a gluon in γ_5' prescription, we need to pick a reading point. As discussed before, the cut-vertex cannot be used because it is not a normal local vertex. Using either one of the two quark-gluon vertices in Figure 3.6(b) as the reading point, the distribution is,

$$\Delta\phi^{(1)}_{q/g}\Big|_{\gamma_5',\mathrm{DR}} = \left(\frac{\mu^2}{\mu_f^2}\right)^{\epsilon}\left[\left(\frac{1}{\epsilon}\right)_{\mathrm{UV}}+\left(-\frac{1}{\epsilon}\right)_{\mathrm{CO}}\right]\left[1+\epsilon\,\ln\left(4\pi\mathrm{e}^{-\gamma_E}\right)\right]\left[\Delta P^{(1)}_{qg}(x)\right] + \text{UV-counterterms}\Big|_{q/g}\,, \tag{3.41}$$

for dimensional collinear regulator. Applying the same $\overline{\mathrm{MS}}$ UV counterterms in Eq. (3.29), we have,

$$\Delta\phi^{(1)}_{q/g}(x)\Big|_{\overline{\mathrm{MS}},\gamma_5',\mathrm{DR}} = \left(\frac{\mu^2}{\mu_f^2}\right)^{\epsilon}\left\{\left(-\frac{1}{\epsilon}\right)_{\mathrm{CO}}\Delta P^{(1)}_{qg}(x) - \left[\Delta P^{(1)}_{qg}(x)\,\ln\left(4\pi\mathrm{e}^{-\gamma_E}\right)\right]_{\mathrm{CO}}\right\}. \tag{3.42}$$

Note that in γ_5' prescription, the first order polarized quark distribution within a gluon does not have any short-distance terms. More discussions on the issue of the so-called anomalous contribution will be given in the next chapter.

At one-loop level, it is found that the gluon distribution within a quark or within a gluon is independent of the choice of γ_5 prescription. Therefore, both $\Delta\phi^{(1)}_{g/q}(x)$ and $\Delta\phi^{(1)}_{g/g}(x)$ in γ_5' prescription are the same as those given by HVBM γ_5 in Eq. (3.34) and Eq. (3.38), respectively,

$$\Delta\phi^{(1)}_{g/q}(x)\Big|_{\overline{\mathrm{MS}},\gamma_5',\mathrm{DR}} = \Delta\phi^{(1)}_{g/q}(x)\Big|_{\overline{\mathrm{MS}},\gamma_5,\mathrm{DR}}\,, \tag{3.43}$$

$$\Delta\phi^{(1)}_{g/g}(x)\Big|_{\overline{\mathrm{MS}},\gamma_5',\mathrm{DR}} = \Delta\phi^{(1)}_{g/g}(x)\Big|_{\overline{\mathrm{MS}},\gamma_5,\mathrm{DR}}\,. \tag{3.44}$$

Off-Shell Momentum Regularization and $\overline{\rm MS}$ Scheme

Parton-level parton distributions are not physical measurables. They depend on CO regularization and UV renormalization. On the other hand, QCD factorization theorem requires all perturbatively calculable partonic quantities to be collinear insensitive. Consequently, dependence on CO regularization in parton-level parton distributions should be canceled when these distributions are used to calculate any short-distance quantities, such as $\Delta C_f(x)$ in polarized DIS. To demonstrate such cancellation in polarized DIS in the next chapter, here we provide both polarized quark distribution within a quark and quark distribution within a gluon with a different collinear regulator — off-shell momentum regulator. In the following, we let the incoming parton momentum p be off-shell, i.e. $p^2 < 0$.

HVBM γ_5 prescription

To derive the quark distribution within a quark, we use the same Feynman diagrams shown in Figure 3.4 or Fig. 3.5 depending on the gauge choice. With HVBM γ_5 prescription and $p^2 \neq 0$ off-shell collinear regulator, we find the parton-level distribution is given by,

$$\begin{aligned}\Delta\phi^{(1)}_{q/q'}(x)\Big|_{\gamma_5,p^2\neq 0} &= \delta_{qq'}\left\{\left(\frac{1}{\epsilon}\right)_{\rm UV}\left(\frac{\mu^2}{\mu_f^2}\right)^{\epsilon}\left[1+\epsilon\,\ln\left(4\pi e^{-\gamma_E}\right)\right]\left[\Delta P^{(1)}_{qq}(x)+\epsilon\,3\,C_F\,(1-x)_{\rm UV}\right]\right.\\ &\quad +\Delta P^{(1)}_{qq}(x)\,\ln\left(\frac{\mu_f^2}{-p^2}\right)-C_F\left[(1+x^2)\left[\frac{\ln(1-x)}{1-x}\right]_+\right.\\ &\quad \left.\left.+\left(\frac{1+x^2}{1-x}\right)\ln(x)+1-\left(\frac{7}{2}-\frac{\pi^2}{3}\right)\delta(1-x)\right]\right\}\\ &\quad +\ \text{UV-counterterms}\Big|_{q/q'}\,. \end{aligned} \tag{3.45}$$

where μ is the renormalization scale, μ_f is the factorization scale, and $\Delta P^{(1)}_{qq}(x)$ is the same quark-to-quark splitting function given in Eq. (3.23). Applying the $\overline{\rm MS}$ UV coun-

terterms given by Eq. (3.25), the $\overline{\rm MS}$ renormalized distribution is,

$$\Delta\phi^{(1)}_{q/q'}(x)\Big|_{\overline{\rm MS},\gamma_5,p^2\neq 0} = \delta_{qq'}\left\{\Delta P^{(1)}_{qq}(x)\,\ln\left(\frac{\mu_f^2}{-p^2}\right) - C_F\left[(1+x^2)\left[\frac{\ln(1-x)}{1-x}\right]_+ + \left(\frac{1+x^2}{1-x}\right)\ln(x) + 1 - \left(\frac{7}{2}-\frac{\pi^2}{3}\right)\delta(1-x)\right]_{\rm CO} + 3\,C_F\,(1-x)_{\rm UV}\right\}, \tag{3.46}$$

As shown in the above equation, after putting the incoming quark momentum p to be off-shell, the CO divergence is regulated as $\ln(-\mu_f^2/p^2)$, while the UV divergence is still the usual $(1/\epsilon)_{\rm UV}$ pole. That is, unlike its divergent collinear DR counterpart, $\Delta\phi^{(1)}_{q/q'}(x)\Big|_{\overline{\rm MS},\gamma_5,p^2\neq 0}$ is finite after renormalization. Furthermore, because the same UV regulator and UV renormalization are used, as expected, the last term in Eq. (3.46) is the same as the last term $3C_F(1-x)_{\rm UV}$ in Eq. (3.26). All other terms depend on the choice of $p^2 \neq 0$ collinear regulator. By comparing the results of different collinear regulator given by Eq. (3.26) and Eq. (3.46), collinear regulator dependence in polarized quark distribution, $\Delta\phi_{q/q'}(x)$, is manifest.

For quark distribution within a gluon, we again evaluate the diagram in Figure 3.6(b). With the HVBM γ_5 prescription and $p^2 \neq 0$ off-shell collinear regulator, the Feynman diagrams give,

$$\Delta\phi^{(1)}_{q/g}(x)\Big|_{\gamma_5,p^2\neq 0} = \left\{\left(\frac{1}{\epsilon}\right)_{\rm UV}\left(\frac{\mu^2}{\mu_f^2}\right)^{\epsilon}\left[1+\epsilon\,\ln\left(4\pi e^{-\gamma_E}\right)\right]\left[\Delta P^{(1)}_{qg}(x) - \epsilon\,2\,T_F\,(1-x)\right] + \Delta P^{(1)}_{qg}(x)\left[\ln\left(\frac{\mu_f^2}{-p^2}\right) - \ln\left[x(1-x)\right] - 1\right]\right\} + \text{UV-counterterms}\Big|_{q/g}. \tag{3.47}$$

Using the same $\overline{\rm MS}$ UV counterterms in Eq. (3.29), we obtain,

$$\Delta\phi^{(1)}_{q/g}(x)\Big|_{\overline{\rm MS},\gamma_5,p^2\neq 0} = \Delta P^{(1)}_{qg}(x)\,\ln\left(\frac{\mu_f^2}{-p^2}\right) - \Delta P^{(1)}_{qg}(x)\left[\ln\left[x(1-x)\right]+1\right]_{\rm CO} - 2\,T_F\,(1-x)_{\rm UV}. \tag{3.48}$$

By comparing the results of different collinear regulators given by Eq. (3.30) and Eq. (3.48), the first order polarized quark distribution within a gluon, $\Delta\phi^{(1)}_{q/g}(x)$, shows an explicit dependence on collinear regulator. Since same UV regulator and UV renormalization are being used, it is expected that Eq. (3.30) and Dimensional Regularization result in Eq. (3.48) share the same short-distance parts.

CFH γ_5 prescription

For quark distribution within a quark in CFH γ_5 prescription, we calculate the Feynman diagrams shown in Figure 3.4 with either one of the two quark-gluon vertices in the diagram as the reading point. Using $p^2 \neq 0$ collinear regulator and $\overline{\rm MS}$ renormalization, we have,

$$\Delta\phi^{(1)}_{q/q'}(x)\Big|_{\overline{\rm MS},\gamma_5',p^2\neq 0} = \delta_{qq'}\left\{\Delta P_{qq}(x)\,\ln\left(\frac{\mu_f^2}{-p^2}\right) - C_F\left[(1+x^2)\left[\frac{\ln(1-x)}{1-x}\right]_+ + \left(\frac{1+x^2}{1-x}\right)\ln(x) + 1 - \left(\frac{7}{2}-\frac{\pi^2}{3}\right)\delta(1-x)\right]_{\rm CO} - C_F\,(1-x)_{\rm UV}\right\}. \tag{3.49}$$

Since the same collinear regulator is being used, the collinear sensitive parts of the results from both γ_5 prescriptions, i.e. Eq. (3.46) and Eq. (3.49), are the same. On the other hand, even with the same renormalization scheme, different γ_5 prescription gives different short-distance parts.

Similarly, to derive the quark distribution within a gluon in CFH γ_5 prescription and $p^2 \neq 0$ off-shell collinear regulator, we evaluate the Feynman diagrams shown in Figure 3.6(b) with either one of the two quark-gluon vertices in the diagram as the reading point. With the $\overline{\rm MS}$ renormalization, we have,

$$\Delta\phi^{(1)}_{q/g}(x)\Big|_{\overline{\rm MS},\gamma_5',p^2\neq 0} = \Delta P^{(1)}_{qg}(x)\,\ln\left(\frac{\mu_f^2}{-p^2}\right) - \Delta P^{(1)}_{qg}(x)\left[\ln\left[x(1-x)\right]+1\right]_{\rm CO}. \tag{3.50}$$

Note that in CFH γ_5 prescription, the first order polarized quark distribution within a gluon does not include any short-distance physics. More discussions on this point will be given later.

In Chapter 4, we use polarized DIS as an example to demonstrate that under QCD factorization theorem, all perturbative calculable quantities are independent of the choice of collinear regulator. Since only $\Delta\phi^{(1)}_{q/q'}(x)$ and $\Delta\phi^{(1)}_{q/g}(x)$ are being used for calculating the one-loop coefficient functions in DIS, we will not present the expressions for $\Delta\phi^{(1)}_{g/q}(x)$ and $\Delta\phi^{(1)}_{g/g}(x)$ in $p^2 \neq 0$ off-shell regulator.

A New Renormalization/Factorization Scheme

In this section, we propose a new renormalization/factorization scheme called UV Subtraction (UVS) scheme. This new scheme is defined by requiring that parton distributions within a parton include *only* collinear sensitive information. That is, UV counterterms are chosen in such a way that all short-distance terms in $\Delta\phi_{a/f}(x)$ are discarded. By employing this new UVS renormalization/factorization scheme, short-distance perturbative quantities are shown to be independent of the choice of γ_5 prescriptions. With all short-distance terms being removed, parton distributions within a parton are now only sensitive to the choice of collinear regulators. However, as we stated earlier, such dependence on collinear regulators is canceled in any perturbatively calculable short-distance quantities.

Presented below is a complete set of next-to-leading order polarized parton distributions within a parton in different collinear regulators. Equipped with these one-loop polarized parton distributions, all next-to-leading order corrections to physical processes involving polarized parton distributions can be uniquely determined.

One-loop polarized parton distributions within a parton

Using Dimensional Regularization for both UV and CO divergences, and HVBM γ_5 prescription, the parton distributions in parton in UVS scheme are given by,

$$\Delta\phi_{q/q'}(1)\Big|_{\rm UVS,\gamma_5,DR} = \delta_{qq'}\left(\frac{\mu^2}{\mu_f^2}\right)^{\epsilon}\left\{\left(-\frac{1}{\epsilon}\right)_{\rm CO}\Delta P_{qq}^{(1)}(x) - \left[\Delta P_{qq}^{(1)}(x)\,\ln\left(4\pi e^{-\gamma_E}\right) + 3\,C_F\,(1-x)\right]_{\rm CO}\right\}, \quad (3.51)$$

$$\Delta\phi_{q/g}^{(1)}(x)\Big|_{\rm UVS,\gamma_5,DR} = \left(\frac{\mu^2}{\mu_f^2}\right)^{\epsilon}\left\{\left(-\frac{1}{\epsilon}\right)_{\rm CO}\Delta P_{qg}^{(1)}(x) - \left[\Delta P_{qg}^{(1)}(x)\,\ln\left(4\pi e^{-\gamma_E}\right) - 2\,T_F\,(1-x)\right]_{\rm CO}\right\}, \quad (3.52)$$

$$\Delta\phi_{g/q}^{(1)}(x)\Big|_{\rm UVS,\gamma_5,DR} = \left(\frac{\mu^2}{\mu_f^2}\right)^{\epsilon}\left\{\left(-\frac{1}{\epsilon}\right)_{\rm CO}\Delta P_{qg}^{(1)}(x) - \left[\Delta P_{qg}^{(1)}(x)\ln\left(4\pi e^{-\gamma_E}\right) + 2\,C_F\,(1-x)\right]_{\rm CO}\right\}, \quad (3.53)$$

$$\Delta\phi_{g/g}^{(1)}(x)\Big|_{\rm UVS,\gamma_5,DR} = \left(\frac{\mu^2}{\mu_f^2}\right)^{\epsilon}\left\{\left(-\frac{1}{\epsilon}\right)_{\rm CO}\Delta P_{gg}^{(1)}(x) - \left[\Delta P_{gg}^{(1)}(x)\ln\left(4\pi e^{-\gamma_E}\right) + 4\,C_A\,(1-x)\right]_{\rm CO}\right\}. \quad (3.54)$$

Because Dimensional Regularization for collinear divergence is being used, the collinear sensitive parton-level parton distributions have dependence in γ_5 prescription. In CFH γ_5 prescription, we have,

$$\Delta\phi_{q/q'}^{(1)}\Big|_{\rm UVS,\gamma_5',DR} = \delta_{qq'}\left(\frac{\mu^2}{\mu_f^2}\right)^{\epsilon}\left\{\left(-\frac{1}{\epsilon}\right)_{\rm CO}\Delta P_{qq}^{(1)}(x) - \left[\Delta P_{qq}^{(1)}(x)\,\ln\left(4\pi e^{-\gamma_E}\right) - C_F\,(1-x)\right]_{\rm CO}\right\}, \quad (3.55)$$

$$\Delta\phi_{q/g}^{(1)}(x)\Big|_{\rm UVS,\gamma_5',DR} = \left(\frac{\mu^2}{\mu_f^2}\right)^{\epsilon}\left\{\left(-\frac{1}{\epsilon}\right)_{\rm CO}\Delta P_{qg}^{(1)}(x) - \left[\Delta P_{qg}^{(1)}(x)\,\ln\left(4\pi e^{-\gamma_E}\right)\right]_{\rm CO}\right\}, \quad (3.56)$$

$$\Delta\phi^{(1)}_{g/q}(x)\Big|_{\rm UVS,\gamma_5',DR} = \left(\frac{\mu^2}{\mu_f^2}\right)^{\epsilon}\left\{\left(-\frac{1}{\epsilon}\right)_{\rm CO}\Delta P^{(1)}_{qg}(x) - \left[\Delta P^{(1)}_{qg}(x)\ln\left(4\pi e^{-\gamma_E}\right) + 2\,C_F\,(1-x)\right]_{\rm CO}\right\}, \quad (3.57)$$

$$\Delta\phi^{(1)}_{g/g}(x)\Big|_{\rm UVS,\gamma_5',DR} = \left(\frac{\mu^2}{\mu_f^2}\right)^{\epsilon}\left\{\left(-\frac{1}{\epsilon}\right)_{\rm CO}\Delta P^{(1)}_{gg}(x) - \left[\Delta P^{(1)}_{gg}(x)\ln\left(4\pi e^{-\gamma_E}\right) + 4\,C_A\,(1-x)\right]_{\rm CO}\right\}. \quad (3.58)$$

As discussed before, this explicit dependence on γ_5 prescription in parton distributions has no effect on any short-distance perturbative quantities.

Using $p^2 \neq 0$ off-shell regulator, the quark distributions within a quark and gluon are independent of γ_5 prescriptions,

$$\begin{aligned}\Delta\phi^{(1)}_{q/q'}(x)\Big|_{\rm UVS,\gamma_5',p^2\neq 0} &= \Delta\phi^{(1)}_{q/q'}(x)\Big|_{\rm UVS,\gamma_5,p^2\neq 0}\\ &= \delta_{qq'}\left\{\Delta P^{(1)}_{qq}(x)\,\ln\left(\frac{\mu_f^2}{-p^2}\right) - C_F\left[(1+x^2)\left[\frac{\ln(1-x)}{1-x}\right]_+ + \left(\frac{1+x^2}{1-x}\right)\ln(x) + 1 - \left(\frac{7}{2}-\frac{\pi^2}{3}\right)\delta(1-x)\right]_{\rm CO}\right\}, \quad (3.59)\\ \Delta\phi^{(1)}_{g/q'}(x)\Big|_{\rm UVS,\gamma_5',p^2\neq 0} &= \Delta\phi^{(1)}_{g/q'}(x)\Big|_{\rm UVS,\gamma_5,p^2\neq 0}\\ &= \Delta P^{(1)}_{qg}(x)\,\ln\left(\frac{\mu_f^2}{-p^2}\right) - \Delta P^{(1)}_{qg}(x)\left[\ln\left[x(1-x)\right]+1\right]_{\rm CO}. \quad (3.60)\end{aligned}$$

Relations between $\overline{\rm MS}$ scheme and the new UVS scheme

Between any two consistent renormalization/factorization, the difference can only be short-distance. These short-distance difference is, in turn, perturbative calculable, and thus completely determined. However, due to the γ_5 dependence in $\overline{\rm MS}$ scheme, the difference between $\overline{\rm MS}$ and UVS schemes also depends on the γ_5 prescription. We summarize the relationship of these two renormalization schemes as conversion tables given in Tables 3.1, 3.2 and 3.3.

Table 3.1 Conversion between UVS and $\overline{\rm MS}$ for one-loop spin-dependent partonic parton distributions $\Delta\phi^{(1)}_{f'/f}(x)$ in HVBM γ_5 prescription with DR collinear regulator.

$\Delta\phi^{(1)}_{q/q'}(x)\Big\vert_{\rm UVS,\gamma_5,DR} - \Delta\phi^{(1)}_{q/q'}(x)\Big\vert_{\overline{\rm MS},\gamma_5,\rm DR}$	$=$	$-\delta_{qq'}\left(\frac{\mu^2}{\mu_f^2}\right)^{\epsilon} 3\,C_F\,(1-x)$
$\Delta\phi^{(1)}_{q/g}(x)\Big\vert_{\rm UVS,\gamma_5,DR} - \Delta\phi^{(1)}_{q/g}(x)\Big\vert_{\overline{\rm MS},\gamma_5,\rm DR}$	$=$	$\left(\frac{\mu^2}{\mu_f^2}\right)^{\epsilon} 2\,T_F\,(1-x)$
$\Delta\phi^{(1)}_{g/q}(x)\Big\vert_{\rm UVS,\gamma_5,DR} - \Delta\phi^{(1)}_{g/q}(x)\Big\vert_{\overline{\rm MS},\gamma_5,\rm DR}$	$=$	$-\left(\frac{\mu^2}{\mu_f^2}\right)^{\epsilon} 2\,C_F\,(1-x)$
$\Delta\phi^{(1)}_{g/g}(x)\Big\vert_{\rm UVS,DR} - \Delta\phi^{(1)}_{g/g}(x)\Big\vert_{\overline{\rm MS},\rm DR}$	$=$	$-\left(\frac{\mu^2}{\mu_f^2}\right)^{\epsilon} 4\,N_c\,(1-x)$

Table 3.2 Conversion between UVS and $\overline{\rm MS}$ for one-loop spin-dependent partonic parton distributions $\Delta\phi^{(1)}_{f'/f}(x)$ in CFH γ_5 prescription with DR collinear regulator.

$\Delta\phi^{(1)}_{q/q'}(x)\Big\vert_{\rm UVS,\gamma_5',DR} - \Delta\phi^{(1)}_{q/q'}(x)\Big\vert_{\overline{\rm MS},\gamma_5',\rm DR}$	$=$	$\delta_{qq'}\left(\frac{\mu^2}{\mu_f^2}\right)^{\epsilon} C_F\,(1-x)$
$\Delta\phi^{(1)}_{q/g}(x)\Big\vert_{\rm UVS,\gamma_5',DR} - \Delta\phi^{(1)}_{q/g}(x)\Big\vert_{\overline{\rm MS},\gamma_5',\rm DR}$	$=$	$\left(\frac{\mu^2}{\mu_f^2}\right)^{\epsilon} 2\,T_F\,(1-x)$
$\Delta\phi^{(1)}_{g/q}(x)\Big\vert_{\rm UVS,\gamma_5',DR} - \Delta\phi^{(1)}_{g/q}(x)\Big\vert_{\overline{\rm MS},\gamma_5',\rm DR}$	$=$	$-\left(\frac{\mu^2}{\mu_f^2}\right)^{\epsilon} 2\,C_F\,(1-x)$
$\Delta\phi^{(1)}_{g/g}(x)\Big\vert_{\rm UVS,DR} - \Delta\phi^{(1)}_{g/g}(x)\Big\vert_{\overline{\rm MS},\rm DR}$	$=$	$-\left(\frac{\mu^2}{\mu_f^2}\right)^{\epsilon} 4\,N_c\,(1-x)$

Table 3.3 Conversion between UVS and $\overline{\rm MS}$ for one-loop spin-dependent partonic quark distributions $\Delta\phi^{(1)}_{q/f}(x)$ in both HVBM and CFH γ_5 prescriptions with off-shell $p^2 \neq 0$ collinear regulator.

$\Delta\phi^{(1)}_{q/q'}(x)\Big\vert_{\rm UVS,\gamma_5,p^2\neq 0} - \Delta\phi^{(1)}_{q/q'}(x)\Big\vert_{\overline{\rm MS},\gamma_5,p^2\neq 0}$	$=$	$-\delta_{qq'}\left(\frac{\mu^2}{\mu_f^2}\right)^{\epsilon} 3\,C_F\,(1-x)$
$\Delta\phi^{(1)}_{q/g}(x)\Big\vert_{\rm UVS,\gamma_5,p^2\neq 0} - \Delta\phi^{(1)}_{q/g}(x)\Big\vert_{\overline{\rm MS},\gamma_5,p^2\neq 0}$	$=$	$\left(\frac{\mu^2}{\mu_f^2}\right)^{\epsilon} 2\,T_F\,(1-x)$
$\Delta\phi^{(1)}_{q/q'}(x)\Big\vert_{\rm UVS,\gamma_5',p^2\neq 0} - \Delta\phi^{(1)}_{q/q'}(x)\Big\vert_{\overline{\rm MS},\gamma_5',p^2\neq 0}$	$=$	$\delta_{qq'}\left(\frac{\mu^2}{\mu_f^2}\right)^{\epsilon} C_F\,(1-x)$
$\Delta\phi^{(1)}_{q/g}(x)\Big\vert_{\rm UVS,\gamma_5',p^2\neq 0} - \Delta\phi^{(1)}_{q/g}(x)\Big\vert_{\overline{\rm MS},\gamma_5',p^2\neq 0}$	$=$	0

4 CASE STUDY: POLARIZED DIS

In this chapter, we use polarized DIS as an example to study both the γ_5 and anomalous ambiguities in polarized distributions in the context of factorization. Furthermore, consistency of various γ_5 prescriptions in d-dimension has been examined by utilizing two different collinear regulators. First, we begin with the kinematics of polarized DIS process.

Kinematics

In longitudinally polarized inclusive deep inelastic scattering, we have the process,

$$l(k, s_l) \; + \; h(p, s_h) \; \rightarrow \; l(k', s_l') \; + \; X, \tag{4.1}$$

where s_l and s_h are the spins of the incoming lepton and hadron (see Figure 4.1). Both s_l' and X are not observed. The differential cross-section written in terms of leptonic and hadronic tensors is given by,

$$d\sigma(s_l, s_h) = \frac{4\alpha_{EM}^2}{S}\frac{1}{Q^4} L^{\mu\nu}(s_l)\, W_{\mu\nu}(s_h) \frac{d^3k'}{2E'}, \tag{4.2}$$

where E' is the energy of the scattered lepton, $S = (p+k)^2$, and $Q^2 = -q^2 = (k-k')^2$. The leptonic tensor and hadronic tensor are defined as,

$$L^{\mu\nu}(s_l) \;=\; \frac{1}{2}\sum_{s_l'} \langle\, l(k, s_l) \,|\, j^\mu(0) \,|\, l(k', s_l') \,\rangle \langle\, l(k', s_l') \,|\, j^\nu(0) \,|\, l(k, s_l) \,\rangle \;, \tag{4.3}$$

$$W_{\mu\nu}(s_h) \;=\; \frac{1}{4\pi}\sum_X \int d\Gamma_X \; \langle h(p, s_h)|\, J_\mu(0) \,|X\rangle \langle X|\, J_\nu(0) \,|h(p, s_h)\rangle \;, \tag{4.4}$$

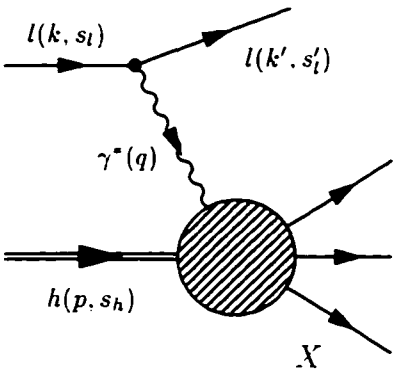

Figure 4.1 Feynman diagram of longitudinal polarized DIS.

where j^μ and J_μ are the leptonic and hadronic EM currents respectively; and $d\Gamma_X$, phase space of X, is given by,

$$d\Gamma_X = \prod_X \frac{d^3p_X}{(2\pi)^3 2E_X} (2\pi)^4 \delta^4 \left(p + q - \sum_X p_X \right) . \tag{4.5}$$

As in deep inelastic region, $Q^2 >> m_l^2$, we can safely assume $m_l \approx 0$ so that the lepton has only $\pm$ helicity states. The leptonic tensor is,

$$L^{\mu\nu}(s_l = \pm) = k^\mu k'^\nu + k^\nu k'^\mu - \frac{Q^2}{2} g^{\mu\nu} \mp i\epsilon^{\mu\nu\alpha\beta} k_\alpha k'_\beta , \tag{4.6}$$

where $\epsilon^{\mu\nu\alpha\beta}$ is the total antisymmetric tensor ($\epsilon_{0123} = 1$).

In longitudinal polarized experiments, it is the spin-dependent differential cross-section being measured. In our convention, we define it as,

$$\begin{aligned} d\Delta\sigma(s_l) &= \frac{1}{2}[\, d\sigma(s_l, s_h = +) - d\sigma(s_l, s_h = -)\,], \\ &= \frac{4\alpha_{EM}^2}{S} \frac{1}{Q^4} L^{\mu\nu}(s_l)\, \Delta W_{\mu\nu} \frac{d^3k'}{2E'}, \end{aligned} \tag{4.7}$$

and the corresponding spin-dependent hadronic tensor $\Delta W_{\mu\nu}$ is simply the antisymmetric part,

$$\Delta W_{\mu\nu} = \frac{1}{2}[\, W_{\mu\nu}(s_h = +) - W_{\mu\nu}(s_h = -)\,] . \tag{4.8}$$

Like its symmetric counterpart, the antisymmetric hadronic tensor can be parameterized by two dimensionless structure functions $g_1(x, Q^2)$ and $g_2(x, Q^2)$,

$$\Delta W_{\mu\nu}(x, Q^2) = i\epsilon_{\mu\nu\alpha\beta}\, q^\alpha \left\{ s_h^\beta\, g_1(x, Q^2) + (s_h^\beta - p^\beta \frac{s\cdot q}{p\cdot q})\, g_2(x, Q^2) \right\} \frac{m_h}{p\cdot q}\,, \tag{4.9}$$

where m_h is the hadron mass and $x = Q^2/2p\cdot q$ is the usual Bjorken variable. The hadron spin vector is defined as $s_h^\beta = (p^\beta - n^\beta p^2/p\cdot n)/m_h$, where $n^\beta = (1, 0, 0, -1)/\sqrt{2}$, so that $s_h^2 = -1$ and $s_h \cdot p = 0$. In longitudinal polarized deep inelastic scattering, the leading contribution to the antisymmetric hadronic tensor is coming from g_1. Whereas the term with g_2 is suppressed by a factor of m_h^2/Q^2. The structure function g_1 can be extracted from the antisymmetric hadronic tensor by,

$$g_1(x, Q^2) = \frac{i}{2}\epsilon_\perp^{\mu\nu}\, \Delta W_{\mu\nu}(x, Q^2)\,, \tag{4.10}$$

where $\epsilon_\perp^{\mu\nu} = \epsilon_{03}{}^{\mu\nu}$, correspondingly $\epsilon_{\perp\mu\nu} = \epsilon_{03\mu\nu}$, and $\epsilon_{0123} = 1$.

Factorization in Polarized DIS

According to factorization theorem, the hadronic structure function g_1^h can be decomposed into two parts,

$$g_1^h = \sum_{f=q,\bar{q},g} \Delta C_f \otimes \Delta\phi_{f/h}. \tag{4.11}$$

In above, structure function g_1^h is a physical observable, and therefore finite and independent of any renormalization and factorization schemes. On the other hand, coefficient functions and parton distributions are not. For instance, the formal definition of parton distributions in $n\cdot A = 0$ light-cone gauge is given by Eq. (3.6),

$$\Delta\phi_{q/h}(x, s_h) = \int \frac{dy^-}{4\pi} e^{ixp^+y^-} \left\langle h(p, s_h) \left| \overline{\psi}_q(y^-)\gamma^+\gamma_5\psi_q(0) \right| h(p, s_h) \right\rangle,$$

where s_h is the spin of the hadron h. Since parton distributions are matrix elements of non-local operators which have to be renormalized, their physical interpretation is not

unique and subjected to factorization/renormalization schemes. The Feynman rules for a more general gauge invariant formulation is given in Appendix B.

Clearly, both hadronic structure function g_1^h and parton distribution $\Delta\phi_{f/h}$ in Eq. (4.11) are not calculable in perturbative QCD. To extract coefficient functions, it is necessary to work on parton states. On partonic level, there are contributions from both quarks and gluons, i.e. g_{1_q} and g_{1_g}. These partonic structure functions are calculable perturbatively by Eq. (4.10). For example, the quark part g_{1_q} is given by,

$$\begin{aligned} g_{1_q} &= \frac{i}{2}\epsilon_\perp^{\mu\nu}\,\Delta W_{\mu\nu}^{(q)}\,, \\ &= \frac{i}{2}\epsilon_\perp^{\mu\nu}\sum_X\int\frac{d\Gamma_X}{8\pi}\Big\{\langle q(p,+)|\,J_\mu(0)\,|X\rangle\,\langle X|\,J_\nu(0)\,|q(p,+)\rangle - \\ &\qquad\qquad \langle q(p,-)|\,J_\mu(0)\,|X\rangle\,\langle X|\,J_\nu(0)\,|q(p,-)\rangle\Big\}\,, \\ &= \sum_X\int\frac{d\Gamma_X}{8\pi}\left(\frac{i}{2}\epsilon_\perp^{\mu\nu}\right)\mathrm{Tr}\left[\gamma_5\gamma\cdot p\,\hat{H}_{\mu\nu}^{(q)}\right]\,, \end{aligned} \tag{4.12}$$

where $\hat{H}_{\mu\nu}^{(q)}$ is the squared amputated matrix element of the process $q(p)+\gamma^*(q)\to X$ in Figure 4.2(a). Similarly, the gluon part g_{1_g} is,

$$\begin{aligned} g_{1_g} &= \frac{i}{2}\epsilon_\perp^{\mu\nu}\sum_X\int\frac{d\Gamma_X}{8\pi}\Big\{\langle g(p,+)|\,J_\mu(0)\,|X\rangle\,\langle X|\,J_\nu(0)\,|g(p,+)\rangle - \\ &\qquad\qquad \langle g(p,-)|\,J_\mu(0)\,|X\rangle\,\langle X|\,J_\nu(0)\,|g(p,-)\rangle\Big\}\,, \\ &= \sum_X\int\frac{d\Gamma_X}{8\pi}\left(\frac{i}{2}\epsilon_\perp^{\mu\nu}\right)\left(-i\,\epsilon_\perp^{\alpha\beta}\right)\hat{H}_{\mu\nu\alpha\beta}^{(g)}\,, \end{aligned} \tag{4.13}$$

where $\hat{H}_{\mu\nu\alpha\beta}^{(g)}$ is the squared amputated matrix element of the process $g(p)+\gamma^*(q)\to X$ in Figure 4.2(b).

Again we apply factorization to g_{1_q} and g_{1_g} as in Eq. (4.11),

$$g_{1_q} = \frac{e_q^2}{2}\left\{\sum_{q'}\Delta C_{q'}\otimes\Delta\phi_{q'/q}+\Delta C_g\otimes\Delta\phi_{g/q}\right\}, \tag{4.14}$$

$$g_{1_g} = \sum_q\frac{e_q^2}{2}\left\{\Delta C_q\otimes\Delta\phi_{q/g}+\Delta C_g\otimes\Delta\phi_{g/g}\right\}, \tag{4.15}$$

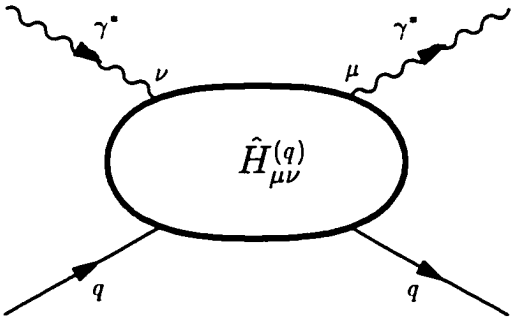

(a)

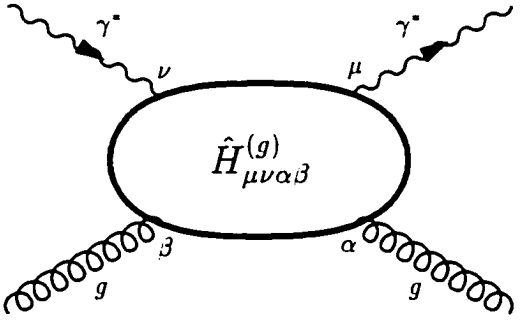

(b)

Figure 4.2 (a) The squared amputated matrix element of the process $q + \gamma^* \to X$. (b) The squared amputated matrix element of the process $g + \gamma^* \to X$.

where $\Delta\phi_{q'/q}$ is the distribution of quark q' inside quark q, $\Delta\phi_{g/q}$ is the distribution of gluon g inside quark q, and etc. Here the coefficient functions $\Delta C_{q'}$ and ΔC_g are redefined so that the factor $e_q^2/2$ is not included. Now both partonic g_1 and $\Delta\phi$ are calculable in perturbative QCD order by order. We expand g_{1_f}, ΔC_q, ΔC_g, and $\Delta\phi_{a/b}$ in the order of $\alpha_s/2\pi$, for example,

$$g_{1_f} = \sum_{n=0}^{\infty} \left(\frac{\alpha_s}{2\pi}\right)^n g_{1_f}^{(n)}, \tag{4.16}$$

$$\Delta\phi_{q'/q} = \sum_{n=0}^{\infty} \left(\frac{\alpha_s}{2\pi}\right)^n \Delta\phi_{q'/q}^{(n)}, \tag{4.17}$$

$$\Delta C_{q'} = \sum_{n=0}^{\infty} \left(\frac{\alpha_s}{2\pi}\right)^n \Delta C_q^{(n)}. \tag{4.18}$$

Using Eq. (4.14) at the leading order (LO), i.e. $n = 0$, the quark part is given by,

$$g_{1_q}^{(0)} = \frac{e_q^2}{2} \left\{ \sum_{q'} \Delta C_{q'}^{(0)} \otimes \Delta\phi_{q'/q}^{(0)} + \Delta C_g^{(0)} \otimes \Delta\phi_{g/q}^{(0)} \right\}. \tag{4.19}$$

Apparently, the zeroth order gluon distribution inside a quark is zero and the quark distribution inside a quark is just the delta function,

$$\Delta\phi_{g/q}^{(0)} = 0, \qquad \Delta\phi_{q'/q}^{(0)} = \delta_{q'q}\,\delta(1-x). \tag{4.20}$$

For $g_{1_q}^{(0)}$, it is corresponding the process $q(p) + \gamma^*(q) \to q(p')$, which can be readily calculated from Eq. (4.12),

$$g_{1_q}^{(0)} = \frac{e_q^2}{2}\,\delta(1-x). \tag{4.21}$$

Thus the zeroth order quark coefficient function is,

$$\Delta C_q^{(0)} = \delta(1-x). \tag{4.22}$$

For the gluon part, using Eq. (4.15) the leading order expansion is given by,

$$g_{1_g}^{(0)} = \sum_q \frac{e_q^2}{2} \left\{ \Delta C_q^{(0)} \otimes \Delta\phi_{q/g}^{(0)} + \Delta C_g^{(0)} \otimes \Delta\phi_{g/g}^{(0)} \right\}. \tag{4.23}$$

Since gluon does not interact directly with the virtual photon, it has no contribution at this order, i.e.

$$\Delta C_g^{(0)} = 0. \tag{4.24}$$

Using Eq. (4.22) and Eq. (4.24), we reproduce the result of the parton model,

$$g_1^h(x,Q^2) = \sum_q \frac{e_q^2}{2}\, \Delta\phi_{q/h}(x,Q^2)\,. \tag{4.25}$$

At leading order, all quantities are finite, and there is no need for renormalization. But it is no longer true at next-to-leading order (NLO) due to the loop structure of the diagrams. As a result, diagrams in g_{1_f} and $\Delta\phi^{(1)}_{f'/f}$ have collinear (CO) and ultraviolet (UV) divergences. (Infrared divergences cancel themselves.) The UV divergences are taken care of by renormalization while the collinear divergences cancel between g_{1_f} and $\Delta\phi^{(1)}_{f'/f}$. In the end, the coefficient functions are finite. The NLO quark part is given by,

$$\begin{aligned}\frac{\alpha_s}{2\pi} g_{1_q}^{(1)} \;=\; & \frac{e_q^2}{2}\left\{ \sum_{q'} \frac{\alpha_s}{2\pi} \Delta C_{q'}^{(0)} \otimes \Delta\phi^{(1)}_{q'/q} \;+\; \frac{\alpha_s}{2\pi} \Delta C_g^{(0)} \otimes \Delta\phi^{(1)}_{g/q} \right. \\ & \left. + \frac{\alpha_s}{2\pi} \sum_{q'} \Delta C_{q'}^{(1)} \otimes \Delta\phi^{(0)}_{q'/q} \;+\; \frac{\alpha_s}{2\pi} \Delta C_g^{(1)} \otimes \Delta\phi^{(0)}_{g/q} \right\}. \end{aligned} \tag{4.26}$$

Using the zeroth order coefficient functions and partonic distributions given by Eqs. (4.22), (4.24) and (4.20), we have,

$$\frac{e_q^2}{2}\, \Delta C_q^{(1)} = g_{1_q}^{(1)} - \frac{e_q^2}{2} \sum_{q'} \Delta\phi^{(1)}_{q'/q}\,. \tag{4.27}$$

Similarly, for the gluon part,

$$\left(\sum_q \frac{e_q^2}{2} \right) \Delta C_g^{(1)} = g_{1_g}^{(1)} - \sum_{q'} \frac{e_q^2}{2}\, \Delta\phi^{(1)}_{q'/g}\,. \tag{4.28}$$

In Eq. (4.27) and Eq. (4.28), the two last terms, $\Delta\phi^{(1)}_{q'/q}$ and $\Delta\phi^{(1)}_{q'/g}$, called subtraction terms, are of crucial importance. They are the collinear contributions residing in the Feynman diagrams of the structure functions. By subtracting them from g_{1_q} and g_{1_g}, we remove the collinear part from the Feynman diagrams and all the remaining is short-distance.

γ_5 Ambiguities in Quark Coefficient Function

In this section, we concentrate on the problem caused by γ_5 ambiguities in polarized parton distributions. To understand this γ_5 problem, we apply the next-leading-order quark distribution within a quark obtained earlier to examine quark coefficient functions in two γ_5 prescriptions and compare their differences. The consistency of the prescriptions are checked by using two different collinear regulators. First, we study the case of HVBM prescription with DR collinear regulator.

HVBM γ_5 with DR collinear regulator

The coefficient function consists of two terms, $g_{1_q}^{(1)}$ and $\Delta\phi_{q'/q}^{(1)}$. For $g_{1_q}^{(1)}$, it can be obtained directly from Eq. (4.12). In Figure 4.3. there are two types of diagrams, virtual and real. Virtual diagrams, namely self-energy and vertex, are relatively simple. They are basically LO diagram with some additional renormalization factors.

$$g_{1_q}^{(1)}\Big|_{\text{vertex}} = g_{1_q}^{(0)} C_F \left(\frac{4\pi\mu^2}{Q^2}\right)^{\epsilon} \frac{\Gamma(1-\epsilon)}{\Gamma(1-2\epsilon)} \left(-\frac{1}{\epsilon^2} - \frac{3}{\epsilon} - 8 - \frac{\pi^2}{3}\right), \tag{4.29}$$

$$g_{1_q}^{(1)}\Big|_{\text{self-energy}} = g_{1_q}^{(0)} C_F \left(\frac{4\pi\mu^2}{Q^2}\right)^{\epsilon} \frac{\Gamma(1-\epsilon)}{\Gamma(1-2\epsilon)} \frac{1}{2} \left(-\frac{1}{\epsilon} + \frac{1}{\epsilon}\right), \tag{4.30}$$

where $C_F = 4/3$ is the color factor, $\epsilon = (4-d)/2$, and $g_{1_q}^{(0)} = \frac{e_q^2}{2}\delta(1-x)$ is the leading order result given by Eq. (4.21). The self-energy diagrams are scaleless, and should be zero. Still we present the full expression here for showing explicitly its soft divergence $(-1/\epsilon)$ and UV divergence $(1/\epsilon)_{\text{UV}}$. In virtual diagrams, there is no UV divergence because of Ward identity — the UV pole of the self-energy diagrams cancel that of the vertex diagram. The total one-loop virtual contribution is,

$$g_{1_q}^{(1v)} = \frac{e_q^2}{2} C_F \left(\frac{4\pi\mu}{Q^2}\right)^{\epsilon} \frac{\Gamma(1-\epsilon)}{\Gamma(1-2\epsilon)} \left(-\frac{2}{\epsilon^2} - \frac{3}{\epsilon} - 8 - \frac{\pi^2}{3}\right) \delta(1-x), \tag{4.31}$$

and all poles are either collinear or IR. As Eq. (4.31) is free of UV divergence, renormalization is not necessary.

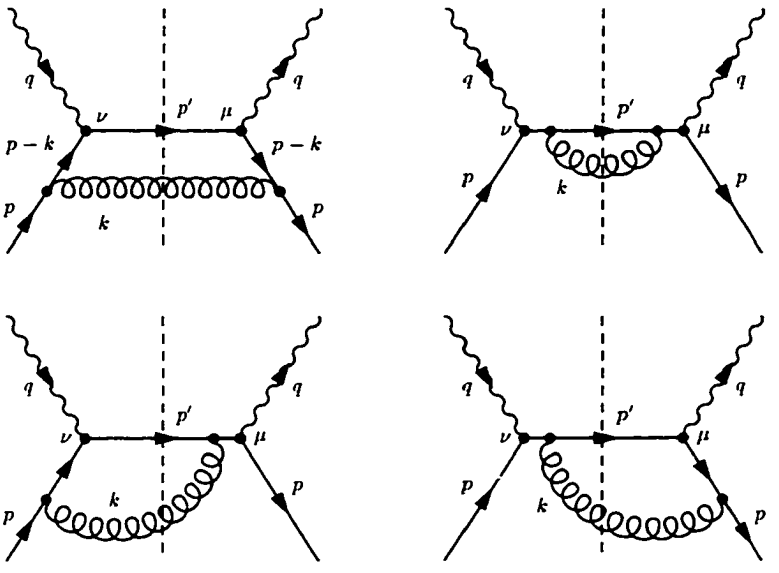

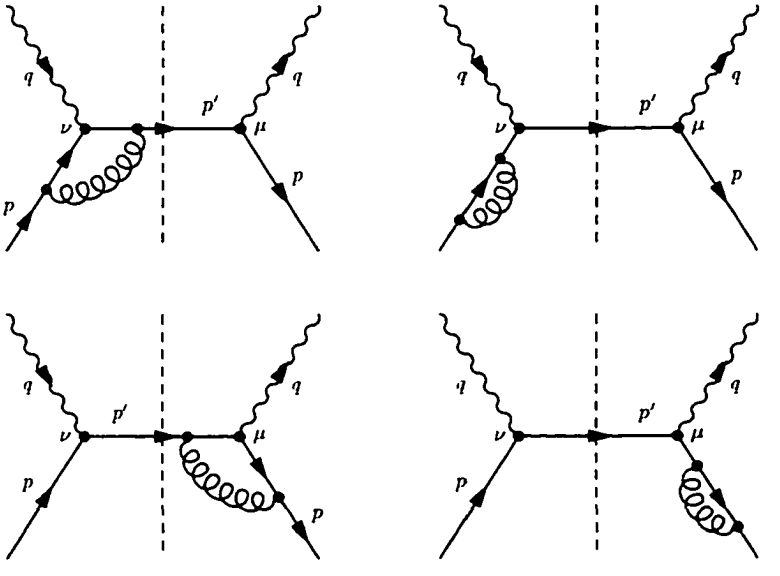

Figure 4.3 Order of α_s diagrams of $\gamma^* + q \rightarrow q + g$. (a) Real diagrams, and (b) virtual diagrams.

However, real diagrams are more complicated due to the emission of a real gluon. The process involved is,

$$q(p) + \gamma^*(q) \rightarrow g(k) + q(p'). \tag{4.32}$$

To simplify the calculation, we adopt the method given by Altarelli, Ellis and Martinelli [40], and work in the C.M. frame of the incoming quark $q(p)$ and virtual photon $\gamma^*(q)$. Define

$$k = (k_0, k_\perp, k_0 \cos\theta), \tag{4.33}$$

$$y = \frac{1}{2}(1 + \cos\theta). \tag{4.34}$$

Then all kinematic variables can be written in terms of x, y and Q^2, e.g.,

$$\begin{aligned} s &= (p+q)^2 = \frac{Q^2(1-x)}{x}, \\ k_0^2 &= \frac{Q^2(1-x)}{4x}, \qquad k_\perp^2 = \frac{Q^2 y(1-y)(1-x)}{x}. \end{aligned} \tag{4.35}$$

The phase space of the final state quark $q(p')$ and gluon $g(k)$ in term of angular variable y is given by,

$$\begin{aligned} \frac{d\Gamma^{(2)}}{8\pi} &= \frac{1}{8\pi}\frac{d^dk}{(2\pi)^d}\frac{d^dp'}{(2\pi)^d}(2\pi)^d\delta(p+q-p-k)(2\pi)\delta_+(p'^2)(2\pi)^2\delta_+(k^2)\,, \\ &= \left(\frac{1}{8\pi}\right)^2\left(\frac{4\pi}{Q^2}\right)^\epsilon \frac{1}{\Gamma(1-\epsilon)}\left[\frac{x}{1-x}\right]^\epsilon y^{-\epsilon}(1-y)^{-\epsilon}\,dy\,. \end{aligned} \tag{4.36}$$

In the last statement, p', k_0 and $k_\perp$ have been integrated. The squared matrix element of all the real diagrams is,

$$\begin{aligned} \frac{i}{2}\epsilon_\perp^{\mu\nu}\mathrm{Tr}\left[\gamma_5\gamma\cdot p\,\hat{H}_{\mu\nu}^{(q,1r)}\right] &= 16\pi\alpha_s e_q^2\mu^{2\epsilon}C_F\left\{\frac{1}{1-y}\left[\frac{1+x^2}{1-x}+3\epsilon(1-x)\right]+4\right. \\ &\left. -\frac{2}{1-x}-2(1-x)+(1-y)\left[\frac{1-\epsilon}{1-x}-2\right]\right\}, \end{aligned} \tag{4.37}$$

After using Eq. (4.12) and integrating over $y \in [0,1]$, all divergences are now regularized

by Dimensional Regularization and expressed as $1/\epsilon$ poles,

$$g_{1_q}^{(1r)} = \frac{e_q^2}{2} C_F \left(\frac{4\pi\mu}{Q^2}\right)^{\epsilon} \frac{\Gamma(1-\epsilon)}{\Gamma(1-2\epsilon)} \left\{ \left(\frac{2}{\epsilon^2} + \frac{3}{2\epsilon} + \frac{7}{2}\right) \delta(1-x) + \left(-\frac{1}{\epsilon}\right) \frac{1+x^2}{(1-x)_+} + \left(1+x^2\right) \left[\frac{\ln(1-x)}{1-x}\right]_+ - \frac{3}{2} \left[\frac{1}{1-x}\right]_+ - \left(\frac{1+x^2}{1-x}\right) \ln x + 5x - 2 \right\}. \quad (4.38)$$

The + distributions, e.g. $1/(1-x)_+$, are the results of expanding $x^\epsilon/(1-x)^{1+\epsilon}$ in the orders of ϵ.

$$\frac{x^\epsilon}{(1-x)^{1+\epsilon}} = -\frac{1}{\epsilon}\delta(1-x) + \frac{1}{(1-x)_+} - \epsilon \left[\frac{\ln(1-x)}{1-x}\right]_+ + \epsilon \frac{\ln x}{1-x} + O(\epsilon^2). \quad (4.39)$$

Combining Eq. (4.31) and Eq. (4.38), the partonic structure function is found to be,

$$g_{1_q}^{(1)}\Big|_{\gamma_5,\mathrm{DR}} = \frac{e_q^2}{2} \left\{ \left(-\frac{1}{\epsilon}\right)_{\mathrm{CO}} \Delta P_{qq}^{(1)}(x) + \ln\left(\frac{Q^2}{\mu_{\overline{\mathrm{MS}}}^2}\right) \Delta P_{qq}^{(1)}(x) + C_F \left[\left(1+x^2\right) \left[\frac{\ln(1-x)}{1-x}\right]_+ - \frac{3}{2} \left[\frac{1}{1-x}\right]_+ - \left(\frac{1+x^2}{1-x}\right) \ln x + 5x - 2 - \left(\frac{9}{2} + \frac{\pi^2}{3}\right) \delta(1-x) \right] \right\}, \quad (4.40)$$

where $\mu_{\overline{\mathrm{MS}}}^2 = 4\pi\mu^2 e^{-\gamma_E}$, γ_E is the usual Euler constant, and $\Delta P_{qq}^{(1)}(x)$ is the well-known quark-to-quark splitting function,

$$\Delta P_{qq}^{(1)}(x) = C_F \left[\frac{1+x^2}{(1-x)_+} + \frac{3}{2}\delta(1-x)\right]. \quad (4.41)$$

Up to this point, there is still no need to perform renormalization — the UV poles of virtual diagrams cancel each other while real diagrams have no UV divergence. That is if there is any γ_5 ambiguity at all in $g_{1_q}^{(1)}$, it must come from the collinear pole. In short, such ambiguity must be part of the collinear sensitive term.

In order to remove the remaining collinear $(-1/\epsilon)_{\mathrm{CO}}$ pole in $g_{1_q}^{(1)}$, it is necessary to compute the subtraction term $\Delta\phi_{q'/q}^{(1)}$, which is represented by the diagrams in Figure 3.5. The detailed gauge invariant Feynman rules for calculating partonic distribution $\Delta\phi_{q'/q}^{(1)}$ are given in Appendix B. From our previous result in Eq. (3.26), the renormalized $\overline{\mathrm{MS}}$

quark distribution is.

$$\Delta\phi_{q/q'}^{(1)}\Big|_{\overline{\rm MS},\gamma_5,{\rm DR}} = \delta_{qq'}\left(\frac{\mu^2}{\mu_f^2}\right)^{\epsilon}\left[\left(-\frac{1}{\epsilon}\right)_{\rm CO}\Delta P_{qq}^{(1)}(x) - \Delta P_{qq}^{(1)}(x)\,\ln\left(4\pi e^{-\gamma_E}\right)\right], \quad (4.42)$$

where we have numerically canceled the $3C_F(1-x)$ in CO and UV parts, and therefore only the collinear pole and the phase factor remain.

Applying Eq. (4.27), the coefficient function in $\overline{\rm MS}$ scheme, HVBM γ_5 prescription and DR collinear regulator is found to be,

$$\begin{aligned}\Delta C_q^{(1)}(x,Q^2/\mu_f^2)\Big|_{\overline{\rm MS},\gamma_5,{\rm DR}} &= \ln\left(\frac{Q^2}{\mu_f^2}\right)\Delta P_{qq}^{(1)}(x) + C_F\left\{\left(1+x^2\right)\left[\frac{\ln(1-x)}{1-x}\right]_+\right.\\ &\quad -\frac{3}{2}\left[\frac{1}{1-x}\right]_+ - \left(\frac{1+x^2}{1-x}\right)\ln x\\ &\quad \left.+5x-2-\left(\frac{9}{2}+\frac{\pi^2}{3}\right)\delta(1-x)\right\}. \end{aligned} \quad (4.43)$$

While using our new UVS scheme, the hard part is given by,

$$\Delta C_q^{(1)}(x,Q^2/\mu_f^2)\Big|_{\rm UVS,\gamma_5,DR} = \Delta C_q^{(1)}(x,Q^2/\mu_f^2)\Big|_{\overline{\rm MS},\gamma_5,{\rm DR}} + 3C_F(1-x). \quad (4.44)$$

As expected, the hard parts in both schemes are now free of any collinear divergence.

HVBM γ_5 with off-shell collinear regulator

Other than using Dimensional Regularization as the collinear regulator, we may put the incoming quark off-shell so that $p^2 \neq 0$. In that case, both structure function and parton distribution look very different from those of Dimensional Regularization. The structure function is,

$$\begin{aligned} g_{1_q}^{(1)}\Big|_{\gamma_5,p^2\neq 0} &= \frac{e_q^2}{2}\left\{\ln\left(\frac{Q^2}{-p^2}\right)\Delta P_{qq}^{(1)}(x) - C_F\left[\frac{3}{2}\left[\frac{1}{1-x}\right]_+\right.\right.\\ &\quad \left.\left.+2\left(\frac{1+x^2}{1-x}\right)\ln x - 2x + \left(1+\frac{2\pi^2}{3}\right)\delta(1-x)\right]\right\}, \end{aligned} \quad (4.45)$$

and from Eq. (3.46) the $\overline{\rm MS}$ renormalized quark distribution within a quark is,

$$\Delta\phi^{(1)}_{q/q'}(x)\Big|_{\overline{\rm MS},\gamma_5,p^2\neq 0} = \delta_{qq'}\left\{\Delta P^{(1)}_{qq}(x)\,\ln\left(\frac{\mu_f^2}{-p^2}\right) - C_F\left[(1+x^2)\left(\frac{\ln(1-x)}{1-x}\right)_+ + \left(\frac{1+x^2}{1-x}\right)\ln(x) + 1 - \left(\frac{7}{2}-\frac{\pi^2}{3}\right)\delta(1-x)\right] + 3\,C_F\,(1-x)\right\}. \tag{4.46}$$

Using Eq. (4.45) and Eq. (4.46) the coefficient function for $p^2 \neq 0$ collinear regulator is,

$$\Delta C^{(1)}_q(x,Q^2/\mu_f^2)\Big|_{\overline{\rm MS},\gamma_5,p^2\neq 0} = \Delta C^{(1)}_q(x,Q^2/\mu_f^2)\Big|_{\overline{\rm MS},\gamma_5,\rm DR}. \tag{4.47}$$

Similarly, for UVS scheme, we have,

$$\Delta C^{(1)}_q(x,Q^2/\mu_f^2)\Big|_{\rm UVS,\gamma_5,p^2\neq 0} = \Delta C^{(1)}_q(x,Q^2/\mu_f^2)\Big|_{\rm UVS,\gamma_5,DR}. \tag{4.48}$$

They are exactly the same as the one obtained by Dimensional Regularization. As is shown, the subtraction term and structure function can be very different in different regularization schemes; nevertheless, the short-distance coefficient function is not affected by the choice of collinear regulators.

CFH γ_5 with both DR and off-shell collinear regulators

In CFH (γ_5) prescription, due to the non-cyclicity of spinor trace, one has to assign a vertex as the reading point for all traces. In our calculation, we choose the quark-gluon vertex. In this prescription, we encounter the same situation as before. The expressions of $g^{(1)}_{1_q}$ and $\Delta\phi^{(1)}_{q'/q}$ are different with different collinear regulators, while the final coefficient function is independent of regulators. The hard parts in $\overline{\rm MS}$ and UVS schemes are,

(i) $\overline{\rm MS}$

$$\Delta C^{(1)}_q(x,Q^2/\mu_f^2)\Big|_{\overline{\rm MS},\gamma_5'} = \Delta C^{(1)}_q(x,Q^2/\mu_f^2)\Big|_{\overline{\rm MS},\gamma_5} + 4C_F(1-x) \tag{4.49}$$

(ii) UVS

$$\Delta C_q^{(1)}(x, Q^2/\mu_f^2)\Big|_{\text{UVS},\gamma_5'} = \Delta C_q^{(1)}(x, Q^2/\mu_f^2)\Big|_{\text{UVS},\gamma_5}, \tag{4.50}$$

for both Dimensional Regularization and $p^2 \neq 0$ collinear regulators.

Chirality and Bjorken sum rule

In the above example, we have seen that the quark coefficient functions obtained from the two γ_5 prescriptions are in general not the same. In $\overline{\text{MS}}$ scheme their differences are actually result of different treatments of chiral symmetry. In HVBM prescription, γ_5 satisfies commutation relation rather than anticommutation relation with the $(d-4)$-dimensional γ-matrices (see Eq. (A.1) and Eq. (A.2)), and is being treated as a 4-dimensional object. Owing to this difference in treating dimensions $\mu = 0, 1, 2, 3$ and $\mu > 3$, we therefore expect that the coefficient function obtained in HVBM prescription does not respect chiral symmetry. To demonstrate this chiral symmetry breaking, we apply the HVBM ($\overline{\text{MS}}$) coefficient function to Bjorken sum rule [4]. Taking the first moment of Eq. (4.11), we have,

$$\begin{aligned}\Gamma_1^h(Q^2) &= \int_0^1 dx\, g_1^h(x, Q^2) \\ &= \sum_q \Delta\bar{C}_q\left(\frac{Q^2}{\mu_f^2}\right)\Delta\bar{\phi}_{q/h}\left(\mu_f^2\right) + \Delta\bar{C}_g\left(\frac{Q^2}{\mu_f^2}\right)\Delta\bar{\phi}_{g/h}\left(\mu_f^2\right).\end{aligned} \tag{4.51}$$

Assuming both proton p and neutron n have the same gluon distribution, the difference between Γ_1^p and Γ_1^n is given by,

$$\begin{aligned}\Gamma_1^p(Q^2) - \Gamma_1^n(Q^2) &= \sum_q \Delta\bar{C}_q\left(\frac{Q^2}{\mu_f^2}\right)\left[\Delta\bar{\phi}_{q/p}\left(\mu_f^2\right) - \Delta\bar{\phi}_{q/n}\left(\mu_f^2\right)\right], \\ &= \left(1 + \frac{\alpha_s}{2\pi}\Delta\bar{C}_q^{(1)} + O(\alpha_s^2)\right) \\ &\quad \times \sum_q \frac{e_q^2}{2}\left[\Delta\bar{\phi}_{q/p}\left(Q^2\right) - \Delta\bar{\phi}_{q/n}\left(Q^2\right)\right].\end{aligned} \tag{4.52}$$

In the last statement, we expand $\Delta\bar{C}_q$ to the order of α_s and assume $\mu_f^2 \approx Q^2$. From the definition of parton distribution given by Eq. (3.6), the axial current is related to

the first moment of the parton distribution by,

$$\begin{aligned} j_{5,+}^{(h)} &= \sum_q e_q^2 \left\langle h(p,s_h) \left| \overline{\psi}_q(0)\gamma_+\gamma_5\psi_q(0) \right| h(p,s_h) \right\rangle , \\ &= 4p_+ \sum_q \frac{e_q^2}{2} \Delta\bar{\phi}_{q/h}. \end{aligned} \tag{4.53}$$

Using the Bjorken sum rule, Eq. (4.52) becomes,

$$\Gamma_1^p - \Gamma_1^n = \frac{1}{4p_+} \left(j_{5,+}^{(p)} - j_{5,+}^{(n)} \right) \left(1 + \frac{\alpha_s}{2\pi} \Delta\bar{C}_q^{(1)} + O(\alpha_s^2) \right) , \tag{4.54}$$

$$= \frac{1}{6} \left| \frac{g_A}{g_V} \right| \left(1 + \frac{\alpha_s}{2\pi} \Delta\bar{C}_q^{(1)} + O(\alpha_s^2) \right) . \tag{4.55}$$

In the last equation, we use the result from Ref. [4],

$$\frac{1}{4p_+} \left(j_{5,+}^{(p)} - j_{5,+}^{(n)} \right) = \frac{1}{6} \left| \frac{g_A}{g_V} \right| . \tag{4.56}$$

Now if we naively apply our result from HVBM ($\overline{\text{MS}}$) γ_5 prescription, the NLO Bjorken sum rule would read,

$$\Gamma_1^p - \Gamma_1^n = \frac{1}{6} \left| \frac{g_A}{g_V} \right| \left(1 - \frac{7}{3} \frac{\alpha_s}{\pi} + O(\alpha_s^2) \right) . \tag{4.57}$$

Of course, this is quite different from the well-known result. The discrepancy is a direct manifestation of chiral symmetry breaking. In using Bjorken sum rule, conservation of axial current j_5^μ is assumed, which is not true in HVBM ($\overline{\text{MS}}$) prescription. In order to remove this spurious anomaly and restore the explicit chiral symmetry in axial current, we apply an overall finite renormalization factor to the axial current j_5^μ in HVBM ($\overline{\text{MS}}$) prescription. Such renormalization factor for HVBM ($\overline{\text{MS}}$) prescription has been worked out in numerous literatures [36, 41, 42, 43, 44]. At the order of the α_s, it is given by,

$$j_5^\mu \Big|_{chiral} = \left(1 - C_F \frac{\alpha_s}{\pi} + O(\alpha_s^2) \right) j_5^\mu \Big|_{\overline{\text{MS}},\gamma_5(HVBM)} . \tag{4.58}$$

To rewrite Eq. (4.54) in terms of chiral axial currents, we multiply the renormalization factor $(1 - C_F \frac{\alpha_s}{\pi})$ to the non-chiral axial currents and $(1 - C_F \frac{\alpha_s}{\pi})^{-1}$ to the coefficient

function. The result is,

$$\Gamma_1^p - \Gamma_1^n = \frac{1}{6}\left|\frac{g_A}{g_V}\right|\left(1 - \frac{\alpha_s}{\pi} + O(\alpha_s^2)\right), \tag{4.59}$$

which is the usual chirality-conserved Bjorken sum rule that we know.

In the case of CFH ($\overline{\rm MS}$) prescription, γ_5' is deliberately constructed so that it anticommutes with all γ-matrices, and hence, respects chiral symmetry. Consequently, there is no need to adjust the axial current. In fact, we can directly apply the coefficient functions obtained in CFH ($\overline{\rm MS}$) prescription. The first moment of coefficient function $\Delta\bar{C}_q^{(1)}\Big|_{\overline{\rm MS},\gamma_5'} = -2$. And the result is, as expected, exactly the same as Eq. (4.59).

Thus, we have demonstrated that the difference of quark coefficient functions from the two γ_5 prescriptions in $\overline{\rm MS}$ scheme is only a result of treating chiral symmetry differently. These two coefficient functions are both consistent with respect to the factorization, and they can be transformed to each other by Eq. (4.49). Furthermore, despite its seeming difficulty of spurious anomaly, HVBM ($\overline{\rm MS}$) prescription can still reproduce the usual chirality-conserved Bjorken sum rule. In fact, as mentioned earlier, there is no a priori reason for polarized parton distributions or coefficient functions to be chiral since they are not direct physical observables. In a sense, whether they respect chiral symmetry or not is only a matter of taste. On the other hand, for any γ_5 prescription, it is crucial to ensure the prescription is consistent with factorization theorem so that we can use the prescription to extracted polarized parton distributions, and have meaningful tests in various polarized experiments. Otherwise, all results will be rendered useless.

Of course this kind of γ_5 ambiguity is intrinsic in any factorization procedure due to the freedom of factorization/renormalization scheme. The goal of the new UVS scheme is to eliminate this extra degree of freedom by demanding all UV related terms in polarized distribution to be removed so that only those collinear sensitive terms will remain. From our examples in Eq. (4.48) and Eq. (4.50), it is confirmed that UV subtraction scheme eliminates this ambiguity and gives unique results of short-distance hard parts.

Anomalous Ambiguities in Gluon Coefficient Functions

In addition to the above γ_5 ambiguities, there is the question of how to handle anomalous contribution in polarized parton distributions [28, 29, 45, 46]. In the following, we again employ the two γ_5 prescriptions, with both collinear regulators, to study this anomalous contribution. The calculation of these gluon parts is almost the same as that of the quark, thus the details are being omitted, and we simply list the results.

HVBM γ_5 with both DR and off-shell collinear regulators

For HVBM prescription, the quark distribution within a gluon and coefficient function have already been studied by Bodwin and Qiu [30] using various collinear regulators. For completeness, their results are listed below. The structure functions $g_{1_g}^{(1)}$, shown in Figure 4.4, are given by,

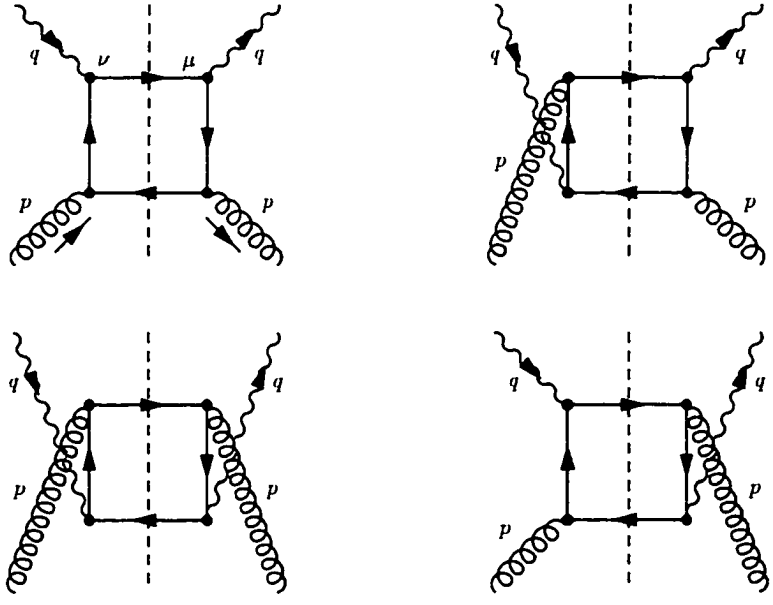

Figure 4.4 Diagrams of order of α_s $\gamma^* + g \rightarrow q + \bar{q}$ process.

(i) Dimensional Regularization (DR)

$$g_{1_g}^{(1)}\Big|_{\gamma_5,\mathrm{DR}} = \left(\sum_q \frac{e_q^2}{2}\right)\left\{\Delta P_{qg}^{(1)}(x)\left[\left(-\frac{1}{\epsilon}\right)_{\mathrm{CO}} + \ln\left(\frac{Q^2}{\mu^2_{\overline{\mathrm{MS}}}}\right) + \ln\left(\frac{1-x}{x}\right) - 1\right] + 2\,T_F(1-x)\right\}, \tag{4.60}$$

(ii) Off-shell ($p^2 \neq 0$)

$$g_{1_g}^{(1)}\Big|_{\gamma_5,p^2\neq 0} = \left(\sum_q \frac{e_q^2}{2}\right)\Delta P_{qg}^{(1)}(x)\left[\ln\left(\frac{Q^2}{-p^2}\right) - \ln(x^2) - 2\right], \tag{4.61}$$

where $T_F = 1/2$ is the color factor and $\Delta P_{qg}^{(1)}(x) = T_F(2x-1)$ is the gluon-to-quark splitting function. And the unrenormalized distributions are,

(i) DR

$$\Delta\phi_{q/g}^{(1)}\Big|_{\gamma_5,\mathrm{DR}} = \left(\frac{\mu^2_{\overline{\mathrm{MS}}}}{\mu_f^2}\right)^{\epsilon}\left[\left(-\frac{1}{\epsilon}\right)_{\mathrm{CO}} + \left(\frac{1}{\epsilon}\right)_{\mathrm{UV}}\right]\left[\Delta P_{qg}^{(1)}(x) - 2\epsilon T_F(1-x)\right], \tag{4.62}$$

(ii) $p^2 \neq 0$

$$\Delta\phi_{q/g}^{(1)}\Big|_{\gamma_5,p^2\neq 0} = \left(\frac{\mu^2_{\overline{\mathrm{MS}}}}{\mu_f^2}\right)^{\epsilon}\left(\frac{1}{\epsilon}\right)_{\mathrm{UV}}\left[\Delta P_{qg}^{(1)}(x) - 2\epsilon T_F(1-x)\right] + \Delta P_{qg}^{(1)}(x)\left[\ln\left(\frac{\mu_f^2}{-p^2}\right) - \ln\Big[x(1-x)\Big] - 1\right]. \tag{4.63}$$

Note that in the last equation, $\left(\mu^2_{\overline{\mathrm{MS}}}/\mu_f^2\right)^{\epsilon} = \left(\mu^2/\mu_f^2\right)^{\epsilon}[1+\ln(4\pi\mathrm{e}^{-\gamma_E})]$. Finally the gluon coefficient functions, calculated from Eq. (4.28), are given by,

(i) $\overline{\mathrm{MS}}$

$$\Delta C_g^{(1)}(x,Q^2/\mu_f^2)\Big|_{\overline{\mathrm{MS}},\gamma_5} = \Delta P_{qg}^{(1)}(x)\left[\ln\left(\frac{Q^2}{\mu_f^2}\right) + \ln\left(\frac{1-x}{x}\right) - 1\right] + 2\,T_F(1-x)\,. \tag{4.64}$$

(i) UVS

$$\Delta C_g^{(1)}(x,Q^2/\mu_f^2)\Big|_{\mathrm{UVS},\gamma_5} = \Delta C_g^{(1)}(x,Q^2/\mu_f^2)\Big|_{\overline{\mathrm{MS}},\gamma_5} - 2T_F(1-x). \tag{4.65}$$

Like their quark counterparts, they are independent of the choice of regulators.

CFH γ_5 with both DR and off-shell collinear regulators

In γ_5' prescription, there is no need to calculate the $g_{1_g}^{(1)}$ term again because it is independent of γ_5. For the distribution term $\Delta\phi_{q/g}^{(1)}$, shown in Figure 3.6, it does depend on the choice of γ_5 prescription. One has to pay extra attention to the choice of the reading point in γ_5' prescription. Since the cut-vertex in Figure 3.6, i.e. the one with γ_5', is non-local, it cannot be used as the reading point. Instead we have to use the quark-gluon vertex, same as the one chosen in the calculation of quark distribution and coefficient function. The unrenormalized quark distributions within a gluon are now,

(i) DR

$$\Delta\phi_{q/g}^{(1)}\Big|_{\gamma_5',\mathrm{DR}} = \left(\frac{\mu_{\overline{\mathrm{MS}}}^2}{\mu_f^2}\right)^{\epsilon}\left[\left(-\frac{1}{\epsilon}\right)_{\mathrm{CO}} + \left(\frac{1}{\epsilon}\right)_{\mathrm{UV}}\right]\Delta P_{qg}^{(1)}(x), \tag{4.66}$$

(ii) $p^2 \neq 0$

$$\begin{aligned}\Delta\phi_{q/g}^{(1)}\Big|_{\gamma_5',p^2\neq 0} &= \left(\frac{\mu_{\overline{\mathrm{MS}}}^2}{\mu_f^2}\right)^{\epsilon}\left(\frac{1}{\epsilon}\right)_{\mathrm{UV}}\Delta P_{qg}^{(1)}(x) \\ &\quad + \Delta P_{qg}^{(1)}(x)\left[\ln\left(\frac{\mu_f^2}{-p^2}\right) - \ln\Big[x(1-x)\Big] - 1\right],\end{aligned} \tag{4.67}$$

In both cases, the unrenormalized distributions differ from their HVBM counterparts. Nevertheless, in Dimensional Regularization the difference does not affect the $\overline{\mathrm{MS}}$ renormalized result. The reason is that in Dimensional Regularization the collinear divergence is exactly the opposite of the UV divergence and the contribution of anomaly is of the order of ϵ; thus, after renormalization, the difference disappears. For off-shell gluon, the situation is very different. The collinear divergence is no longer the opposite of the UV divergence, consequently, the difference shows up in the short-distance coefficient function,

(i) DR

$$\begin{aligned}\Delta C_g^{(1)}(x,Q^2/\mu_f^2)\Big|_{\overline{\mathrm{MS}},\gamma_5',\mathrm{DR}} &= \Delta P_{qg}^{(1)}(x)\left[\ln\left(\frac{Q^2}{\mu_f^2}\right) + \ln\left(\frac{1-x}{x}\right) - 1\right] \\ &\quad + 2\,T_F(1-x),\end{aligned} \tag{4.68}$$

(ii) $p^2 \neq 0$

$$\Delta C_g^{(1)}(x, Q^2/\mu_f^2)\Big|_{\overline{\rm MS},\gamma_5',p^2\neq 0} = \Delta C_g^{(1)}(x, Q^2/\mu_f^2)\Big|_{\overline{\rm MS},\gamma_5',\rm DR} - 2T_F(1-x). \quad (4.69)$$

For the new UVS scheme, since there is no ϵ term associated with the UV $(1/\epsilon)_{\rm UV}$ pole, the results are the same as $\overline{\rm MS}$.

(i) DR

$$\Delta C_g^{(1)}(x, Q^2/\mu_f^2)\Big|_{\rm UVS,\gamma_5',DR} = \Delta C_g^{(1)}(x, Q^2/\mu_f^2)\Big|_{\overline{\rm MS},\gamma_5',\rm DR}, \quad (4.70)$$

(ii) $p^2 \neq 0$

$$\Delta C_g^{(1)}(x, Q^2/\mu_f^2)\Big|_{\rm UVS,\gamma_5',p^2\neq 0} = \Delta C_g^{(1)}(x, Q^2/\mu_f^2)\Big|_{\overline{\rm MS},\gamma_5',p^2\neq 0}. \quad (4.71)$$

Apparently in γ_5' prescription, the gluon coefficient function in $\overline{\rm MS}$ depends on the choice of collinear regulators. Such unexpected collinear dependence, as discussed before, implies inconsistency in the scheme. This inconsistency arises from the presence of anomaly in the triangular diagram. As pointed out by Körner, Kreimer and Schilcher [47] that in the presence of anomaly, one has to use the axial vertex, i.e γ_5' vertex, as the reading point. However, for $\Delta\phi_{q/g}^{(1)}$, such possibility is being ruled out due to the non-local nature of the cut-vertex. For this reason, the quark distribution within a gluon obtained by using $p^2 \neq 0$ collinear regulator contains no anomalous contribution which, of course, is incorrect. Therefore, we may label the gluon coefficient function in Eq. (4.69) as,

$$\Delta C_g^{(1)}(x, Q^2/\mu_f^2)\Big|_{\overline{\rm MS},\gamma_5',\text{no-anomaly}} = \Delta P_{qg}^{(1)}(x)\left[\ln\left(\frac{Q^2}{\mu_f^2}\right) + \ln\left(\frac{1-x}{x}\right) - 1\right]. \quad (4.72)$$

To confirm that Eq. (4.68) is indeed the coefficient function contains correct anomalous contribution, we treat the axial cut-vertex as if it were local, and choose it as the reading point. Then the anomalous contribution should be correctly included. The distributions $\Delta\phi_{q/g}^{(1)}\Big|_{\gamma_5'}$ in both regulators now are given by,

(i) DR, Axial-vertex reading point

$$\Delta\phi_{q/g}^{(1)}\Big|_{\gamma_5',\mathrm{DR,Axial}} = \Delta\phi_{q/g}^{(1)}\Big|_{\gamma_5,\mathrm{DR}}, \tag{4.73}$$

(ii) $p^2 \neq 0$, Axial-vertex reading point

$$\Delta\phi_{q/g}^{(1)}\Big|_{\gamma_5',p^2\neq 0,\mathrm{Axial}} = \Delta\phi_{q/g}^{(1)}\Big|_{\gamma_5,p^2\neq 0}. \tag{4.74}$$

From which the coefficient function can be extracted, and is the same for both collinear regulators and also identical to those obtained in HVBM prescription,

$$\Delta C_g^{(1)}(x,Q^2/\mu_f^2)\Big|_{\overline{\mathrm{MS}},\gamma_5',\mathrm{Axial}} = \Delta C_g^{(1)}(x,Q^2/\mu_f^2)\Big|_{\overline{\mathrm{MS}},\gamma_5}, \tag{4.75}$$

$$\Delta C_g^{(1)}(x,Q^2/\mu_f^2)\Big|_{\mathrm{UVS},\gamma_5',\mathrm{Axial}} = \Delta C_g^{(1)}(x,Q^2/\mu_f^2)\Big|_{\mathrm{UVS},\gamma_5}. \tag{4.76}$$

Although it may seem plausible to forget about the non-local nature of the cut-vertex and "define" the distributions $\Delta\phi_{q/g}^{(1)}$ by using the γ_5' vertex as the reading point. Such redefinition has shown to cause problem in polarized Drell-Yan processes [37].

Finally, the explicit expression of the anomalous contribution in x-space can be extracted by taking the difference of Eq. (4.72) and Eq. (4.75),

$$\begin{aligned}\Delta C_g^{(1)}(x,Q^2/\mu_f^2)\Big|_{\mathrm{anomaly}} &= \Delta C_g^{(1)}(x,Q^2/\mu_f^2) - \Delta C_g^{(1)}(x,Q^2/\mu_f^2)\Big|_{\mathrm{no\text{-}anomaly}} \\ &= 2\,T_F(1-x).\end{aligned} \tag{4.77}$$

Or, if one prefers the anomalous contribution inside $\Delta\phi_{q/g}^{(1)}$,

$$\begin{aligned}\Delta\phi_{q/g}^{(1)}(x)\Big|_{\mathrm{anomaly}} &= \Delta\phi_{q/g}^{(1)}(x) - \Delta\phi_{q/g}^{(1)}(x)\Big|_{\mathrm{no\text{-}anomaly}} \\ &= -2\,T_F(1-x).\end{aligned} \tag{4.78}$$

As pointed out previously, the above result is in x-space which means it is non-local; only its first moment can be regarded as anomaly in the axial current.

Axial Ward identity and anomalous contribution

So far, we have calculated the explicit anomalous contribution term by deliberately using the wrong reading point in CFH γ_5 prescription. But, it is also possible to calculate the anomalous contribution term directly by imposing the axial current Ward identity to the axial vertex in the triangular diagram in Figure 3.6. Consider the axial current j_5^μ in HVBM prescription,

$$j_5^\mu(x) \;=\; \frac{1}{2}\,\bar{\psi}_q(x)\,[\,\gamma^\mu,\gamma_5\,]\,\psi_q(x). \tag{4.79}$$

The commutator is inserted to make sure $j_5^\mu(x)$ is Hermitian. For an axial vertex attached with two propagators, as in Figure 4.5(a), it can be written as,

$$\Gamma_5^\mu(k',k) = \frac{\gamma\cdot k'}{k'^2}\,\bar{\gamma}^\mu\gamma_5\,\frac{\gamma\cdot k}{k^2}. \tag{4.80}$$

The definitions of $\bar{\gamma}^\mu$ and $\hat{\gamma}^\mu$ are given in Appendix A. Contract the vertex with $(k'-k)^\mu$,

$$\begin{aligned}(k'-k)_\mu\Gamma_5^\mu(k',k) \;=\; & \left[\gamma_5\frac{\gamma\cdot\bar{k}}{k^2} + \frac{\gamma\cdot\bar{k}'}{k'^2}\gamma_5\right] + \gamma_5\frac{\gamma\cdot\hat{k}}{k^2} + \gamma_5\frac{\gamma\cdot\hat{k}'}{k'^2} \\ & - \frac{\gamma\cdot k'}{k'^2}\left(\gamma\cdot\hat{k}'+\gamma\cdot\hat{k}\right)\gamma_5\frac{\gamma\cdot k}{k^2}\end{aligned} \tag{4.81}$$

The first two terms in square brackets are merely the usual axial Ward identity, i.e. the chiral symmetry conserving parts. Whereas the last three terms violate chirality and contribute to anomaly residing in the parton distribution $\Delta\phi_{q/g}^{(1)}$. As we may expect, these chirality breaking terms vanish as $d\to 4$ (i.e. $\hat{k}',\hat{k}\to 0$). Therefore, we may write the chirality breaking terms as,

$$(k'-k)_\mu\Gamma_5^\mu\Big|_{cb}(k',k) = \gamma_5\frac{\gamma\cdot\hat{k}}{k^2} + \gamma_5\frac{\gamma\cdot\hat{k}'}{k'^2} - \frac{\gamma\cdot k'}{k'^2}\left(\gamma\cdot\hat{k}'+\gamma\cdot\hat{k}\right)\gamma_5\frac{\gamma\cdot k}{k^2}, \tag{4.82}$$

where the subscript cb denotes chirality breaking. By writing $k'\to k+p/2$ and $k\to k-p/2$ and taking the derivative of p, it becomes,

$$\Gamma_5^\mu\Big|_{cb}(k,k) = \frac{1}{2}\left(\frac{\partial}{\partial k'_\mu}-\frac{\partial}{\partial k_\mu}\right)\Big|_{p_\mu=0}\frac{\gamma\cdot k'}{k'^2}\left(\gamma\cdot\hat{k}'+\gamma\cdot\hat{k}\right)\gamma_5\frac{\gamma\cdot k}{k^2}, \tag{4.83}$$

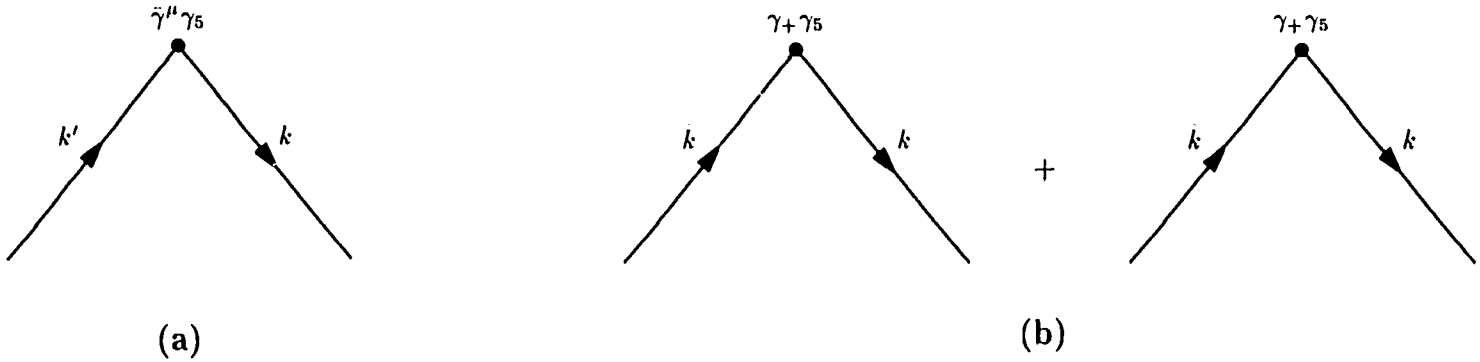

Figure 4.5 (a) The Γ_5^μ vertex in HVBM prescription. (b) The chirality breaking parts of the vertex.

where we have used the relation,

$$\frac{\partial}{\partial p_\mu}\Big|_{p_\mu=0} = \frac{1}{2}\left(\frac{\partial}{\partial k'_\mu} - \frac{\partial}{\partial k_\mu}\right)\Big|_{p_\mu=0}. \tag{4.84}$$

The component of interest is along the + direction and given by (see Figure 4.5(b)),

$$\Gamma_{5,+}\Big|_{cb}(k,k) = \frac{\gamma\cdot\hat{k}}{k^2}\gamma_+\gamma_5\frac{\gamma\cdot k}{k^2} + \frac{\gamma\cdot k}{k^2}\gamma_+\gamma_5\frac{\gamma\cdot\hat{k}}{k^2}, \tag{4.85}$$

which are the chirality breaking terms, or anomalous contribution parts, associated with the axial vertex $\gamma_+\gamma_5$. In Figure 4.6, this anomalous contribution in the subtraction term $\Delta\phi^{(1)}_{q/g}$ is represented by two Feynman diagrams, whose UV part can be readily calculated,

$$\Delta\phi^{(1)}_{q/g}(x)\Big|_{\text{anomaly, UV}} = -2T_F(1-x), \tag{4.86}$$

and is exactly the same as we have found earlier in Eq. (4.78). Since we have used DR for both UV and collinear divergences, the collinear part of the diagrams in Figure 4.5(b) is just the same except for a sign difference, i.e. $\Delta\phi^{(1)}_{q/g}(x)\Big|_{\text{anomaly, CO}} = 2T_F(1-x)$. As stated in earlier chapter, the inclusion of this UV term is scheme dependent. In fact, in

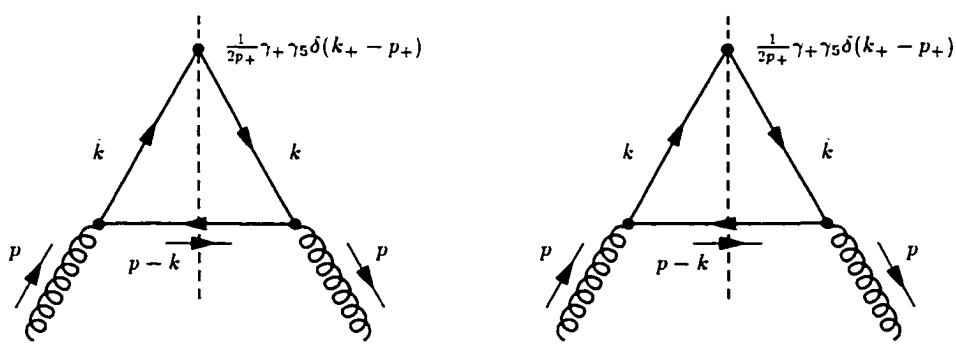

Figure 4.6 Feynman diagrams for chirality breaking parts of the $O(\alpha_s)$ quark distribution inside a gluon.

the new UVS scheme, this UV anomalous contribution $-2T_F(1-x)$ is eliminated from $\Delta\phi^{(1)}_{q/g}(x)$ because of its short-distance nature.

Although it is tempting to extend the above analysis to quark distribution and coefficient function, the method will fail. The reason is that Eq. (4.85) is not gauge invariant and for $\Delta\phi^{(1)}_{q'/q}$, such gauge dependence is crucial as we can see a gluon is always present in all the diagrams (see Figure 3.5 and Figure 3.4). However, in the special case of first order gluon subtraction term the lack of gauge invariance poses no problem since $\Delta\phi^{(1)}_{q/g}$ itself is gauge independent.

Finally, the results of the quark and gluon coefficient functions from different γ_5 prescriptions and collinear regulators are summarized in Tables 4.1, 4.2 and 4.3.

Table 4.1 Coefficient functions from $\overline{\rm MS}$ HVBM γ_5 prescription.

Collinear Regulator: DR	
$g_{1_q}^{(1)}(x,Q^2)$	$\frac{e_q^2}{2}\left\{\left(-\frac{1}{\epsilon}\right)_{\rm CO}\Delta P_{qq}^{(1)}(x)+\ln\left(Q^2/\mu^2_{\overline{\rm MS}}\right)\Delta P_{qq}^{(1)}(x)+C_F\left[\left(1+x^2\right)\left[\frac{\ln(1-x)}{1-x}\right]_+\right.\right.$ $\left.\left.-\frac{3}{2}\left[\frac{1}{1-x}\right]_+-\left(\frac{1+x^2}{1-x}\right)\ln x+5x-2-\left(\frac{9}{2}+\frac{\pi^2}{3}\right)\delta(1-x)\right]\right\}$
$\Delta\phi_{q'/q}^{(1)}(x)$	$\delta_{q'q}\left(\mu^2_{\overline{\rm MS}}/\mu_f^2\right)^{\epsilon}\left[\left(-\frac{1}{\epsilon}\right)_{\rm CO}+\left(\frac{1}{\epsilon}\right)_{\rm UV}\right]\left[\Delta P_{qq}^{(1)}(x)+3\epsilon C_F(1-x)\right]$
$\Delta C_q^{(1)}(x,Q^2/\mu_f^2)$	$\ln\left(Q^2/\mu_f^2\right)\Delta P_{qq}^{(1)}(x)+C_F\left\{\left(1+x^2\right)\left[\frac{\ln(1-x)}{1-x}\right]_+-\frac{3}{2}\left[\frac{1}{1-x}\right]_+\right.$ $\left.-\left(\frac{1+x^2}{1-x}\right)\ln x+5x-2-\left(\frac{9}{2}+\frac{\pi^2}{3}\right)\delta(1-x)\right\}$
$g_{1_g}^{(1)}(x)$	$\left(\sum_q\frac{e_q^2}{2}\right)\left\{\Delta P_{qg}^{(1)}(x)\left[\left(-\frac{1}{\epsilon}\right)_{\rm CO}+\ln\left(Q^2/\mu^2_{\overline{\rm MS}}\right)+\ln\left(\frac{1-x}{x}\right)-1\right]+2T_F(1-x)\right\}$
$\Delta\phi_{q/g}^{(1)}(x)$	$\left(\mu^2_{\overline{\rm MS}}/\mu_f^2\right)^{\epsilon}\left[\left(-\frac{1}{\epsilon}\right)_{\rm CO}+\left(\frac{1}{\epsilon}\right)_{\rm UV}\right]\left[\Delta P_{qg}^{(1)}(x)-2\epsilon T_F(1-x)\right]$
$\Delta C_g^{(1)}(x,Q^2/\mu_f^2)$	$\Delta P_{qg}^{(1)}(x)\left[\ln\left(Q^2/\mu_f^2\right)+\ln\left(\frac{1-x}{x}\right)-1\right]+2T_F(1-x)$
Collinear Regulator: $p^2\neq 0$	
$g_{1_q}^{(1)}(x,Q^2)$	$\frac{e_q^2}{2}\left\{\ln\left(\frac{Q^2}{-p^2}\right)\Delta P_{qq}^{(1)}(x)+C_F\left[-\frac{3}{2}\left[\frac{1}{1-x}\right]_+-2\left(\frac{1+x^2}{1-x}\right)\ln x\right.\right.$ $\left.\left.+2x-\left(1+\frac{2\pi^2}{3}\right)\delta(1-x)\right]\right\}$
$\Delta\phi_{q'/q}^{(1)}(x)$	$\delta_{q'q}\left\{\left(\frac{1}{\epsilon}\right)_{\rm UV}\left(\mu^2_{\overline{\rm MS}}/\mu_f^2\right)^{\epsilon}\left[\Delta P_{qq}^{(1)}(x)+3\epsilon C_F(1-x)\right]+\ln\left(\frac{\mu_f^2}{-p^2}\right)\Delta P_{qq}^{(1)}(x)\right.$ $\left.-C_F\left[\left(1+x^2\right)\left[\frac{\ln(1-x)}{1-x}\right]_+\right.\right.$ $\left.\left.+\left(\frac{1+x^2}{1-x}\right)\ln x+1-\left(\frac{7}{2}-\frac{\pi^2}{3}\right)\delta(1-x)\right]\right\}$
$\Delta C_q^{(1)}(x,Q^2/\mu_f^2)$	$\ln\left(Q^2/\mu_f^2\right)\Delta P_{qq}^{(1)}(x)+C_F\left\{\left(1+x^2\right)\left[\frac{\ln(1-x)}{1-x}\right]_+-\frac{3}{2}\left[\frac{1}{1-x}\right]_+\right.$ $\left.-\left(\frac{1+x^2}{1-x}\right)\ln x+5x-2-\left(\frac{9}{2}+\frac{\pi^2}{3}\right)\delta(1-x)\right\}$
$g_{1_g}^{(1)}(x)$	$\left(\sum_q\frac{e_q^2}{2}\right)\Delta P_{qg}^{(1)}(x)\left[\ln\left(\frac{Q^2}{-p^2}\right)-\ln(x^2)-2\right]$
$\Delta\phi_{q/g}^{(1)}(x)$	$\left(\mu^2_{\overline{\rm MS}}/\mu_f^2\right)^{\epsilon}\left(\frac{1}{\epsilon}\right)_{\rm UV}\left[\Delta P_{qg}^{(1)}(x)-2\epsilon T_F(1-x)\right]$ $+\Delta P_{qg}^{(1)}(x)\left[\ln\left(\frac{\mu_f^2}{-p^2}\right)-\ln[x(1-x)]-1\right]$
$\Delta C_g^{(1)}(x,Q^2/\mu_f^2)$	$\Delta P_{qg}^{(1)}(x)\left[\ln\left(Q^2/\mu_f^2\right)+\ln\left(\frac{1-x}{x}\right)-1\right]+2T_F(1-x)$

Table 4.2 Coefficient functions from $\overline{\rm MS}$ CFH γ_5 prescription.

Collinear Regulator: DR	
$g_{1_q}^{(1)}(x,Q^2)$	$\frac{e_q^2}{2}\left\{\left(-\frac{1}{\epsilon}\right)_{\rm CO}\Delta P_{qq}^{(1)}(x)+\ln\left(Q^2/\mu^2_{\overline{\rm MS}}\right)\Delta P_{qq}^{(1)}(x)+C_F\left[\left(1+x^2\right)\left[\frac{\ln(1-x)}{1-x}\right]_+\right.\right.$ $\left.\left.-\frac{3}{2}\left[\frac{1}{1-x}\right]_+-\left(\frac{1+x^2}{1-x}\right)\ln x+x+2-\left(\frac{9}{2}+\frac{\pi^2}{3}\right)\delta(1-x)\right]\right\}$
$\Delta\phi_{q'/q}^{(1)}(x)$	$\delta_{q'q}\left(\mu^2_{\overline{\rm MS}}/\mu_f^2\right)^{\epsilon}\left[\left(-\frac{1}{\epsilon}\right)_{\rm CO}+\left(\frac{1}{\epsilon}\right)_{\rm UV}\right]\left[\Delta P_{qq}^{(1)}(x)-\epsilon C_F(1-x)\right]$
$\Delta C_q^{(1)}(x,Q^2/\mu_f^2)$	$\ln\left(Q^2/\mu_f^2\right)\Delta P_{qq}^{(1)}(x)+C_F\left\{\left(1+x^2\right)\left[\frac{\ln(1-x)}{1-x}\right]_+-\frac{3}{2}\left[\frac{1}{1-x}\right]_+\right.$ $\left.-\left(\frac{1+x^2}{1-x}\right)\ln x+x+2-\left(\frac{9}{2}+\frac{\pi^2}{3}\right)\delta(1-x)\right\}$
$g_{1_g}^{(1)}(x)$	$\left(\sum_q\frac{e_q^2}{2}\right)\left\{\Delta P_{qg}^{(1)}(x)\left[\left(-\frac{1}{\epsilon}\right)_{\rm CO}+\ln\left(Q^2/\mu^2_{\overline{\rm MS}}\right)+\ln\left(\frac{1-x}{x}\right)-1\right]+2T_F(1-x)\right\}$
$\Delta\phi_{q/g}^{(1)}(x)$	$\left(\mu^2_{\overline{\rm MS}}/\mu_f^2\right)^{\epsilon}\left[\left(-\frac{1}{\epsilon}\right)_{\rm CO}+\left(\frac{1}{\epsilon}\right)_{\rm UV}\right]\left[\Delta P_{qg}^{(1)}(x)\right]$
$\Delta C_g^{(1)}(x,Q^2/\mu_f^2)$	$\Delta P_{qg}^{(1)}(x)\left[\ln\left(Q^2/\mu_f^2\right)+\ln\left(\frac{1-x}{x}\right)-1\right]+2T_F(1-x)$
Collinear Regulator: $p^2\neq 0$	
$g_{1_q}^{(1)}(x,Q^2)$	$\frac{e_q^2}{2}\left\{\ln\left(\frac{Q^2}{-p^2}\right)\Delta P_{qq}^{(1)}(x)+C_F\left[-\frac{3}{2}\left[\frac{1}{1-x}\right]_+-2\left(\frac{1+x^2}{1-x}\right)\ln x\right.\right.$ $\left.\left.+2x-\left(1+\frac{2\pi^2}{3}\right)\delta(1-x)\right]\right\}$
$\Delta\phi_{q'/q}^{(1)}(x)$	$\delta_{q'q}\left\{\left(\frac{1}{\epsilon}\right)_{\rm UV}\left(\mu^2_{\overline{\rm MS}}/\mu_f^2\right)^{\epsilon}\left[\Delta P_{qq}^{(1)}(x)-\epsilon C_F(1-x)\right]+\ln\left(\frac{\mu_f^2}{-p^2}\right)\Delta P_{qq}^{(1)}(x)\right.$ $\left.-C_F\left[\left(1+x^2\right)\left[\frac{\ln(1-x)}{1-x}\right]_+\left(\frac{1+x^2}{1-x}\right)\ln x+1-\left(\frac{7}{2}-\frac{\pi^2}{3}\right)\delta(1-x)\right]\right\}$
$\Delta C_q^{(1)}(x,Q^2/\mu_f^2)$	$\ln\left(Q^2/\mu_f^2\right)\Delta P_{qq}^{(1)}(x)+C_F\left\{\left(1+x^2\right)\left[\frac{\ln(1-x)}{1-x}\right]_+-\frac{3}{2}\left[\frac{1}{1-x}\right]_+\right.$ $\left.-\left(\frac{1+x^2}{1-x}\right)\ln x+x+2-\left(\frac{9}{2}+\frac{\pi^2}{3}\right)\delta(1-x)\right\}$
$g_{1_g}^{(1)}(x)$	$\left(\sum_q\frac{e_q^2}{2}\right)\Delta P_{qg}^{(1)}(x)\left[\ln\left(\frac{Q^2}{-p^2}\right)-\ln(x^2)-2\right]$
$\Delta\phi_{q/g}^{(1)}(x)$	$\left(\mu^2_{\overline{\rm MS}}/\mu_f^2\right)^{\epsilon}\left(\frac{1}{\epsilon}\right)_{\rm UV}\left[\Delta P_{qg}^{(1)}(x)\right]$ $+\Delta P_{qg}^{(1)}(x)\left[\ln\left(\frac{\mu_f^2}{-p^2}\right)-\ln[x(1-x)]-1\right]$
$\Delta C_g^{(1)}(x,Q^2/\mu_f^2)$	$\Delta P_{qg}^{(1)}(x)\left[\ln\left(Q^2/\mu_f^2\right)+\ln\left(\frac{1-x}{x}\right)-1\right]$

Table 4.3 Conversion between USV and $\overline{\rm MS}$ for one-loop polarized DIS coefficient functions $\Delta C_f^{(1)}(x, Q^2/\mu_f^2)$ (with anomalous contribution).

$\Delta C_q^{(1)}(x,Q^2/\mu_f^2)\Big\vert_{\rm UVS} - \Delta C_q^{(1)}(x,Q^2/\mu_f^2)\Big\vert_{\overline{\rm MS},\gamma_5}$	$=$	$3\,C_F\,(1-x)$
$\Delta C_g^{(1)}(x,Q^2/\mu_f^2)\Big\vert_{\rm UVS} - \Delta C_g^{(1)}(x,Q^2/\mu_f^2)\Big\vert_{\overline{\rm MS},\gamma_5}$	$=$	$-2\,T_F\,(1-x)$
$\Delta C_q^{(1)}(x,Q^2/\mu_f^2)\Big\vert_{\rm UVS} - \Delta C_q^{(1)}(x,Q^2/\mu_f^2)\Big\vert_{\overline{\rm MS},\gamma_5'}$	$=$	$-\,C_F\,(1-x)$
$\Delta C_g^{(1)}(x,Q^2/\mu_f^2)\Big\vert_{\rm UVS} - \Delta C_g^{(1)}(x,Q^2/\mu_f^2)\Big\vert_{\overline{\rm MS},\gamma_5'}$	$=$	$-2\,T_F\,(1-x)$

5 IMPACTS ON DRELL-YAN PROCESS

Although we have been so far concentrating only on the discussion of polarized deep inelastic scattering, ambiguities of γ_5 and anomalous contribution are indeed present in all measurements involving spin-dependent parton distributions.

γ_5 and Anomalous Ambiguities in Drell-Yan

In this Chapter, we use the results obtained from DIS and some very simple physical arguments to demonstrate the effects of these γ_5 and anomalous ambiguities in polarized Drell-Yan Production. For a more detailed analysis, it can be found in Ref. [37]. Consider the longitudinal polarized Drell-Yan process,

$$h_1(P_1, s_1) + h_2(P_2, s_2) \rightarrow l(l_1) + \bar{l}(l_2) + X. \tag{5.1}$$

As usual, $S = (P_1 + P_2)^2$ is the squared total C.M. energy of h_1 and h_2, $Q^2 = (l_1 + l_2)^2$ is the squared invariant mass of the lepton pair $l\bar{l}$, and s_1 and s_2 are the spins of hadrons h_1 and h_2 respectively. The factorized longitudinal spin-dependent differential cross-section is given by,

$$\frac{d\Delta\sigma_{h_1h_2}}{dQ^2} = \sum_{f_1,f_2=q,\bar{q},g} \int dx_1 dx_2 \Delta\phi_{f_1/h_1}(x_1, \mu_f^2) \Delta H_{f_1f_2}(x_1, x_2, \frac{Q^2}{\mu_f^2}) \Delta\phi_{f_2/h_2}(x_2, \mu_f^2). \tag{5.2}$$

To show the explicit γ_5 dependence of the hard part, it is sufficient to consider the quark-antiquark hard part $\Delta H_{q\bar{q}_1'}$. As usual we extract $\Delta H_{q\bar{q}_1'}$ order by order on parton

states. At leading order,

$$\begin{aligned}\frac{d\Delta\sigma^{(0)}_{q\bar{q}'}}{dQ^2} &= \sum_{q_1,\bar{q}'_1}\int dx_1\, dx_2\, \Delta\phi^{(0)}_{q_1/q}(x_1,\mu_f^2)\, \Delta H^{(0)}_{q_1\bar{q}'_1}(x_1,x_2,\frac{Q^2}{\mu_f^2})\, \Delta\phi^{(0)}_{\bar{q}'_1/\bar{q}'}(x_2,\mu_f^2) \\ &= \Delta H^{(0)}_{q\bar{q}'}, \end{aligned} \tag{5.3}$$

where we have used,

$$\begin{aligned}\Delta\phi^{(0)}_{q_1/q}(x_1) &= \delta_{q_1 q}\delta(1-x_1), \\ \Delta\phi^{(0)}_{\bar{q}'_1/\bar{q}'}(x_2) &= \delta_{\bar{q}'_1\bar{q}'}\delta(1-x_2). \end{aligned} \tag{5.4}$$

Therefore, at leading order the quark-antiquark hard part $\Delta H^{(0)}_{q\bar{q}'}$ is nothing but the zeroth order partonic differential cross-section $d\Delta\sigma^{(0)}_{q\bar{q}'}/dQ^2$ of the quark-antiquark annihilation, $q+\bar{q}'\to\gamma^*\to l+\bar{l}$, which can be directly calculated. The results are,

(i) HVBM (γ_5)

$$\Delta H^{(0)}_{q\bar{q}'}\Big|_{\gamma_5} = \delta_{q\bar{q}'}\,\zeta(\epsilon)\,\mu^{2\epsilon}\,(1+\epsilon)\,\frac{e_q^2}{N_c}\,\frac{\sigma_0}{S}\,\delta(1-\frac{\tau}{x_1x_2}), \tag{5.5}$$

(ii) CFH (γ'_5)

$$\Delta H^{(0)}_{q\bar{q}'}\Big|_{\gamma'_5} = \delta_{q\bar{q}'}\,\zeta(\epsilon)\,\mu^{2\epsilon}\,(1-\epsilon)\,\frac{e_q^2}{N_c}\,\frac{\sigma_0}{S}\,\delta(1-\frac{\tau}{x_1x_2}), \tag{5.6}$$

where N_c is the number of colors, $\sigma_0 = 4\pi\alpha^2/3Q^2$, $\tau = Q^2/S$, and,

$$\zeta(\epsilon) = \left(\frac{4\pi\mu^2}{Q^2}\right)^{\epsilon}\,\frac{\Gamma(1-\epsilon)}{\Gamma(2-2\epsilon)}\,\frac{3-3\epsilon}{3-2\epsilon}, \tag{5.7}$$

which is an overall normalization factor, and $\zeta(\epsilon)\to 1$ as $\epsilon\to 0$. As expected, at leading order both prescriptions reproduce the parton model result after taking $\epsilon\to 0$. The factor $\zeta(\epsilon)\mu^{2\epsilon}(1\pm\epsilon)$ is present in all order of calculation. For the sake of consistency and simplicity, we will take it out from all calculation and treat it as an overall factor. Thus from now on, it should be kept in mind that there is always an implicit factor $\zeta(\epsilon)\mu^{2\epsilon}(1\pm\epsilon)$ in all the terms below.

For next-to-leading order quark-antiquark hard part $\Delta H^{(1)}_{q\bar{q}'}$, since $\Delta\phi^{(0)}_{q/g} = \Delta\phi^{(0)}_{g/q} = 0$, the only remaining terms are those with $\Delta\phi^{(1)}_{q_1/q}$ or $\Delta\phi^{(1)}_{\bar{q}'_1/\bar{q}'}$. And from Eq (5.2), we have,

$$\begin{aligned}\Delta H^{(1)}_{q\bar{q}'} &= \frac{d\Delta\sigma^{(1)}_{q\bar{q}'}}{dQ^2} - \sum_{q_1}\int dx_1\,\Delta\phi^{(1)}_{q_1/q}(x_1)\,\Delta H^{(0)}_{q_1\bar{q}'}(x_1, x_2 = 1) \\ &\quad - \sum_{\bar{q}'_1}\int dx_2 \Delta H^{(0)}_{q\bar{q}'_1}(x_1 = 1, x_2)\;\Delta\phi^{(1)}_{\bar{q}'_1/\bar{q}'}(x_2). \qquad (5.8)\end{aligned}$$

At this order, there are divergences; and we need regularization. To simplify our analysis, we employ the off-shell ($p^2 \neq 0$) collinear regulator — collinear pole will appear as $\ln(-p^2/Q^2)$ and $1/\epsilon$ pole is only of UV divergence — so that calculations are effectively performed in 4-dimension instead of d-dimension. As for IR divergences, they will cancel each other after all diagrams are taken into account; therefore, we can safely ignore them. For $\Delta\phi^{(1)}_{q_1/q}$, after renormalization it no longer has any $1/\epsilon$ pole; consequently, all the $O(\epsilon)$ terms in $\Delta H^{(0)}_{q\bar{q}'}$ can be dropped, i.e.,

$$\Delta H^{(1)}_{q\bar{q}'} = \frac{d\Delta\sigma^{(1)}_{q\bar{q}'}}{dQ^2} - 2\,\frac{e_q^2}{N_c}\,\frac{\sigma_0}{S}\,\Delta\phi^{(1)}_{q/\bar{q}'}(\tau)\,, \qquad (5.9)$$

for both HVBM and CFH γ_5 prescriptions. That means the differences between the two γ_5 prescriptions in $\overline{\rm MS}$ and UVS are,

(i) $\overline{\rm MS}$

$$\begin{aligned}\Delta H^{(1)}_{q\bar{q}'}\Big|_{\overline{\rm MS},\gamma_5} - \Delta H^{(1)}_{q\bar{q}'}\Big|_{\overline{\rm MS},\gamma'_5} &= \left.\frac{d\Delta\sigma^{(1)}_{q\bar{q}'}}{dQ^2}\right|_{\gamma_5} - \left.\frac{d\Delta\sigma^{(1)}_{q\bar{q}'}}{dQ^2}\right|_{\gamma'_5} \\ &\quad - 8\,\delta_{q\bar{q}'}\,\frac{e_q^2}{N_c}\,\frac{\sigma_0}{S}\,\frac{\alpha_s}{2\pi}\,C_F\,(1-\tau), \qquad (5.10)\end{aligned}$$

(ii) UVS

$$\Delta H^{(1)}_{q\bar{q}'}\Big|_{\rm UVS,\gamma_5} - \Delta H^{(1)}_{q\bar{q}'}\Big|_{\rm UVS,\gamma'_5} = \left.\frac{d\Delta\sigma^{(1)}_{q\bar{q}'}}{dQ^2}\right|_{\gamma_5} - \left.\frac{d\Delta\sigma^{(1)}_{q\bar{q}'}}{dQ^2}\right|_{\gamma'_5}, \qquad (5.11)$$

where we have used the results in Table 4.1 and Table 4.2. Note that there is no $\overline{\rm MS}$ or UVS label for $d\Delta\sigma^{(1)}_{q\bar{q}'}/dQ^2$ terms. As we are going to see, there is no UV divergence in them, thus no need for renormalization. However, even if there were UV poles, they would already be uniquely fixed by the renormalization scheme of the renormalized QCD Lagrangian. In that case, they should be all renormalized by $\overline{\rm MS}$. In short, all ambiguities associated with γ_5 come from factorization/renormalization of the polarized parton distributions.

In the calculation of the differential cross-section $d\Delta\sigma^{(1)}_{q\bar{q}'}/dQ^2$, we know real diagrams have no UV divergence and all collinear divergences are regulated as $\ln(-p^2/Q^2)$, i.e. real diagrams are finite. Therefore, for the real diagrams, the difference of the two γ_5 prescriptions can only be $O(\epsilon)$,

$$\left.\frac{d\Delta\sigma^{(1,real)}_{q\bar{q}'}}{dQ^2}\right|_{\gamma_5} - \left.\frac{d\Delta\sigma^{(1,real)}_{q\bar{q}'}}{dQ^2}\right|_{\gamma_5'} = O(\epsilon) \tag{5.12}$$

In the case of virtual diagrams, their contribution can be written as,

$$\frac{d\Delta\sigma^{(1,virtual)}_{q\bar{q}'}}{dQ^2} = \mathcal{R}\,\Delta H^{(0)}_{q\bar{q}'}, \tag{5.13}$$

where $\mathcal{R}$ is some renormalization factor and independent of γ_5 prescriptions. In other words, all γ_5 dependence of $d\Delta\sigma^{(1)}_{q\bar{q}'}/dQ^2$ is coming from $\Delta H^{(0)}_{q\bar{q}'}$. Owing to the Ward identity, UV divergence of the vertex diagram cancels that of the self-energy diagrams (see Figure 5.1). As a result, the renormalization factor $\mathcal{R}$ has no $(1/\epsilon)_{\rm UV}$ pole, which implies,

$$\left.\frac{d\Delta\sigma^{(1,virtual)}_{q\bar{q}'}}{dQ^2}\right|_{\gamma_5} - \left.\frac{d\Delta\sigma^{(1,virtual)}_{q\bar{q}'}}{dQ^2}\right|_{\gamma_5'} = O(\epsilon). \tag{5.14}$$

In summary, the differences of the hard parts in the two γ_5 prescriptions in $\overline{\rm MS}$ and UVS are given by,

(i) $\overline{\rm MS}$

$$\Delta H^{(1)}_{q\bar{q}'}\Big|_{\overline{\rm MS},\gamma_5} - \Delta H^{(1)}_{q\bar{q}'}\Big|_{\overline{\rm MS},\gamma_5'} = -8\,\delta_{q\bar{q}'}\,\frac{e_q^2}{N_c}\,\frac{\sigma_0}{S}\,\frac{\alpha_s}{2\pi}\,C_F\,(1-\tau). \tag{5.15}$$

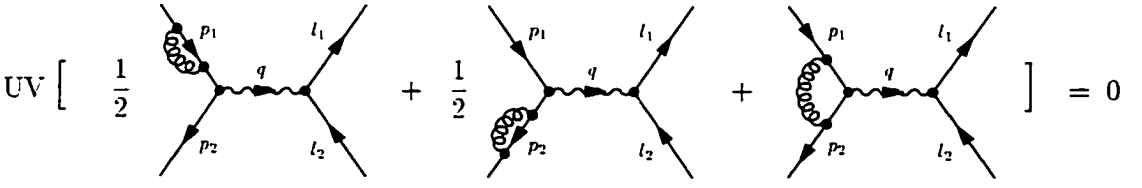

Figure 5.1 Cancellation of UV divergences in the virtual part of the $O(\alpha_s)$ $q + \bar{q} \to l + \bar{l}$ Drell-Yan process.

(ii) UVS

$$\Delta H^{(1)}_{q\bar{q}'}\Big|_{\text{UVS},\gamma_5} - \Delta H^{(1)}_{q\bar{q}'}\Big|_{\text{UVS},\gamma_5'} = 0. \tag{5.16}$$

For anomalous ambiguity, we examine the quark-gluon hard part ΔH_{qg}. As gluon does not interact directly with photon, it has no zeroth order contribution, i.e. $\Delta H^{(0)}_{qg} = 0$. The lowest contribution is from first order. Since $\Delta\phi^{(0)}_{q/g} = \Delta\phi^{(0)}_{g/q} = 0$, the only surviving term is $\Delta H^{(1)}_{qg}$,

$$\Delta H^{(1)}_{qg} = \frac{d\Delta\sigma^{(1)}_{qg}}{dQ^2} - \sum_{\bar{q}'} \int dx_2\, \Delta H^{(0)}_{q\bar{q}'}(x_1 = 1, x_2)\; \Delta\phi^{(1)}_{\bar{q}'/g}(x_2). \tag{5.17}$$

Using arguments as in quark-antiquark hard part, we know there is no UV divergence in $d\Delta\sigma^{(1)}_{qg}/dQ^2$, i.e no $1/\epsilon$ pole. As all collinear divergences are regulated as $\ln(-p^2/Q^2)$, the differential cross-section $d\Delta\sigma^{(1)}_{qg}/dQ^2$ is finite. Therefore, $d\Delta\sigma^{(1)}_{qg}/dQ^2$ in different γ_5 can only have difference in order of ϵ. That is, if there is any γ_5 ambiguity in $\Delta H^{(1)}_{qg}$, it must come from $\Delta\phi^{(1)}_{\bar{q}'/g}$. Using the off-shell results in Table 4.1 and Table 4.2, we find,

$$\Delta H^{(1)}_{qg}\Big|_{\overline{\text{MS}},\gamma_5} - \Delta H^{(1)}_{qg}\Big|_{\overline{\text{MS}},\gamma_5'} = \frac{e_q^2}{N_c}\frac{\sigma_0}{S}\, 2T_F(1-\tau), \tag{5.18}$$

Moreover, $\Delta H^{(1)}_{qg}$ can still have ambiguity related to anomalous contribution. In fact, the presence of the quark distribution within gluon, $\Delta\phi^{(1)}_{\bar{q}'/g}$, proves this. Applying

Eq. (4.86) to Eq. (5.17), we find,

$$\Delta H_{qg}^{(1)} - \Delta H_{qg}^{(1)}\Big|_{\text{no-anomaly}} = \frac{e_q^2}{N_c}\frac{\sigma_0}{S} 2T_F(1-\tau), \tag{5.19}$$

where all uninteresting ϵ terms are dropped.

As we have seen from above examples, due to the ambiguities of parton distributions, the hard parts of polarized Drell-Yan process inevitably inherit those same problems of polarized DIS [48]. In fact, all factorization calculations that involve polarized parton distributions have to face these ambiguities. Consequently, in order to have any meaningful comparison of results from various polarized processes, it is important to make sure these ambiguities are handled consistently.

6 SUMMARIES AND CONCLUSIONS

Deep Inelastic Scattering is a powerful probe for studying the internal structure of nucleons. It has greatly advanced our knowledge of parton interactions inside nucleons. Recently, polarized DIS that studies nucleon spin structure has become a big excitement. This sudden surge of interest is the result of the so-called "Spin Crisis", which has caused both the experimental and theoretical communities to rethink their understanding on nucleon spin structure. The direct consequence of this "Spin Crisis" is the abundance and availability of the newly measured high quality experimental data. However, in order to improve our understanding on nucleon spin, better theoretical models and predictions are also needed. And because of this, numerous studies have been carried out to extract more accurate polarized parton distribution functions from data. Nevertheless, due to the intrinsic ambiguities in the definition of polarized parton distributions, there have been lot of debates and confusions in the community.

Theoretically, parton distributions inside hadrons are defined as matrix elements of non-local operators on hadron states. These hadronic matrix elements are neither direct physical observables nor calculable in perturbative QCD. Their usefulness rests on the QCD factorization theorem. QCD factorization theorem states that for many hadronic processes, e.g. DIS, Drell-Yan, Direct Photon, etc, the involved physical observables can be decomposed into two parts: The universal long-distance non-perturbative parton distributions and the short-distance calculable coefficient functions. The predicting power of parton distributions comes from their universality. By using parton distributions extracted from one process, predictions can be made and tested in other processes. In view

of the numerous soon-to-be-on-line polarized hadronic experiments, it is important to have a set of reliable and consistent parton distributions. To achieve such a goal, it is crucial to pin point exactly what are these ambiguities in polarized parton distributions and how they affect the extracted numerical results.

Ambiguities in parton-level parton distributions affect the analytical expressions of the short-distance coefficient functions, which in turns affect the result of parton distributions in hadrons extracted from experimental data. Hadronic parton distributions are very different from parton-level parton distributions. They correspond to the matrix elements of the same non-local operator on different states — hadron states or parton states. Parton distributions in hadrons are non-perturbative. They can only be extracted from experimental data after we pick a particular choice of coefficient functions. Whereas, parton-level parton distributions are calculable order by order from a known set of Feynman rules. In calculation of any coefficient functions, parton-level parton distributions are needed to cancel the collinear divergence from factorization. In short, the ambiguities of hadronic parton distributions are result of ambiguous parton-level parton distributions.

All ambiguities in parton-level parton distributions come from the freedom in choosing renormalization/factorization scheme. In principle, the renormalization scheme for all physical observables are fixed once that of the Lagrangian is fixed. But since parton distributions are not physical observables, they can have any renormalization scheme — as long as it is handled consistently. This extra scheme freedom is well-known in the case of unpolarized distributions. However, due to the presence of γ_5 and $\epsilon_{\mu\nu\alpha\beta}$ tensor in their operator definitions, polarized distributions have additional complications. One obvious question is how to define γ_5 in d-dimension in terms of Dimensional Regularization. Another less-known problem is the proper treatment of anomalous contribution. When using different scheme of γ_5 or anomalous contribution, different numerical polarized hadronic parton distributions will be extracted from experimental data. Thus, in order

to have meaningful tests and predictions from these extracted polarized hadronic parton distributions, it is essential to have a systematic and consistent approach to handle these ambiguities.

The question concerning γ_5 in d-dimension originates from Dimensional Regularization. As in d-dimension, it is possible to define γ_5 in more than one way. In usual physical observables calculation, the most important point is to conform with the well-defined 4-dimensional behavior and consistent with dimensional renormalization procedure. However, in calculating polarized parton-level distributions, consistency with QCD factorization must also be satisfied.

For anomalous contribution, it is a result of the anomaly in the triangular diagram in Figure 3.6(b). As is shown in Chapter 3, this anomalous contribution is a remainder of UV origin. Therefore, whether to include it in the parton-level $\Delta\phi^{(1)}_{q/g}$ is subjected to debate. On one hand, since it is short-distance, its presence does not affect the validity of the factorization procedure; and in the spirit of $\overline{\text{MS}}$ scheme, such term should not be removed. On the other hand, this anomalous contribution violates the conservation of axial current and is, as mentioned, short-distance so it would be preferable to subtract it from the parton-level distributions. But, not until now, the exact expression of this troublesome term was unknown. In our study, we provide methods to extract it explicitly and hence open the possibility of consistent treatment.

Since all these ambiguities arise from renormalization/factorization scheme freedom, we have calculated in Chapter 3 a complete set of unrenormalized first order parton distributions within partons. Also, results from two different γ_5 prescriptions and collinear regulators are given so that explicit comparison between different prescriptions and regulators is possible. With this set of distributions, one can easily derive any renormalized first order parton distributions within partons once the renormalization scheme is fixed. Moreover, we have proposed a new renormalization scheme, called UV Subtraction (UVS) scheme that is designed to remove all UV sensitive terms in partonic parton dis-

tributions. In principle, all consistent renormalization schemes are equivalent. But this UVS scheme is especially useful: Under UVS scheme all ambiguities from various γ_5 prescriptions and treatments of anomalous contribution are eliminated. Furthermore, UVS renormalized partonic distributions are by definition entirely collinear; consequently, the hard coefficient functions in UVS scheme preserve all short-distance physics of the corresponding partonic scattering process. To facilitate the transformation between $\overline{\rm MS}$ and UVS schemes, conversion tables for the first order parton distributions within partons are given in Chapter 3.

Using polarized DIS as an example, we have presented a complete analysis of the one-loop polarized coefficient functions in two different γ_5 prescriptions, HVBM and CFH, in d-dimension. In order to check the consistency of these two γ_5 prescriptions, results obtained from two different collinear regulators are also given. It is found that for quark coefficient function $\Delta C_q^{(1)}$, different γ_5 prescription gives different result, but is independent of the choice of collinear regulators. The difference is a consequence of chirality conservation - chirality is violated in HVBM prescription but conserved in CFH. Nevertheless, with an additional renormalization constant, it is still possible to derive the usual Bjorken sum rule result from $\overline{\rm MS}$ HVBM quark coefficient function.

In addition, the anomalous contribution terms in both coefficient function $\Delta C_g^{(1)}$ and partonic distribution $\Delta\phi_{q/g}^{(1)}$ are given. We have found that the anomalous contribution term in $\Delta\phi_{q/g}^{(1)}$ is of UV origin. Thus, whether to include it in partonic parton distribution is simply a choice of renormalization scheme. Nevertheless, such a choice is important in extracting hadronic parton distributions from experimental data. For instance, if anomalous contribution is chosen not to be included in parton-level parton distributions, there will be a non-zero contribution from polarized gluon to Γ_1^h. The anomalous contribution term is given in x-dependent form so that one may readily use them to extract parton distributions inside nucleons.

After studying carefully the two γ_5 prescriptions, we have found problem in CFH

scheme. Despite its appealing simple definition, which manifestly respects chiral symmetry, CFH prescription has difficulty in treating anomaly consistently under factorization theorem. For any results to be valid, it is required for all γ_5 prescriptions, besides consistent with renormalization procedures, to conform with factorization theorem, i.e. the short-distance hard parts must not depend on the choice of collinear regulators. However, CFH γ_5 prescription seems to fail this requirement. This poses serious question on the validity of CFH prescription, and any results obtained by it, in calculations involved factorization.

In Chapter 5, the effects of these ambiguities on the hard parts of polarized Drell-Yan are discussed. Applying the results obtained in polarized DIS, we conclude that both γ_5 and anomalous contribution ambiguities exist in polarized Drell-Yan. These ambiguities in Drell-Yan hard parts are direct consequence of ambiguous parton distributions within partons. In fact, these ambiguities are present in any calculation that uses parton distributions within partons. Therefore, in order to have any meaningful predictions and comparisons between different hadronic processes, it is crucial to make sure that same renormalization scheme and treatment of ambiguities are being used throughout the analysis.

We have so far concentrated on the effects of these ambiguities to the extraction of parton distributions in nucleons. However, their impact is much more far-reaching. Consider the evolution of parton distributions. The Renormalization Group Equation requires,

$$\frac{d}{d\ln\mu_f^2} g_1^h(x,Q^2) = \frac{d}{d\ln\mu_f^2}\left(\Delta C_a(x,Q^2/\mu_f^2)\otimes\Delta\phi_{a/h}(x,\mu_f^2)\right) = 0, \tag{6.1}$$

or,

$$\Delta C_a(x,Q^2/\mu_f^2)\otimes\frac{d}{d\ln\mu_f^2}\Delta\phi_{a/h}(x,\mu_f^2) = -\left(\frac{d}{d\ln\mu_f^2}\Delta C_a(x,Q^2/\mu_f^2)\right)\otimes\Delta\phi_{a/h}(x,\mu_f^2). \tag{6.2}$$

Clearly, evolution kernel of the distributions depends on the exact expressions of coefficients, which in turns depend on the scheme used in partonic parton distributions.

Finally, partonic distributions may still have an additional ambiguity from the total anti-symmetric tensor $\epsilon_{\mu\nu\alpha\beta}$. Up to this point, we have only assumed it is the usual 4-dimensional Levi-Civita tensor. As the total anti-symmetric tensor is closely related to γ_5, it seems that HVBM prescription works fine with a 4-dimensional $\epsilon_{\mu\nu\alpha\beta}$. But, for CFH γ_5, this 4-dimensional $\epsilon_{\mu\nu\alpha\beta}$ may not be sufficient. More work still need to be done to see if it is possible to define a truly d-dimensional $\epsilon_{\mu\nu\alpha\beta}$ in such a way that it is consistent with the CFH prescription and take care of the problem of anomalous contribution.

APPENDIX A DEFINITIONS OF VARIOUS γ_5 PRESCRIPTIONS

Here we present the definitions of both 't Hooft, Veltman, Breitenlohner and Maison (HVBM) and Modified Chanowitz, Furman and Hinchliffe (CFH) γ_5 prescriptions.

't Hooft, Veltman, Breitenlohner and Maison (HVBM) Prescription

HVBM prescription is the first d-dimensional γ_5 prescription and perhaps the most widely used. It was first proposed by 't Hooft and Veltman [33] in the context of Dimensional Regularization and then systematized by Breitenlohner and Maison [39]. It has been proven to be consistent with anomaly and dimensional renormalization procedures [36, 39]. In this prescription, γ_5 is defined to anticommute only with 4-dimensional Dirac γ-matrices.

$$\bar{g}^{\mu\nu} \{ \gamma_5 , \gamma_\nu \} = \{ \gamma_5 , \bar{\gamma}_\mu \} = 0, \tag{A.1}$$

$$\hat{g}^{\mu\nu} [\gamma_5 , \gamma_\nu] = [\gamma_5 , \hat{\gamma}_\mu] = 0, \tag{A.2}$$

where

$$\bar{g}^{\mu\nu} = \begin{cases} g^{\mu\nu} & \mu, \nu = 0, 1, 2, 3 \\ 0 & \text{else,} \end{cases} \tag{A.3}$$

$$\hat{g}^{\mu\nu} = \begin{cases} g^{\mu\nu} & \mu, \nu > 3 \\ 0 & \text{else.} \end{cases} \tag{A.4}$$

Here we give some important properties of γ_5 (HVBM):

$$\gamma_5^2 = 1, \tag{A.5}$$

$$\mathrm{Tr}\left[\gamma_5\gamma_{\mu_1}\gamma_{\mu_2}\gamma_{\mu_3}\gamma_{\mu_4}\right] = 4\,i\,\epsilon_{\mu_1\mu_2\mu_3\mu_4}, \tag{A.6}$$

$$\mathrm{Tr}\left[\gamma_5\gamma_{\mu_1}\gamma_{\mu_2}\cdots\gamma_{\mu_{2n+1}}\right] = 0, \tag{A.7}$$

$$\mathrm{Tr}\left[\gamma_5\gamma_{\mu_1}\gamma_{\mu_2}\cdots\gamma_{\mu_n}\right] = \mathrm{Tr}\left[\gamma_{\mu_n}\gamma_5\gamma_{\mu_1}\gamma_{\mu_2}\cdots\gamma_{\mu_{n-1}}\right], \tag{A.8}$$

where $\epsilon_{\mu_1\mu_2\mu_3\mu_4}$ is the usual total antisymmetric tensor in 4-dimension. The last equation states that γ_5 (HVBM) preserves the cyclic property of trace.

Despite its simple definition, HVBM prescription has been known to violate chiral symmetry and lead to so called *spurious anomalies* in addition to the true anomaly [36, 43, 44, 49]. This can be understood by simply examining the definition given in Eq. (A.1) and Eq. (A.2). Obviously, certain "directions" ($\mu = 0, 1, 2, 3$) are different from the others ($\mu > 3$). This different treatment of "directions" is the source of this spurious chiral symmetry violation. Nevertheless, these spurious anomalies can be removed by redefining the axial current with an extra finite renormalization constant [36, 43, 44, 49].

Modified Chanowitz, Furman and Hinchliffe (CFH) Prescription

Due to the inconvenience of spurious anomalies in HVBM prescription, numerous γ_5 prescriptions that manifestly respect chiral symmetry have been introduced. However, a lot of them turned out to have various problems. (For a more detailed discussion, one can consult the review by Bonneau [50].) Here, a modified version of CFH γ_5 prescription [51] is being considered because it has been systematized by Körner, Kreimer and Schilcher [47] with the criticisms of Bonneau in mind. Furthermore, in their paper, they have shown that this version of CFH prescription gives the correct anomaly in the AVV triangular diagram.

To distinguish from the γ_5 proposed by HVBM, we write $\gamma_5' \equiv \gamma_5(\mathrm{CFH})$. That is,

γ_5 is always γ_5(HVBM) unless it is specified to be otherwise. In this prescription, γ_5' anticommutes with all γ-matrices,

$$\left\{ \gamma_5' , \gamma_\mu \right\} = 0. \tag{A.9}$$

Some important properties are:

$$\gamma_5'^{\,2} = 1, \tag{A.10}$$

$$\mathrm{Tr}\left[\gamma_5' \gamma_{\mu_1} \gamma_{\mu_2} \gamma_{\mu_3} \gamma_{\mu_4}\right] = 4\, i\, \epsilon_{\mu_1\mu_2\mu_3\mu_4}, \tag{A.11}$$

$$\mathrm{Tr}\left[\gamma_5' \gamma_{\mu_1} \gamma_{\mu_2} \cdots \gamma_{\mu_{2n+1}}\right] = 0, \tag{A.12}$$

$$\mathrm{Tr}\left[\gamma_5' \gamma_{\mu_1} \gamma_{\mu_2} \cdots \gamma_{\mu_n}\right] = \mathrm{Tr}\left[\gamma_5' \gamma_{\mu_n} \gamma_{\mu_{n-1}} \cdots \gamma_{\mu_1}\right], \tag{A.13}$$

$$\mathrm{Tr}\left[\gamma_5' \gamma_{\mu_1} \gamma_{\mu_2} \cdots \gamma_{\mu_n}\right] \neq \mathrm{Tr}\left[\gamma_{\mu_n} \gamma_5' \gamma_{\mu_1} \gamma_{\mu_2} \cdots \gamma_{\mu_{n-1}}\right] \quad \text{for } n > 4. \tag{A.14}$$

Here $\epsilon_{\mu_1\mu_2\mu_3\mu_4}$ is still the usual 4-dimensional Levi-Civita tensor. In general, trace with odd numbers of γ_5''s is not cyclic. The lost of cyclicity in trace is the price to pay for having γ_5' anticommuting with all γ_μ. Because of this special feature, the trace of all diagrams has to start at the same vertex. This particular chosen vertex is called the *reading point*. In the present of anomaly, the reading point has to be chosen at the axial vertex so that the anomaly is correctly included. This is of crucial importance when we are dealing with the triangular diagram of the gluon coefficient function.

APPENDIX B GAUGE INVARIANT FEYNMAN RULES FOR PARTON DISTRIBUTIONS

In Chapter 2, we have introduced the definition of parton distributions on light-cone, i.e. in $n \cdot A$ gauge ($n^\mu = \delta^{\mu -}$). In light-cone formulation, the gluon's propagator and polarization must also be in physical gauge so that all unphysical degrees of freedom are explicitly eliminated. By using this gauge choice, the bi-local operator and the path-ordered phase are reduced to a simple cut-vertex as given by Mueller [38]. However, sometimes it is more convenient and favorable to work in a gauge invariant formulation. Here we summarize the gauge invariant definitions and Feynman rules given by Collins and Soper [25].

In fact, the only difference between the light-cone formulation and the gauge invariant formulation is the additional Wilson line, which is constructed so that the bi-local operator is manifestly gauge invariant. The unpolarized and polarized quark distributions in a hadron h with momentum $p^\mu = p^+$ are,

$$\phi_{q/h}(x) = \int \frac{dy^-}{2\pi} e^{-ixp^+y^-} \langle h(p)|\bar{\psi}_q(y^-) \frac{\gamma^+}{2} \mathcal{P} \psi_q(0)|h(p)\rangle , \tag{B.1}$$

$$\Delta\phi_{q/h}(x) = \int \frac{dy^-}{2\pi} e^{-ixp^+y^-} \langle h(p,s)|\bar{\psi}_q(y^-) \frac{\gamma^+\gamma_5}{2} \mathcal{P} \psi_q(0)|h(p,s)\rangle , \tag{B.2}$$

where $\mathcal{P}$ is the Wilson line mentioned before,

$$\mathcal{P} = P \exp\left[-ig \int_0^{y^-} dy'^- \, A_a^+(0, y'^-, 0_\perp)\, t_a\right] , \tag{B.3}$$

and t_a is the generator of the color SU(3). It is basically a path-ordered phase between the positions of the two quarks fields.

For gluon, the definitions are similar,

$$\phi_{g/h}(x) = \frac{1}{xp^+}\int \frac{dy^-}{2\pi} e^{-ixp^+y^-} \left(-\frac{g_{\mu\nu}}{2}\right) \langle h(p)|\, F^{+\mu}(y^-)\, \mathcal{P}\, F^{+\nu}(0)\, |h(p)\rangle\,, \tag{B.4}$$

$$\Delta\phi_{g/h}(x) = \frac{1}{xp^+}\int \frac{dy^-}{2\pi} e^{-ixp^+y^-} \left(-\frac{i}{2}\epsilon_{\perp\mu\nu}\right) \langle h(p,s)|\, F^{+\mu}(y^-)\, \mathcal{P}\, F^{+\nu}(0)\, |h(p,s)\rangle. \tag{B.5}$$

But now $\mathcal{P}$ has a different generator T_a,

$$\mathcal{P} = P \exp\left[-ig\int_0^{y^-} dy'^-\, A_a^+(0,y'^-,0_\perp)\, T_a\right], \tag{B.6}$$

and T_a is the generator of the adjoint representation of SU(3). Note the extra $1/xp^+$ factor for gluon distributions.

In perturbative calculations, we are mostly interested in the parton-level parton distributions or parton distributions within parton $\Delta\phi_{f'/f}(x)$. The definitions are the same except replacing the hadron state h by parton state f. The general Feynman diagrams for quark and gluon distributions within parton f, $f = q, \bar{q}, g$, are given by Figure B.1. In Figure B.1, the dotted line represents a generic initial state parton f

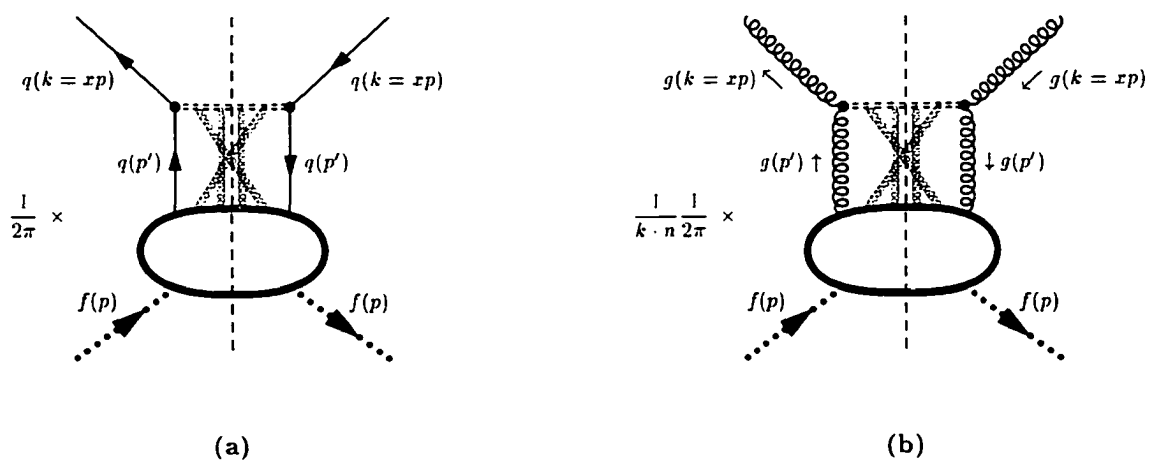

Figure B.1 (a) Quark distribution within parton f. (b) Gluon distribution within parton f. Note the extra factors $\frac{1}{2\pi}$ and $\frac{1}{k\cdot n}\frac{1}{2\pi}$.

with momentum $p^\mu = p^+$. All "outgoing" quark and gluon have momentum $k = xp$, which is a result of collinear expansion. The double-dashed eikonal line represents the Wilson line $\mathcal{P}$. Clearly from its definition given by Eq. (B.3) and Eq. (B.6), the eikonal line connects the two patron fields at different positions. Since only gluon is present in the path-ordered exponential, the only eikonal-eikonal interaction allowed is the eikonal-gluon-eikonal vertex. That is why gluons are the only partons linking the middle of the eikonal line and the blob in Figure B.1.

The Feynman rules for both unpolarized and polarized quarks and gluon distributions are:

(1) Eikonal Propagator

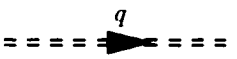

$$\frac{i}{q \cdot n + i\epsilon} \tag{B.7}$$

(2) Cut-eikonal line

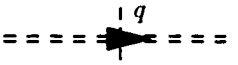

$$2\pi\,\delta(q \cdot n) \tag{B.8}$$

(3) Vertices

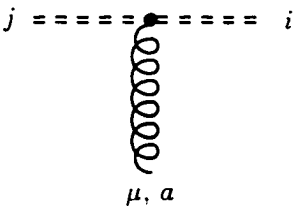

$$i\,g\,n_\mu t^a_{ij} \tag{B.9}$$

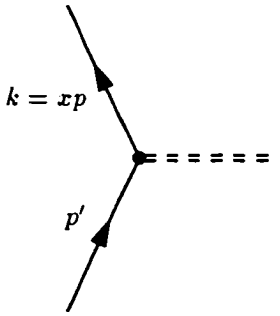

$$1 \tag{B.10}$$

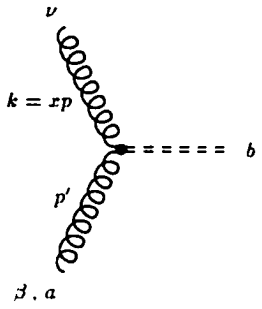

$$i(k \cdot n\, g^{\beta\nu} - p'^{\nu}\, n^{\beta})\delta_{ba} \tag{B.11}$$

(4) Initial/"Incoming" Partons

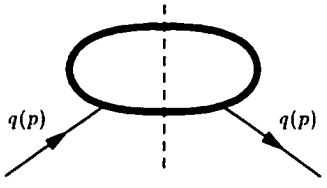

unpolarized: $\frac{\gamma\cdot p}{2}$

polarized: $\frac{\gamma_5\,\gamma\cdot p}{2}$ (B.12)

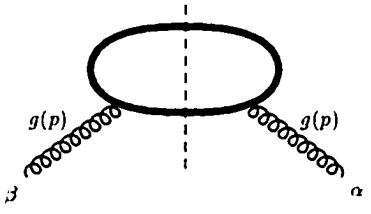

unpolarized: $-\frac{g_{\perp\alpha\beta}}{2}$

polarized: $-\frac{i\epsilon_{\perp\alpha\beta}}{2}$ (B.13)

(5) Cut-vertex/"Outgoing" Partons

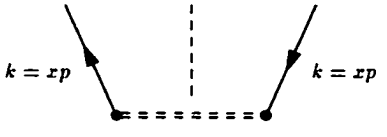

unpolarized: $\frac{\gamma\cdot n}{2}$

polarized: $\frac{\gamma\cdot n\,\gamma_5}{2}$ (B.14)

unpolarized: $-g_{\mu\nu}$

polarized: $i\epsilon_{\perp\mu\nu}$ (B.15)

Just a reminder, the Greek indices like α, β denote the Lorentz indices, while alphabetical indices a, b and etc denote the color indices. Also in our notation, $\epsilon_{0123} = 1$ and $\epsilon_{\perp\alpha\beta} = \epsilon_{\perp}^{\alpha\beta} = \epsilon_{03\alpha\beta}$. For initial state gluon, the polarization tensor for spin-averaged gluons is given by $(-g_{\perp_{\alpha\beta}}/2)$ so that only physical helicities are summed. The definition of $g_{\perp_{\alpha\beta}}$ is,

$$g_{\perp_{\alpha\beta}} = \begin{cases} 0 & \mu,\nu = 0,3 \\ g_{\alpha\beta} & \text{else.} \end{cases} \tag{B.16}$$

This complication arises from the non-abelian nature of QCD, i.e. the presence of tri-gluon vertex. If there is no triple-gluon interaction in the diagrams concerned, one may safely replace $(-g_{\perp_{\alpha\beta}}/2)$ by $(-g_{_{\alpha\beta}}/2)$. Strictly speaking the cut-vertex, or "outgoing", gluon is not a gluon, it is drawn as gluon so that diagrams look more like the usual Feynman diagrams. Thus for the "outgoing" gluon, the situation is very different from that of the initial state. The spin-averaged "outgoing" gluon tensor is always $-g_{\mu\nu}$ because it is a formal derivation from the decoupling of Lorentz indices in Eq.(3.10) and Eq. (B.4). The rigorous definition of the tensor relies on Eq. (B.4), that is $(-g_{_{\mu\nu}}/2)$. To see how to apply these Feynman rules, two example calculations are presented in the followings.

First, we consider the simpler case — the zeroth order gluon distribution within a gluon. The Feynman diagram is given by Figure B.2. Since it is a gluon distribution, we have to add the extra factor $\frac{1}{k\cdot n}\frac{1}{2\pi}$, and the unpolarized diagrams reads,

$$\begin{aligned} \phi^{(0)}_{g/g}(x) &= \frac{1}{k\cdot n}\frac{1}{2\pi}\left(-\frac{g_{\perp\alpha\beta}}{2}\right)(-g_{\mu\nu})\,(k\cdot n\, g^{\alpha\mu} - p^{\mu}\, n^{\alpha})(k\cdot n\, g^{\beta\nu} - p^{\nu}\, n^{\beta}) \\ &\quad \times 2\,\pi\,\delta((p-k)\cdot n) \\ &= \delta(1-x)\,. \end{aligned} \tag{B.17}$$

As there is no tri-gluon vertices in Figure B.2, we can just as well use $g_{_{\alpha\beta}}$ in the above

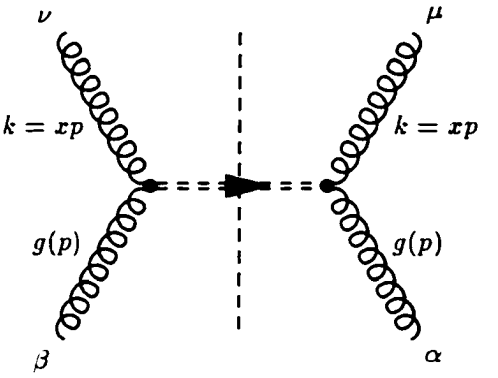

Figure B.2 Zeroth order gluon distribution within a gluon.

equation, and the result is the same. For the polarized diagrams,

$$\begin{aligned}\Delta\phi^{(0)}_{g/g}(x) &= \frac{1}{k\cdot n}\frac{1}{2\pi}\left(-\frac{i\epsilon_{\perp\alpha\beta}}{2}\right)(i\epsilon_{\perp\mu\nu})\,(k\cdot n\,g^{\alpha\mu}-p^{\mu}\,n^{\alpha})(k\cdot n\,g^{\beta\nu}-p^{\nu}\,n^{\beta}) \\ &\quad\times 2\,\pi\,\delta((p-k)\cdot n) \\ &= \delta(1-x)\,. \end{aligned} \tag{B.18}$$

In the last statement, we use the result $\epsilon_{\perp}^{\mu\nu}\epsilon_{\perp\mu\nu}=2$. Also, we have ignored the uninteresting color sum, which is obviously 1.

The next example is a bit more complicated. The diagram we are about to calculate is given in Figure B.3(a). It is one of the virtual diagrams in first order polarized quark distribution within a quark. The diagram itself is divergent so we need to choose a regularization procedure. Here Dimensional Regularization is used for treating all divergences for its simplicity. The gluon propagator is chosen to be in Feynman gauge and the γ_5 prescription is HVBM. (However, for this special case, both CFH and HVBM give the same answer.) We first take care of the color factor. Color factor $C_F = \sum_a \mathrm{Tr}\,[t^a t^a]/N_c = 4/3$. Since it is a quark distribution, the factor $\frac{1}{2\pi}$ is needed. The diagram is,

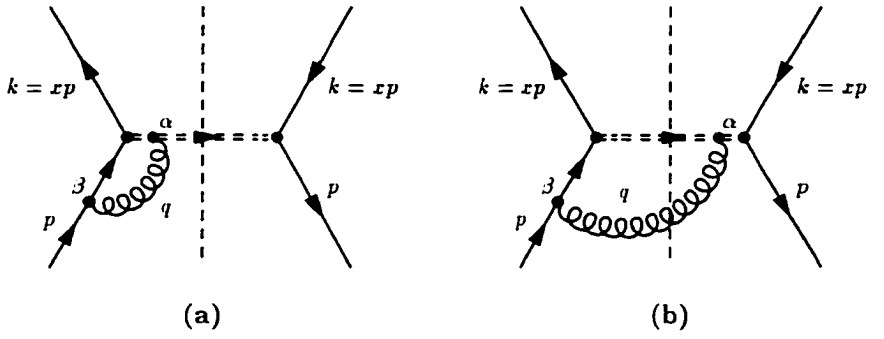

Figure B.3 Two example diagrams in first order polarized quark distribution within a quark.

$$\Delta\phi^{(1a)}_{q/q}(x) = \frac{1}{2\pi}C_F\int\frac{d^dq}{(2\pi)^d}\,\mathrm{Tr}\left[\left(\frac{\gamma_5\gamma\cdot p}{2}\right)\left(\frac{i\gamma\cdot n\gamma_5}{2}\right)\left(\frac{i\gamma\cdot k'}{k'^2+i\epsilon}\right)(-ig\mu^\epsilon\gamma_\beta)\right](-ig\mu^\epsilon n_\alpha)$$
$$\times\left(\frac{i}{(p-q-k)\cdot n+i\epsilon}\right)\left(\frac{-ig^{\alpha\beta}}{q^2+i\epsilon}\right)2\,\pi\,\delta((p-k)\cdot n)\,, \tag{B.19}$$
$$= \frac{ig^2\mu^{2\epsilon}}{(2\pi)^d}C_F\,\delta(1-x)\int\frac{d^dq}{q^+}\,\frac{1}{-2q^-(p^+-q^+)-q_\perp^2+i\epsilon}$$
$$\times\frac{p^+-q^+}{2q^+q^--q_\perp^2+i\epsilon}\,. \tag{B.20}$$

In the q^- plane, there are two poles, $(q_\perp^2-i\epsilon)/2q^+$ and $(-q_\perp^2+i\epsilon)/2(p^+-q^+)$. In order to have one pole above the real axis while the other below, q^+ must satisfy $0<q^+<p^+$. Otherwise, both poles are either below or above the real axis, and it is possible to choose a contour that encloses no pole. In that case, the integral is zero. Therefore, the only non-zero kinematic region for q^+ is $0<q^+<p^+$. Using $0<q^+<p^+$ and perform the q^- contour integral, we find,

$$\Delta\phi^{(1a)}_{q/q}(x) = \frac{g^2\mu^{2\epsilon}}{(2\pi)^{d-1}}C_F\,\delta(1-x)\int_0^1 dz\,\frac{z}{1-z}\int\frac{d^{d-2}q_\perp}{q_\perp^2}, \tag{B.21}$$

where $z=1-q^+/p^+$. Now the $q_\perp$ integral can be easily calculated by using the trick,

$$\int\frac{d^{d-2}q_\perp}{q_\perp^2}=\frac{\Omega_{d-3}}{2}\left[\int_0^{\mu_f^2}+\int_{\mu_f^2}^{\infty}\right]\frac{dq_\perp^2}{(q_\perp^2)^{1+\epsilon}}\,, \tag{B.22}$$

where Ω_{d-3} is the angular volume in $(d-2)$-dimension, and μ_f is the artificial cut-off that separate the soft part and the hard part. The cut-off μ_f is generally referred to as the factorization scale. In the first integral, the divergence comes from the soft, $q_\perp^2 \to 0$, region, thus we label it collinear (CO). To regularized it, we need to treat ϵ as if it were negative so that the collinear pole will appear as $(-1/\epsilon)_{\rm CO}$. For the hard part, the divergence comes from the region $q_\perp^2 \to \infty$; thus we treat ϵ as positive so that the UV singularity will become $(1/\epsilon)_{\rm UV}$. Finally putting all these together, we have,

$$\begin{aligned}\Delta\phi_{q/q}^{(1a)}(x) &= -\frac{\alpha_s}{2\pi}C_F\left(\frac{\mu^2}{\mu_f^2}\right)^\epsilon\left[1+\epsilon\ln(4\pi e^{-\gamma_E})\right]\left[\left(\frac{1}{\epsilon}\right)_{\rm UV}+\left(-\frac{1}{\epsilon}\right)_{\rm CO}\right]\\ &\quad\times\delta(1-x)\int_0^1 dz\,\frac{z}{1-z}\,,\end{aligned} \tag{B.23}$$

where γ_E is the usual Euler constant. The z integral is obviously divergent but this singularity will be cancel by the diagram in Figure B.3(b). The combined result will be in terms of the familiar $\left(\frac{z}{1-z}\right)_+$ distribution.

BIBLIOGRAPHY

[1] E.D. Bloom *et al.*, Phys. Rev. Lett. **23**, 930 (1969); M. Breidenbach *et al.*, Phys. Rev. Lett. **23**, 933 (1969); J.L. Friedman and H.W. Kendall, Annual Reviews of Nuclear Science **22**, 203 (1972).

[2] G. Altarelli and G. Parisi, Nucl. Phys. **B126**, 298 (1977); L.N. Lipatov, Sov. J. Nucl. Phys. **20**, 95 (1975); V.N. Gribov and L.N. Lipatov, Sov. J. Nucl. Phys. **15**, 438 (1972); Yu.L. Dokshitzer, Sov. Phys. JETP **46**, 641 (1977).

[3] SLAC E80 Collaboration, M.J. Alguard *et al.*, Phys. Rev. Lett. **37**, 1261 (1976); Phys. Rev. Lett. **41**, 70 (1978); SLAC E130 Collaboration, G. Baum *et al.*, Phys. Rev. Lett. **51**, 1135 (1983).

[4] J.D. Bjorken, Phys. Rev. **148**, 1467 (1966).

[5] J. Ellis and R.L. Jaffe, Phys. Rev. D **9**, 1444 (1974); Phys. Rev. D **10**, 1669 (1974).

[6] EMC Collaboration, J. Ashman *et al.*, Phys. Lett. B **206**, 364 (1988); Nucl. Phys. **B328**, 1 (1989).

[7] M. Gell-Mann, Phys Lett. **8**, 214 (1964); G. Zweig, CERN Report 8182/TH.401 (1964).

[8] F.D. Close and R.G. Roberts, Phys. Lett. B **316**, 165 (1993).

[9] SMC Collaboration, B. Adeva *et al.*, Phys. Lett. **B369**, 93 (1996); D. Adams *et al.*, Phys. Lett. B **357**, 248 (1995).

[10] L. Sehgal, Phys. Rev. D **10**, 1663 (1974).

[11] F.E. CLose, Preprint HEP-PH 9306288, talk presented at the 6th ICTP workshop, Treste, Italy.

[12] R.L. Jaffe, Physics Today, September 1995, 24.

[13] Particle Data Group, Review of Particle Physics, Phys. Rev. D **54** (1996).

[14] X. Ji, J. Tang, and P. Hoodbhoy, Phys. Rev. Lett. **76**, 740 (1996); X. Ji, Phys. Rev. Lett. **78**, 610 (1997).

[15] SMC Collaboration, D. Adams *et al.*, Phys. Rev. D **56**, 5330 (1997).

[16] HERMES Collaboration, K. Ackerstaff *et al.*, Phys.Lett. **B404**, 383 (1997).

[17] E143 Collaboration, K. Abe *et al.*, Phys. Rev. Lett. **76**, 587 (1996); **74**, 346 (1995); Phys. Lett. B **364**, 61 (1995).

[18] H.-Y. Cheng and S.-N. Lai, Phys. Rev. D **41**, 91 (1990).

[19] H.-Y. Cheng and C.F. Wai, Phys. Rev. D **46**, 125 (1992).

[20] T. Gehrmann and W. J. Stirling, Phys. Rev. D **53**, 6100 (1996).

[21] G. Altarelli, R. Ball, S. Forte, and G. Ridolfi, Preprint hep-ph 9803237.

[22] G. Altarelli, R.K. Ellis, G. Martinelli, and S.Y. Pi, Nucl. Phys. **B160**, 301 (1979).

[23] G. Gurci, W. Furmanski, and Petronzio, Nucl. Phys. **B175**, 27 (1980).

[24] J.C. Collins, D.E. Soper, and G. Sterman, in *Perturbative Quantum Chromodynamics*, edited by A.H. Mueller (World Scientific, Singapore, 1989).

[25] J.C. Collins and D.E. Soper, Nucl. Phys. **B194**, 445 (1982).

[26] M. Stratmann, A. Weber, and W. Vogelsang, Phys. Rev. D **53**, 138 (1996).

[27] A. Weber, Nucl. Phys. **B382**, 63 (1992).

[28] G. Altarelli and G.G. Ross, Phys. Lett. B **212**, 391 (1988).

[29] R.D. Carlitz, J.C. Collins, and A.H. Mueller, Phys. Lett. B **214**, 229 (1988).

[30] G.T. Bodwin and J. Qiu, Phys. Rev. D **41**, 2755.

[31] M.E. Fisher and D.S. Grant, Phys. Rev. A **133**, 224 (1964).

[32] K.G. Wilson and M.E. Fisher, Phys. Rev. Lett. **28** 240 (1972).

[33] G. 't Hooft and M. Veltman, Nucl. Phys. **B44**, 189 (1972).

[34] G. 't Hooft, Nucl. Phys. **B33**, 173 (1971).

[35] G. 't Hooft, Nucl. Phys. **B35**, 167 (1971).

[36] J.C. Collins, *Renormalization* (Cambridge University Press, 1984).

[37] E.L. Berger, Y.-W. Law and J. Qiu, *Definitions of Polarized Parton Distributions*, in preparation; Y.-W. Law and J. Qiu, γ_5 *Ambiguity in Polarized Drell-Yan Process*, in preparation.

[38] A.H. Mueller, Phys. Rep. **73**, 236 (1981).

[39] P. Breitenloher and D. Mason, Commun. Math. Phys. **52**, 11 (1977).

[40] G. Altarelli, R.K. Ellis, and G. Martinelli, Nucl. Phys. **B157**, 461 (1979).

[41] J. Kodaira, S. Matsuda, K. Sasaki, and T. Uematsu, Nucl. Phys. **B159**, 99 (1979).

[42] J. Kodaira, S. Matsuda, T. Muta, K. Sasaki, and T. Uematsu, Phys. Rev. D **20**, 627 (1979).

[43] S.A. Larin and J.A.M. Vermaseren, Phys. Lett. B **259**, 345 (1991).

[44] S.A. Larin, Phys. Lett. B **334**, 192 (1994).

[45] S.L. Adler, Phys. Rev. **177**, 2426 (1969); J.S. Bell and R. Jackiw, Nuovo Cimento A **51**, 47 (1969).

[46] R.L. Jaffe and A. Manohar, Nucl. Phys. **B337**, 509 (1990).

[47] J.D. Körner, D. Kreimer, and K. Schilcher, Z Phys. C **54**, 503 (1992).

[48] B. Kamal, Phys. Rev. D **53**, 1142 (1996).

[49] T.L. Trueman, Z Phys. C **69**, 525 (1996).

[50] G. Bonneau, Int. J. Mod. Phys. **A5**, 3831 (1990).

[51] M. Chanowitz, M. Furman, and I. Hinchliff, Nucl. Phys. **B159**, 225 (1979).

IMAGE EVALUATION TEST TARGET (QA-3)

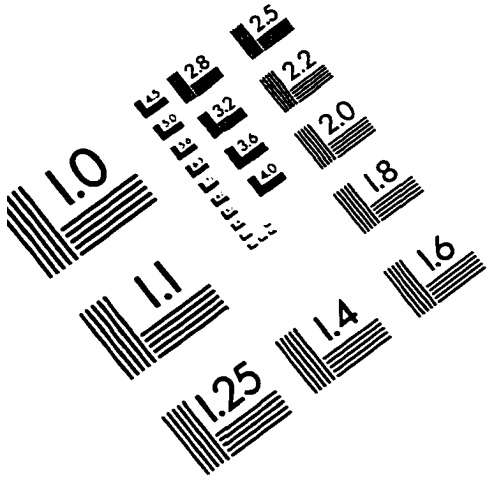

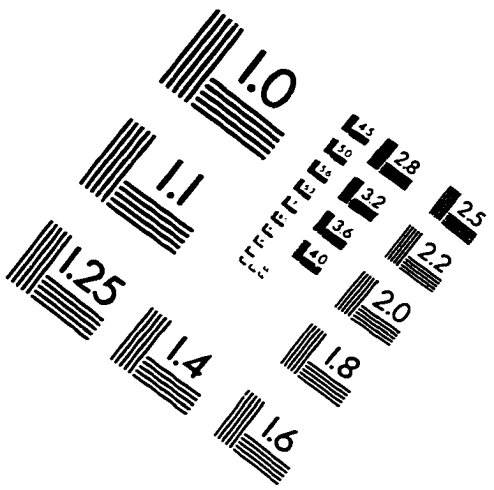

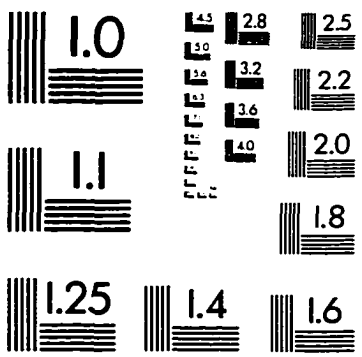

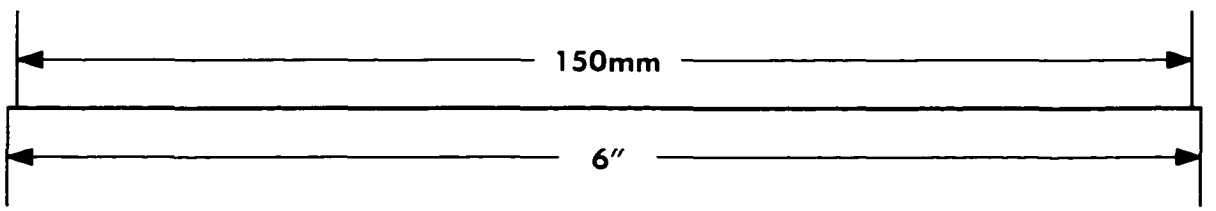

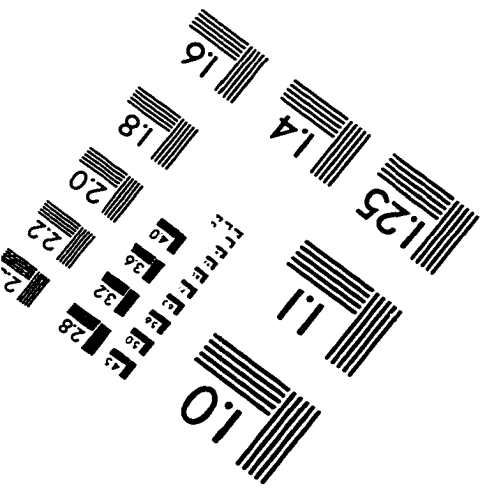

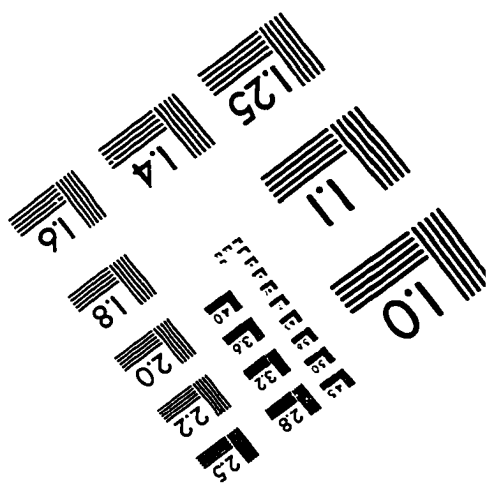

APPLIED IMAGE, Inc
1653 East Main Street
Rochester, NY 14609 USA
Phone: 716/482-0300
Fax: 716/288-5989